IDENTIFICATION OF IMMUNE-RESPONSIVE CIRCULAR RNAs IN SHRIMP

(*Litopenaeus vannamei*) UPON YELLOW HEAD VIRUS INFECTION

Amarin   Massu

A Thesis Submitted in Partial Fulfillment of the Requirements for the

Degree of Master of Science in Biotechnology

Suranaree University of Technology

Academic Year 2023

การจำแนกอาร์เอนเอชนิดวงกลมที่ตอบสนองต่อระบบภูมิคุ้มกันจากกุ้งขาวที่ติดเชื้อไวรัสหัวเหลือง

นายอัมรินทร์ มัสสุ

IDENTIFICATION OF IMMUNE-RESPONSIVE CIRCULAR RNAs IN SHRIMP (*Litopenaeus vannamei*) UPON YELLOW HEAD VIRUS INFECTION

Suranaree University of Technology has approved this thesis submitted in partial fulfillment of the requirements for a Master's Degree.

Thesis Examining Committee

_____
(Prof. Dr. Neung Teaumroong)
Chairperson

_____
(Assist. Prof. Dr. Pakpoom   Boonchuen)
Member (Thesis Advisor)

_____
(Assoc. Prof. Dr. Parinya   Noisa)
Member

_____
(Dr. Phattarunda   Jaree)
Member

_____
(Assoc. Prof. Dr. Yupaporn Ruksakulpiwat)
Vice Rector for Academic Affairs
and Quality Assurance

_____
(Prof. Dr. Neung Teaumroong)
Dean of Institute of Agricultural
Technology

อัมรินทร์ มัสสุ : การจำแนกอาร์เอนเอชนิดวงกลมที่ตอบสนองต่อระบบภูมิคุ้มกันจากกุ้งขาว
ที่ติดเชื้อไวรัสหัวเหลือง (IDENTIFICATION OF IMMUNE-RESPONSIVE CIRCULAR RNAs
IN SHRIMP (*Litopenaeus vannamei*) UPON YELLOW HEAD VIRUS INFECTION)
อาจารย์ที่ปรึกษา : ผู้ช่วยศาสตราจารย์ ดร.ภาคภูมิ บุญชื่น, 83 หน้า.

คำสำคัญ: อาร์เอนเอชนิดวงกลม/ไวรัสหัวเหลือง/กุ้งขาว/การหาลำดับนิวคลิโอไทด์ของอาร์เอนเอ
ชนิดวงกลม

อาร์เอนเอชนิดวงกลมเป็นอาร์เอนเอที่ไม่มีการถอดรหัส ถูกสังเคราะห์มาจากกระบวนการ
backsplicing อาร์เอนเอชนิดวงกลมมีบทบาทสำคัญในการความคุมกระบวนการต่าง ๆ ทางชีวภาพ
ในปัจจุบันอาร์เอนเอชนิดวงกลม พบว่ามีส่วนร่วมในการตอบสนองต่อการติดเชื้อไวรัสในเซลล์ของ
สัตว์เลี้ยงลูกด้วยนม อย่างไรก็ตามยังไม่มีการจำแนกอาร์เอนเอชนิดวงกลมที่ตอบสนองต่อเชื้อไวรัสหัว
เหลืองในกุ้งขาว (*Litopenaeus vannamei*) ดังนั้นการศึกษานี้มีจุดประสงค์เพื่อจำแนกอาร์เอนเอ
ชนิดวงกลมในเลือดของกุ้งขาวที่ติดเชื้อไวรัสหัวเหลือง พบว่ามีอาร์เอนเอชนิดวงกลมทั้งหมด 358
ชนิดที่มีการแสดงออกที่เปลี่ยนไปหลังจากกุ้งขาวติดเชื้อไวรัสหัวเหลือง โดยมี 177 ชนิดที่มีการ
แสดงออกเพิ่มขึ้น และ 181 ชนิดที่มีการแสดงออกลดลง จากนั้นสุ่มเลือกอาร์เอนเอชนิดวงกลมที่มี
การแสดงออกเปลี่ยนแปลงไปหลังจากกุ้งขาวติดเชื้อไวรัสหัวเหลือง 8 ชนิด ประกอบด้วย
circ_alpha-1 -inhibitor 3 , circ_CDC4 2 small effector protein 2 , circ_hemicentin 2 ,
circ_integrin alpha V, circ_kazal-type proteinase inhibitor, circ_phenoloxidase 3 ,
circ_related protein rab-8B, และ circ_protein toll-likeมาตรวจสอบคุณลักษณะของอาร์เอนเอ
ชนิดวงกลมด้วยเทคนิค PCR, RNase R treatment และ Sanger sequencing พบว่า ทั้ง 8 ชนิดมี
ลักษณะของอาร์เอนเอชนิดวงกลม การค้นพบนี้ทำให้เข้าใจในความเกี่ยวข้องของอาร์เอนเอชนิด
วงกลมในการตอบสนองต่อการติดเชื้อไวรัสหัวเหลืองในกุ้งมากยิ่งขึ้น

สาขาวิชาเทคโนโลยีชีวภาพ   ลายมือชื่อนักศึกษา____อัมรินทร์ มัสสุ____

ปีการศึกษา 2566   ลายมือชื่ออาจารย์ที่ปรึกษา_____

AMARIN MASSU : IDENTIFICATION OF IMMUNE-RESPONSIVE CIRCULAR RNAs IN
SHRIMP (*Litopenaeus vannamei*) UPON YELLOW HEAD VIRUS INFECTION
THESIS ADVISOR : ASSIST. PROF. Pakpoom Boonchuen, Ph.D., 83 PP.

Keywords: CircRNA/Yellow head virus/*Litopenaeus vannamei*/CircRNA sequencing

Circular RNAs (circRNAs) are a subclass of non-coding RNAs (ncRNAs) formed through a process known as back-splicing. They play a crucial role in the genetic regulation of various biological processes. Currently, circRNAs have been identified as participants in the antiviral response within mammalian cells. However, circRNAs in shrimp infected with the yellow head virus (YHV) remain largely unexplored. Therefore, this study aims to identify circRNAs in the hemocytes of *Litopenaeus vannamei* during YHV infection. The 358 differentially expressed circRNAs (DECs) were discovered, with 177 of them being up-regulated and 181 down-regulated. Subsequently, 8 DECs, including circ_alpha-1-inhibitor 3, circ_CDC42 small effector protein 2, circ_hemicentin 2, circ_integrin alpha V, circ_kazal-type proteinase inhibitor, circ_phenoloxidase 3, circ_related protein rab-8B, and circ_protein toll-like, were randomly selected for analysis of their expression patterns during YHV infection using qRT-PCR. Furthermore, the circRNAs' characteristics were confirmed through PCR, RNase R treatment, and Sanger sequencing, all of which were consistent with the features of circRNAs. These findings contribute to a better understanding of circRNAs' involvement in the antiviral response in shrimp.

School of Biotechnology   Student's Signature _____

Academic Year 2023   Advisor's Signature _____

ACKNOWLEDGEMENTS

CONTENTS

CONTENTS

LIST OF TABLES

LIST OF FIGURES

LIST OF FIGURES (Continued)

LIST OF ABBREVIATIONS

°C	Degree celsius
μ	Micro
×g	Relative centrifugal force
3′ UTR	3′ untranslated region
AHPND	Acute hepatopancreatic necrosis disease
ALFs	Anti-lipopolysaccharide factors
AMPs	Antimicrobial peptides
bp	Base pair
CAMs	Cell adhesion molecules
CDC42SE2	CDC42 small effector protein 2
cDNA	Complementary DNA
CIK	Cytokine-induced killer cell
circRNAs	Circular RNAs
ciRNA	Intronic circRNAs
clip-SP	clip-domain serine proteinase
DECs	Differentially expressed circular RNAs
DEPC	Diethyl pyrocarbonate
DNA	Deoxyribonucleic acid
dsDNA	Double-stranded DNA
dsRNA	Double-stranded RNA
ECM	extracellular matrix
EDTA	Ethylenediaminetetraacetic acid
EF-1α	Elongation factor-1 alpha
EHP	*Enterocytozoon hepatopenaei*
EMS	Early mortality syndrome
ElcircRNAs	Exon-intron circRNAs
eRNAs	Enhancer RNAs

LIST OF ABBREVIATIONS (Continued)

g	Gram
GAV	Gill associated virus
GCRV	Grass carp reovirus
gDNA	Genomic DNA
GLU	β-glucans
GO	Gene Ontology
h	Hour
HCV	Hepatitis C virus
HP	Hepatopancrease
hpi	Hour post-infection
HPM	Hepatopancreatic microsporidiosis
IAV	Influenza A virus
IHHNV	Infectious hypodermal and hematopoeitic necrosis virus
IL	Interleukin
Imd	Immune deficiency
IMN	Infectious myonecrosis
IMNV	Infectious myonecrosis virus
KEGG	Kyoto encyclopedia of genes and genomes
KSHV	Kaposi's sarcoma-associated herpesvirus
l	Liter
LGBD	LPS and GLU-binging protein
li-RNAs	Linear RNAs
lncRNAs	Long non-coding RNAs
LPS	Lipopolysaccharide
LTA	Lipoteichoic acid
*Lv*HMC	*Litopenaeus vannamei* hemocyanin
m	Milli
M	Molar
MG	Midgut

LIST OF ABBREVIATIONS (Continued)

min	Minute
miRNAs	MicroRNAs
mRNA	Messenger RNA
N	Nuclease
n	Nano
NaCl	Normal saline
ncRNAs	Non-coding RNAs
nt	Nucleotide
ORFs	Open reading frams
PAMPs	Pathogen-associated molecular patterns
PE	Paired-end
PEDV	Porcine endemic diarrhea virus
PEN	Penaedin
PGBD	PGN-binding protein
PGN	Peptidoglycans
pH	Potential of hydrogen ion
Pi	Primary
piRNAs	Piwi-interaction RNAs
PO	Phenoloxidase
Pol	RNA Polymerase
PPAE	proPO-activating enzyme
Pre	Precursor
PPRs	Pattern-recognition receptors
proPO	Prophenoloxidase
q	Quantitative
RDS	Runt-deformity syndrome
RISC	RNA-induced silencing complex
RNA	Ribonucleic acid
RNAi	RNA interference

LIST OF ABBREVIATIONS (Continued)

ROS	Reactive oxygen species
rRNA	Ribosomal RNA
RT	Reverse transcription
SCRV	*Siniperca chuatsi* rhabdovirus
SD	Standard deviation
Seq	Sequencing
siRNAs	Small interfering RNAs
sncRNAs	Small non-coding RNAs
snoRNAs	Small nucleolar RNAs
snRNAs	Small nuclear RNAs
ssDNA	Single-stranded DNA
ssRNA	Single-stranded RNA
ST	Stomach
TNFα	Tumor necrosis alpha
tRNA	Transfer RNA
TSD	Taura syndrome disease
TSV	Taura syndrome virus
UK	United Kingdom
USA	United States
v/v	Volume per volume
w/v	Weight per volume
WSSV	White spot syndrome virus
YHD	Yellow head disease
YHV	Yellow head virus
α	Alpha
β	Beta
βGBD	GLU-binding protein
%	Percent

CHAPTER I

INTRODUCTION

1.1 Background and Rationale

Yellow head virus (YHV) stands as one of the major virulent pathogens responsible for causing yellow head disease (YHD), which has resulted in extensive economic losses in shrimp aquaculture. YHV is characterized as a single-stranded RNA virus featuring a spiked envelope and a positive-sense genome. The YHV genome comprises approximately 27,000 nucleotides, placing the virus within the family *Roniviridae*, specifically in the genus *Okavirus* (Walker et al., 2005; Wongteerasupaya et al., 1995). Infection with YHV in Pacific white shrimp (*Litopenaeus vannamei*) can lead to mortality rates of up to 100% within 3–5 days following the initial appearance of gross YHD symptoms. Clinical manifestations of YHD encompass a pallid body complexion and a yellowish discoloration of the cephalothorax (Chantanachookin et al., 1993). Nevertheless, an effective vaccine for curing or preventing YHD remains elusive, given that shrimp lack adaptive immunity.

As invertebrates, shrimp rely solely on their innate immune system to defend against pathogen infections. While the innate immune system lacks specificity, it does boast a relatively rapid response time. Innate immunity swiftly identifies pathogen-associated molecular patterns (PAMPs), such as lipopolysaccharide (LPS), peptidoglycans (PGN), β-glucans (GLU), or double-stranded RNA (dsRNA), through pattern-recognition receptors (PRRs). This recognition leads to the activation of pro-inflammatory cytokines (IL-1, IL-6, IL-8, and TNF-α), chemokines, and transcription factors (Kulkarni et al., 2021). Additionally, non-coding RNAs (ncRNAs) play pivotal roles in regulating the immune response. ncRNAs are RNA molecules that are not encoded for protein production and can be categorized into two types: housekeeping gene ncRNAs, including transfer RNA and ribosomal RNA, and regulatory ncRNAs, such as small interfering RNAs (siRNAs), microRNAs (miRNAs), and circular RNAs (circRNAs) (Zhang et al., 2019).

In shrimp, the expression level of numerous miRNAs are increased during white spot syndrome virus (WSSV) infections (Zhang et al., 2019). They exert their influence by downregulating immune response genes through binding to the 3′ untranslated region (3′UTR) of messenger RNA (mRNA) seed sequences, thereby interfering with the translation process. For instance, miR-589-5p was found to reduce the expression of *L. vannamei* hemocyanin (*Lv*HMC), resulting in high shrimp mortality following WSSV infection (Bao et al., 2020).

Circular RNAs (circRNAs) represent a category of non-coding RNAs (ncRNAs) that form a closed-loop structure, lacking both the 5′ and 3′ terminals (Chen et al., 2015; Qu et al., 2015). Typically, circRNAs arise from back-splicing events where the upstream splice acceptor connects with the downstream splice donor region. Three distinct types of circRNAs exist, categorized based on their formation location: exonic circRNAs, exonic-intronic circRNAs, and intronic circRNAs (Kristensen et al., 2019; Wang et al., 2017). Numerous studies have underscored the significant biological roles played by circRNAs. In human cells, distinct classes of circRNAs displayed up-regulation or down-regulation in hepatitis C virus (HCV)-infected cells. Notably, one up-regulated circRNA, circPSD3, exhibited a substantial impact on viral RNA levels in both HCV- and Dengue virus-infected cells (Chen et al., 2020). In *Drosophila melanogaster*, circRNA profiling revealed an age-related accumulation pattern from 10 to 40 days, extending the observations of Westholm et al. This provides evidence that global circRNA levels continue to rise from 20 to 40 days of age (Westholm et al., 2014). The white-spotted bamboo shark (*Chiloscyllium plagiosum*) employs at least two circRNAs, circ-38-1717 and circ-6-1096, which act as miRNA sponges (Zhang et al., 2020). Furthermore, circRNAs have been implicated in immune regulation in fish species, including grass carp (*Ctenopharyngodon idella*) (He et al., 2017), tilapia (*Oreochromis niloticus*) (Fan et al., 2019), Miiuy croaker (*Miichthys miiuy*) (Xin et al., 2022), crucian carp (*Carassis auratus gibelio*) (Hu et al., 2019), and blunt snout bream (*Megalobrama amblycephala*) (Wang et al., 2021). When fish encounter bacterial or viral infections, differentially expressed circRNAs (DECs) containing miRNA binding sites may interact with miRNAs, influencing the expression of immunomodulatory proteins and thereby enhancing the immune response.

In shrimp, the presence of circRNAs in WSSV-infected shrimp has been unveiled.

Among the 290 circRNAs, 160 DECs were up-regulated, while 130 DECs were down-regulated following WSSV infection. This discovery sheds light on the landscape of WSSV-responsive circRNAs and their potential functions (Limkul et al., 2023). However, the identification and characteristics of YHV-responsive circRNAs have not been reported.

In this study, we aimed to identify circRNAs associated with the response of *L. vannamei* to YHV infection. To achieve this, the expression profiles of circRNAs in the hemocytes of both control and YHV-infected shrimp were analyzed using the high-throughput next-generation sequencing technique on the Illumina HiSeq 2500 platform. The immune-related differentially expressed circRNAs (DECs) from six libraries were quantitatively identified and subsequently validated and confirmed them through quantitative reverse transcription-PCR (qRT-PCR), RNase R treatment, and Sanger sequencing. These findings lay the groundwork for future investigations into circRNAs in shrimp, elucidating their characteristic features and shedding light on their roles in shrimp immunity.

1.2 Research objectives

The objectives of this study are as below:

1.2.1 To identify YHV-responsive circRNAs in shrimp using omics technology

1.2.2 To analyze the expression of YHV-responsive circRNAs in shrimp using qRT-PCR

1.2.3 To verify the structural and chemical characteristics of YHV-responsive circRNAs in shrimp using PCR, Sanger sequencing, and RNase R treatment

CHAPTER II

LITERATURE REVIEW

2.1 Taxonomy of the Pacific white shrimp

Pacific white shrimp (*Litopenaeus vannamei*) is classified into the phylum Arthropoda, which is the largest phylum in the animal kingdom. The taxonomic definition of the Pacific white shrimp is as follows (Bailey-Brock and Moss, 1992);

Domain: Eukarya

  Kingdom: Animalia

    Phylum: Arthropoda

      Subphylum: Crustacea

        Class: Malacostraca

          Subclass: Eumalacostraca

            Superorder: Eucarida

              Order: Decapoda

                Suborder: Dendrobranchiata

                  Superfamily: Penaeoidea

                    Family: Penaeidae

                      Genus: *Litopenaeus*

                        Species: *Litopenaeus vannamei*

Common name: Pacific white shrimp (USA), White shrimp (Peru), Whiteleg shrimp (UK, USA), Valkokatkarapu (Finland), Crevette pattes blanches (France), Mazzancolla tropicale (Italy), Camaron blanco (Ecuado and Mexico), Camaron café (Columbia), Camaron ecuatoriano o penaeus (Chile), Chamaron patiblanco (Spain), and Kung-kao (Thailand)

F.A.O. Names: Whiteleg shrimp, Crevette pattes blanches, Camaron patiblanco.

2.2 Morphology of Pacific white shrimp (*L. vannamei*)

The external morphology of *L. vannamei*, illustrated in Figure 1, showcases distinct anatomical features. The Pacific white shrimp consists of 19 pairs of body segments, each serving specific functions. The primary five pairs constitute the cephalon (head region), while the subsequent eight pairs form the thorax. These segments merge to form the cephalothorax (pereon), providing structural integrity. The exoskeleton covering the cephalothorax safeguards vital structures such as the gills and the gill chamber (branchiostegite). The remaining six pairs form the abdomen, housing the swimming legs (pleopods) on the first five pairs and concluding with the tail fan. This terminal segment features two pairs of uropods and the telson, facilitating rapid backward movement in response to threats (Ruppert and Barnes, 1994).
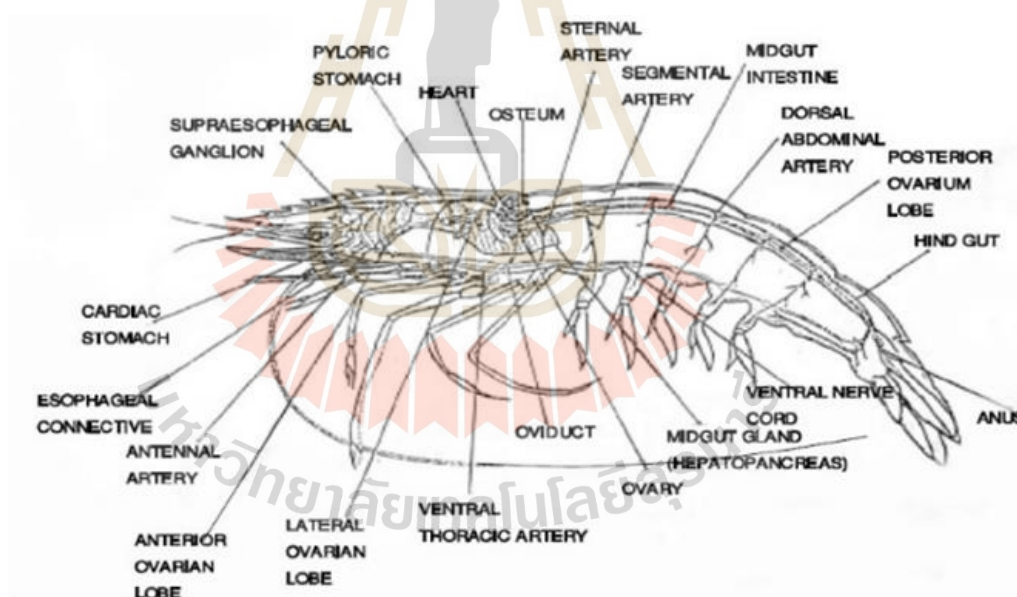
Figure 1. Morphology of Pacific white shrimp (*L. vannamei*) (Dugassa and Gaetan, 2018).

2.3 Infectious diseases in shrimp

The outbreak of infectious diseases in shrimp has resulted in considerable losses within shrimp production, impacting both fisheries and aquaculture industries economically. The infectious disease outbreaks have been caused by a major shrimp

pathogen, especially bacteria, viruses, and fungi (Table 1). Bacterial infections such as *Vibrio haveyi* and *V. parahaemolyticus* (VP$_{AHPND}$), have been reported in shrimp. As well, various viruses, such as white spot syndrome virus (WSSV), infectious hypodermal and hematopoeitic necrosis virus (IHHNV), infectious myonecrosis virus (IMNV), yellow head virus (YHV), taura syndrome virus (TSV), have been identified, causing high mortality, reduced production, and increased economic losses (El-Saadony et al., 2022; Lee et al., 2022). Additionally, *Enterocytozoon hepatopenaei* (EHP) is a microsporidian parasite classified as a group of fungi that causes extensive economic damage in shrimp (T. S. Kumar et al., 2022).

Table 1 The major causes of the infectious disease in shrimp.

Disease	Pathogen	References
Vibriosis	Vibrio species	(Chen, 1992)
Acute hepatopancreatic necrosis disease (AHPND)	Vibrio species	(Tran et al., 2013)
White spot syndrome disease (WSV)	White spot syndrome virus (WSSV)	(Flegel, 2006)
Infectious hypodermal and hematopoietic necrosis (IHHN) disease or runt-deformity syndrome (RDS)	Infectious hypodermal and hematopoietic necrosis virus (IHHNV)	(Motte et al., 2003)
Yellow head disease (YHD)	Yellow head virus (YHV) and Gill associated virus (GAV)	(Flegel, 2006)
Taura syndrome disease (TSD) (Red-Tail)	Taura syndrome virus (TSV)	(Srisuvan et al., 2005)
Infectious myonecrosis (IMN)	Infectious myonecrosis virus (IMNV)	(Tang et al., 2005)
Hepatopancreatic microsporidiosis (HPM)	*Enterocytozoon hepatopenaei* (EHP)	(Chayaburakul et al., 2004)

2.3.1 Bacterial diseases

2.3.1.1 Vibriosis

Vibriosis stands out as a significant bacterial disease affecting shrimp farms, attributable to gram-negative bacterial species within the Vibrionaceae family, including *V. harveyi*, *V. parahaemolyticus*, *V. vulnificus*, *V. splendidus*, *V. penaeicida*, *V. cholera*, and *V. alginolyticus* (Jayasree et al., 2006). *V. harveyi* is recognized as one of the primary causative agents responsible for mass mortalities in shrimp larval systems (Chandrakala and Priya, 2017). It is a gram-negative, rod-shaped, motile bacterium with luminescent properties. Clinical signs include shrimp becoming luminescent, reddish discoloration, and the formation of black spots of melanization on the cephalothorax (Figure 2). Infection can lead to mortality rates of up to 100% in affected shrimp.

Figure 2. The clinical signs of vibriosis (BioAqua and Kerala Agricultural Univesity). (A) Luminescence exhibited by the shrimp and (B) the appearance of black spots on the cephalothorax, attributed to melanization.

2.3.1.2 Early Mortality Syndrome

Early Mortality Syndrome (EMS), also known as Acute Hepatopancreatic Necrosis Disease (AHPND), is a newly emerged shrimp disease responsible for severe 100% mortalities in shrimp aquaculture. It has led to substantial losses in shrimp production globally. This disease was first discovered in Chaina in 2009 and spread to other countries (Tran et al., 2013). In Thailand, the shrimp production in 2013 has

decreased nearly 30% because of AHPND (Flegel, 2012; Leaño and Mohan, 2012). The causative agent of AHPND has been identified as a distinct strain of the bacterium *V. parahaemolyticus* (VP$_{AHPND}$), characterized by the presence of a 69 kbp plasmid containing two genes encoding Pir toxin-like proteins, namely pirA and pirB (Han et al., 2015; Yang et al., 2014). These toxin proteins were proven to be the key factors that cause AHPND symptoms (Lee et al., 2015). Clinical signs reported in VP$_{AHPND}$-infected shrimp include an empty digestive tract and a pale to white, atrophied hepatopancreas (Figure 3) (Kumar et al., 2020).
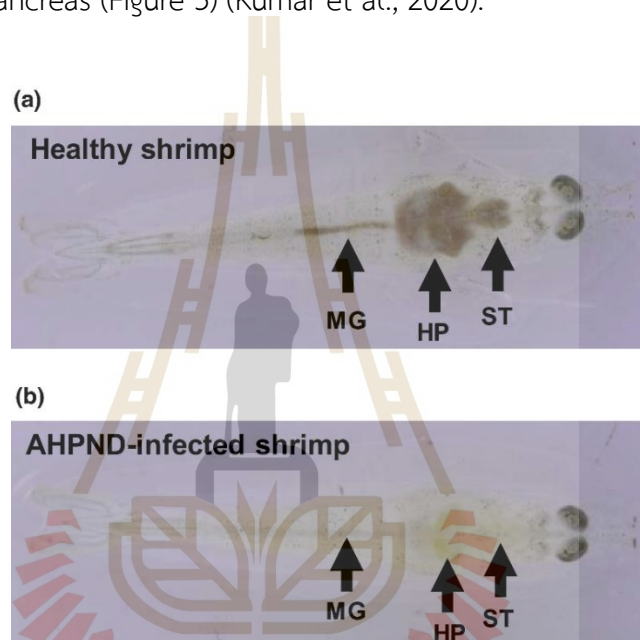
Figure 3. The clinical sign of VP$_{AHPND}$-infected shrimp (Kumar et al., 2020). (a) Healthy shrimp. (b) VP$_{AHPND}$-infected shrimp. Midgut (MG), hepatopancreas (HP), and stomach (ST).

2.3.2 Viral diseases

2.3.2.1 White spot syndrome disease

White spot syndrome disease (WSD) is a highly severe infectious disease in shrimp that caused by white spot syndrome virus (WSSV). WSSV was first reported in Taiwan shrimp farms in 1992 (Chou et al., 1995) and subsequently reported in many countries worldwide (Karunasagar et al., 1997; Park et al., 1998; Zhan et al., 1998). Clinical signs of WSSV infection include the appearance of white spots on the exoskeleton (carapace) and reddish-brown discoloration of the body

(Figure 4). Additionally, WSSV-infected shrimp typically exhibit reduced food consumption, shell loss, and lethargy. Mortality rates of 80-100% can occur within 3-5 days post-infection, leading to significant economic losses in shrimp aquaculture (Qiu et al., 2021).
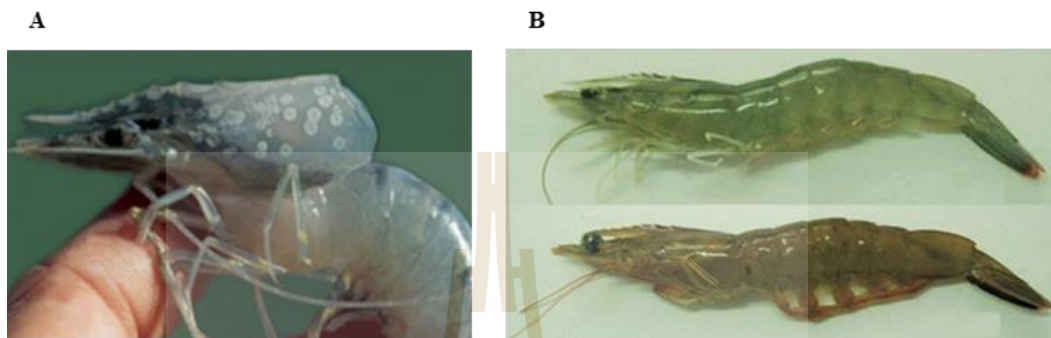
Figure 4. The clinical signs of white spot syndrome disease (R. Kumar et al., 2022). (A) The presence of white spots on the carapace is attributed to the accumulation of calcium salts within the cuticular chitin. (B) Reddish-brown body discoloration, typical of the acute phase of infection.

WSSV is a rod-shaped, enveloped, large circular double-strand DNA (dsDNA) virus with a 300 kbp genome. The virion is a large 80-120 × 250-380 nm, particle structure quite similar to baculovirus shape. WSSV is classified in the family Nimaviridae, genus *Whispovirus* (Sánchez-Paz, 2010). It had been proposed to encode 181 functional open reading frames (ORFs) (Leu et al., 2009). WSSV virion particles are ellipsoid, with three layers: a lipid-containing envelope, a tegument, and a nucleocapsid enclosing genomic DNA (Tsai et al., 2006). Electron micrographs of virion particles are illustrated in Figure 5.
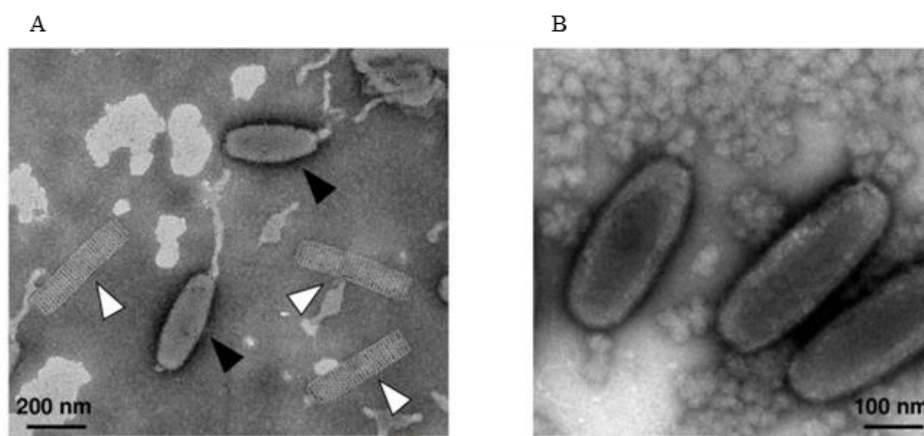
Figure 5. Electron micrographs of WSSV virions (R. Kumar et al., 2022). (A) Mature WSSV virions featuring characteristic tail-like structures. (B) The WSSV virion particles lacked a tail-like structure.

2.3.2.2 Yellow head disease

Yellow head disease (YHD) is one of the infectious diseases that has been caused by yellow head virus (YHV). YHD was first observed in the black tiger shrimp (*Penaeus monodon*) in central Thailand in 1990 (Boonyaratpalin et al., 1993). It causes mass mortality of the species and substantial economic losses to the shrimp industry. Observations of YHV-infected shrimp typically reveal a pale body appearance along with yellowish discoloration of the cephalothorax (Figure 6). The YHV type-1 reported from Thailand causes severe mortality of *P. monodon* while the second type (YHV type-2), is named a gill-associated virus (GAV) (Dhar et al., 2004; Wijegoonawardane et al., 2008). Among the eight identified genotypes, recognizable symptoms of YHV infection in shrimp are only documented for YHV genotype 1 (Li et al., 2019).

Most aquacultured species of penaeid shrimp, including *P. stylirotris*, *P. aztecus*, *P. duorarum*, *L. vannamei*, are susceptible to YHV infection. YHV infection also caused high mortality in *P. stylirotris*, *P. aztecus*, *P. duorarum*, and *L. vannamei*, and *P. monodon* was the most affected (Cedano-Thomas et al., 2010; Cowley et al., 2004).

Figure 6. The clinical signs of yellow head disease. The red arrow indicated the YHV-infected shrimp which shows a yellowish discoloration of the cephalothorax compared to the normal shrimp (left) (Amarakoon and Wijegoonawardane, 2017).

YHV is a rod-shaped, positive sense, enveloped single-stranded RNA (ssRNA) genome with virions of 40-60 nm × 150-200 nm and internal helical nucleocapsids of 15 nm in diameter 80-450 nm in length (Figure 7) (Lee et al., 2022). The YHV genome spans approximately 27,000 nucleotide (nt), and the virus is classified within the newly established family Roniviridae, genus *Okavirus* (Walker et al., 2005; Wongteerasupaya et al., 1995). Three structural proteins of YHV have been identified, including two envelope glycoproteins, gp116 and gp64, and a nucleocapsid protein, p20 (Assavalapsakul et al., 2005; Jitrapakdee et al., 2003; Sittidilokratna et al., 2008). After YHV infection, extensive necrosis is observed in various shrimp tissues, including the lymphoid organ, gills, connective tissues, hemocytes, and hematopoietic organs. Histopathological studies and YHV receptor investigations suggest that the lymphoid organ may be the primary target of YHV. Mortality of YHV-infected shrimp typically occurs within 3-5 days after the onset of clinical signs, with cumulative mortality rates reaching up to 100% (Chantanachookin et al., 1993). Resulting in rapid damage to shrimp production.
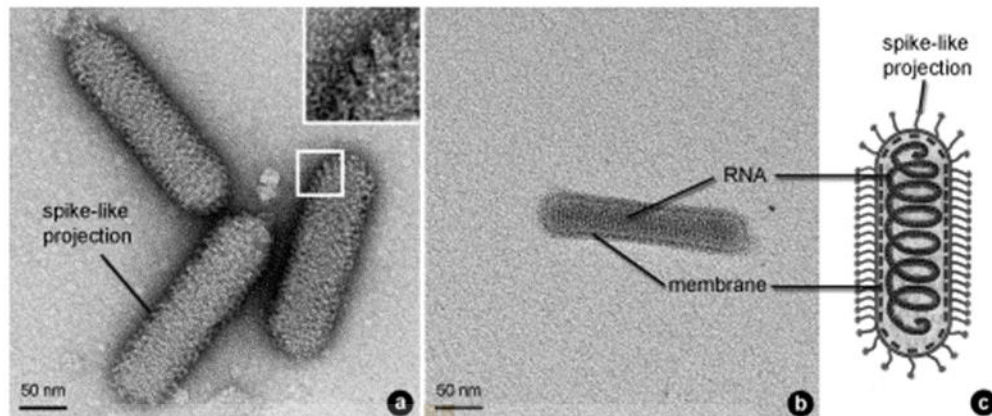
Figure 7. Electron microscopic of YHV (Duangsuwan et al., 2011). (a) The spike-like projection surrounds YHV. (b-c) The YHV nucleocapsid, which has a rod-shaped and a helical structure with 40-50 turns.

2.3.2.3 Runt-deformity syndrome

Runt-deformity syndrome (RDS) is attributed to the infectious hypodermal and hematopoietic necrosis virus (IHHNV), which is a linear single-stranded DNA (ssDNA) virus with an estimated length of 3900 nt. It is a non-enveloped, icosahedral linear virion with a diameter ranging from 20 to 23 nm (Shen et al., 2015). It was first discovered in infectious Pacific blue shrimp (*P. stylirostris*) and Pacific white shrimp (*L. vannamei*) in Hawaii in 1981 (Lightner et al., 1983) and subsequently detected in other penaeid species around the world (Flegel, 1997; Lightner, 1996). RDS does really affect shrimp growth, with IHHNV-infected shrimp exhibiting reduced and irregular growth patterns (cuticular deformities of the rostrum, antennae, thoracic and abdominal areas) (Figure 8).
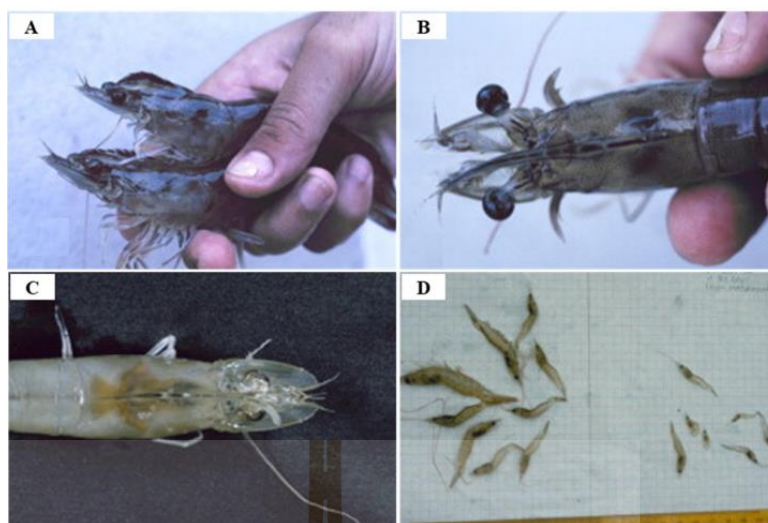
Figure 8. The clinical signs of runt-deformity syndrome (Lightner, 2011). (A, B) The bent (to the left) rostrums of *L. vannamei*. (C) The discoloration and deformity of the body on *L. vannamei*. (D) The abdominal deformities and size variation of IHHNV-infected shrimp.

2.3.2.4 Taura syndrome disease

Taura syndrome disease (TSD) inflicts substantial economic losses on the shrimp farming industry and affects the trade and transportation of shrimp between countries. The cause of TSD is the taura syndrome virus (TSV), which was first reported in 1992 and classified in the *Aparavirus* genus belonging to the Dicistroviridae family (Cruz-Flores et al., 2021). TSV is an icosahedral-shaped, positive-sense, non-enveloped ssRNA virus with a genome of 10,200 nt and a diameter of about 32 nm (Fadilah and Fasya, 2021). Shrimp infected with TSV typically display clinical signs such as a reddish discoloration of the body, particularly noticeable on the tail, uropods, and appendages, attributed to chromatophore expansion. They may also develop irregular black spots, known as melanization, beneath the cuticle layer (Figure 9). Furthermore, affected shrimp may demonstrate symptoms including loss of appetite, erratic swimming behavior, lethargy, soft cuticles, flaccid bodies, and opaque musculature (Dhar et al., 2004; Fadilah and Fasya, 2021).
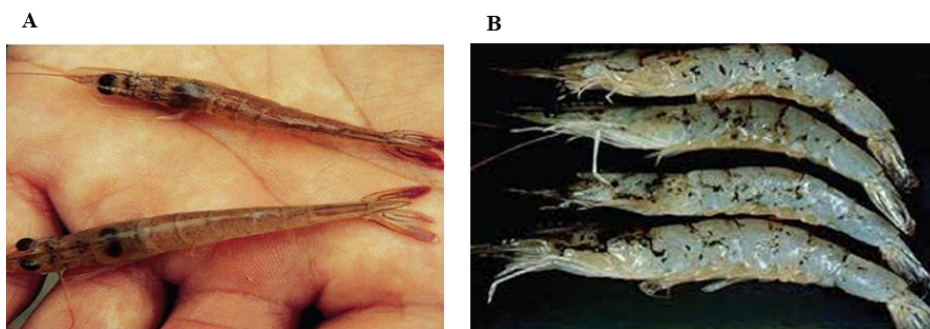
Figure 9. The clinical signs of TSV-infected shrimp (Samocha, 2019). (A) The red tail fans and reddish discoloration of the body. (B) Dark melanised lesions on the carapace.

2.3.2.5 Infectious myonecrosis

The infectious myonecrosis virus (IMNV) causes infectious myonecrosis (IMN) and significantly impacts the shrimp aquaculture industry. IMNV comprises a double-stranded RNA (dsRNA), forming a monopartite genome approximately 8,000 bp in length, with two open reading frames (ORFs). It is a non-enveloped icosahedral virus with a diameter of 40 nm and fiber-like protrusions on the surface (Borsa et al., 2011; Sahul Hameed et al., 2017). The host of IMNV is the *L. vannamei*, which typically shows symptoms approximately 7 days after infection, resulting in a cumulative mortality rate of 70%. In addition, IMNV infection has also been found in other shrimp species, such as *P. sylirostris*, *P. monodon*, and *P. subtiltis*. The clinical signs of IMNV infection are typically identified through the observation of chronic symptoms in the host. Symptoms exhibited by IMNV-infected shrimp include focal to extensive white necrotic areas in the striated muscle, particularly in the distal abdominal segments and tail fan (Figure 10), as well as gradual mortality that persists throughout the culture period (Poulos et al., 2006).

Figure 10. The clinical sign of IMNV-infected shrimp (Sahul Hameed et al., 2017). (a, b) The reddish opaque muscle at distal abdominal segments.

2.3.3 Fungal diseases

2.3.3.1 Hepatopancreatic microsporidiosis

Hepatopancreatic microsporidiosis (HPM), caused by *Enterocytozoon hepatopenaei* (EHP), is a disease affecting shrimp. This microsporidian parasite was first characterized in black tiger shrimp (*P. monodon*) in Thailand in 2009 (Chayaburakul et al., 2004). It was also affecting Pacific white shrimp (*L. vannamei*). EHP belongs to the *Enterocytozoonidae* family. The characteristics of EHP suggest a eukaryotic cell structure (unicellular), but it lacks mitochondria and peroxisomes. It is a spore-forming parasite (Jaroenlak et al., 2018). The spore is oval-shaped, measuring 0.7-1.1 µm in size. EHP does not typically result in mass mortalities. While there are no specific clinical signs of EHP infection, it is frequently linked with stunted growth, wide size variation, and the occurrence of white feces syndrome (Suresh et al., 2018). This makes the causative agent EHP an economically significant pathogen for shrimp aquaculture.

Figure 11. The clinical sign of HPM (Suresh et al., 2018). The size variation of EHP-infected shrimp.

2.4 The immune system in shrimp

As invertebrates, shrimp rely solely on their innate immune system to defend against pathogen infections. Although the innate immune system cannot respond to specific pathogens, its response time is relatively rapid. The shrimp's innate immune system can be divided into 2 groups of cellular and humoral immunity components to fight invading microbes (Bachère et al., 2004). The cellular immunity involves phagocytosis, nodule formation, encapsulation, and melanization, while the humoral immune component includes reactive oxygen species (ROS), antioxidant defense enzymes, lysosomal enzymes, proteinase inhibitors, antimicrobial peptides (AMPs), prophenoloxidase-activating system (proPO system), blood clotting cascade and agglutinins and cytokine-like factors (Bachère et al., 2004; Cerenius et al., 2010). The innate immune response in shrimp is triggered by engaging pathogen-associated molecular patterns (PAMPs) through pattern recognition receptors (PRRs). The PAMPs include lipopolysaccharides (LPS), peptidoglycans (PGN), double-stranded RNA (dsRNA), and β-glucans (GLU) (Kulkarni et al., 2021). These conserved molecules are located on the surface of invading pathogens. The interaction of PRRs with their PAMPs triggers the expression and up-regulation of appropriate pro-inflammatory cytokines and antimicrobial molecules during infection, leading to the activation of the host defense system (Figure 12).
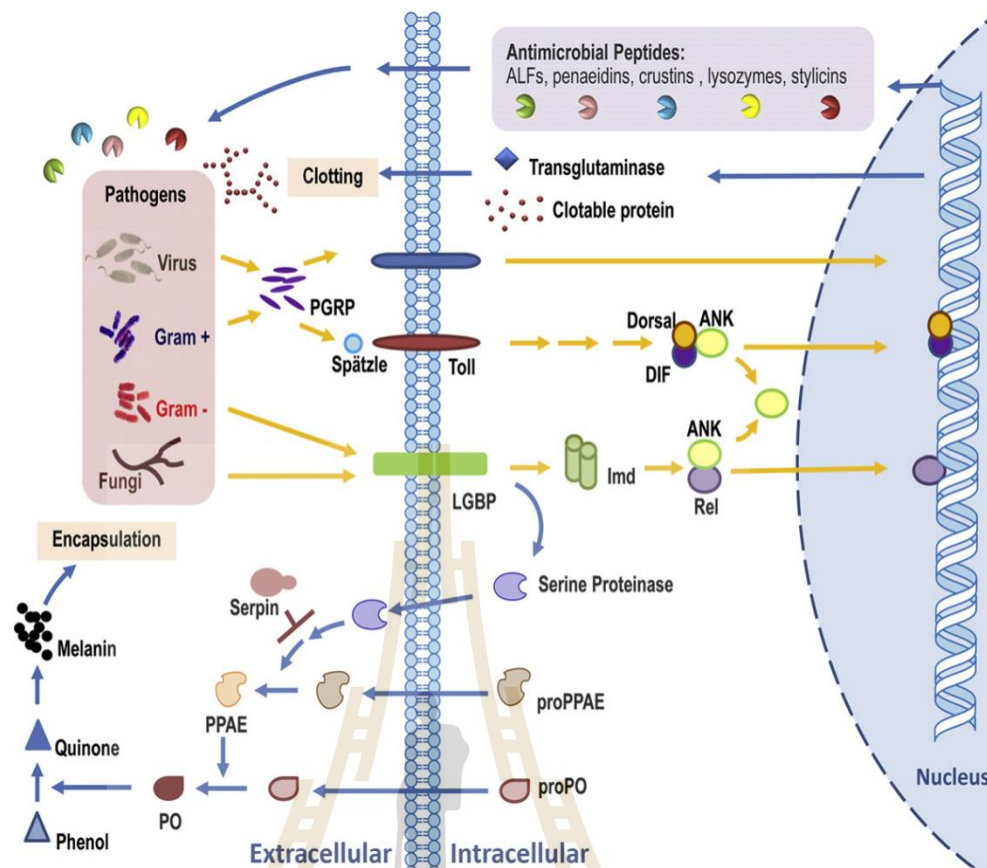
Figure 12. A schematic model of the shrimp immune system (Tassanakajon et al., 2013).

2.4.1 Cellular immune response

Penaeid shrimp hemocytes serve as the primary cells of the innate immune system, playing crucial roles in host defense and maintaining homeostasis. These hemocytes are classified into three categories: hyalinocytes, semi-granulocytes, and granulocytes (Figure 13) (Zhang et al., 2006). The various immune response molecules are synthesized and accumulated within the granules of hemocytes before being released into the hemolymph to combat invading pathogens (Tassanakajon et al., 2013).

Hyalinocytes, also known as hyalin cells, possess a small nucleus relative to their cytoplasm and typically lack cytoplasmic granules. These cells play roles primarily associated with clotting and phagocytosis. Each species of shrimp has a different amount of agranulocytes (Figure 13A). For example, *Pacitastacus leniusculus* and *P. japonicus* have 3% and 10% of circulating hemocyte, respectively. But agranulocyte have not found in *Macrobrachium rosenbergii*.

Semi-granulocytes, also known as semi-granular cells, are characterized by the presence of numerous small eosinophilic granules (Figure 13B). These cells have the function involved in encapsulation, phagocytosis, and coagulation. The semi-granulocytes are responsible for recognizing and responding to pathogen that invaded shrimp and binding to the surface of foreign (Kobayashi et al., 1990).

Granulocytes, also referred to as granular cells or eosinophilic granulocytes, are characterized by their small nucleus and abundance of cytoplasmic granules (Figure 13C). These cells exhibit phagocytic activity and serve as reservoirs for the enzyme prophenoloxidase (proPO). Stimulation by β-1,3-glucans (GLU), peptidoglycans (PG), and lipopolysaccharides (LPS) can trigger exocytosis and enzyme release. Their functions include encapsulation, initiation of the proPO cascade, and phagocytosis (Lin and Söderhäll, 2011).
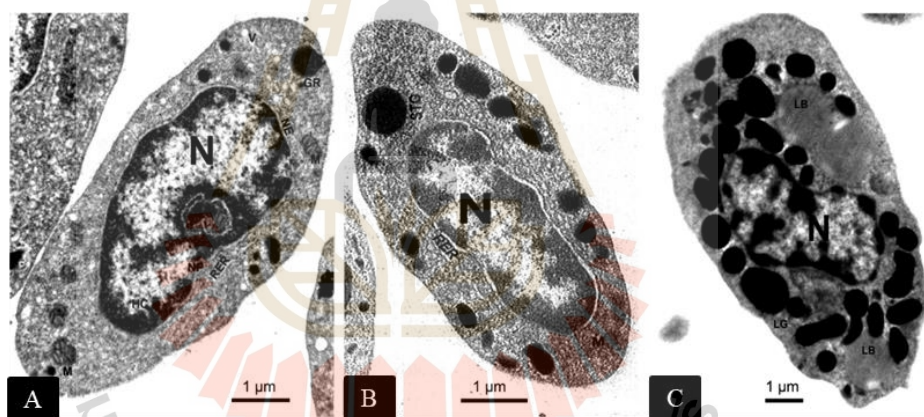
Figure 13. The transmission electron micrograph of the crustacean hemocytes (mud crab, *Scylla serrata*) (Kumar et al., 2013). (A) Hyalinocytes. (B) Semi-granulocytes. (C) Granulocytes. Nuclease (N).

Their biological properties and functions can be classified into phagocytosis, which is carried out by semi-granulocytes and granulocytes capable of sensing and internalizing into the phagosome able to degrade the ingested particle (Canton, 2014), and encapsulation; i.e., semi-granulocytes are responsible for the recognition of the invading agents, which are formed by numerous hemocytes acting synergistically to trap microorganisms or big antigens that cannot be removed by phagocytosis (Aguirre-Guzman et al., 2009).

2.4.2 Humoral immune response

The humoral responses of shrimp play a crucial role in their immune defense system, serving as the first line of defense against pathogen infections. The shrimp immune system is involved in various functions, including recognizing foreign antigens, eliminating different types of pathogens, and minimizing tissue damage to the host (Beutler, 2004).

2.4.2.1 Pattern recognition proteins

The pattern recognition proteins (PRPs) are lectins that identified the molecules like PGN, LPS, bacterial lipoteichoic acid (LTA), fungal β-1,3-glucans, and viral RNA (Lee and Söderhäll, 2002). They facilitate the activation of specific defense mechanisms by the host. The biological functions of PRPs include initiating protein cascades and/or signaling pathways for defense mechanisms, as well as eliminating invaders from the blood system (Aguirre-Guzman et al., 2009). When detection of antigens by PRPs, the hemocytes are migrating to their location by chemotaxis, initiating an inflammatory response. The crustacean's open circulatory system facilitates this process, enabling a rapid and efficient defense mechanism against pathogens (Robalino et al., 2004).

The innate immune system identifies pathogens through PRPs and their corresponding PRRs, which are also proteins. Two major signaling immune pathways, known as the Toll and Imd (immune deficiency) pathways, are directly involved in these responses. These distinct signaling pathways regulate the expression of different sets of antimicrobial peptides (AMPs) (Figure 14). They may also act in parallel in response to different kinds of microorganisms (Li and Xiang, 2013a).
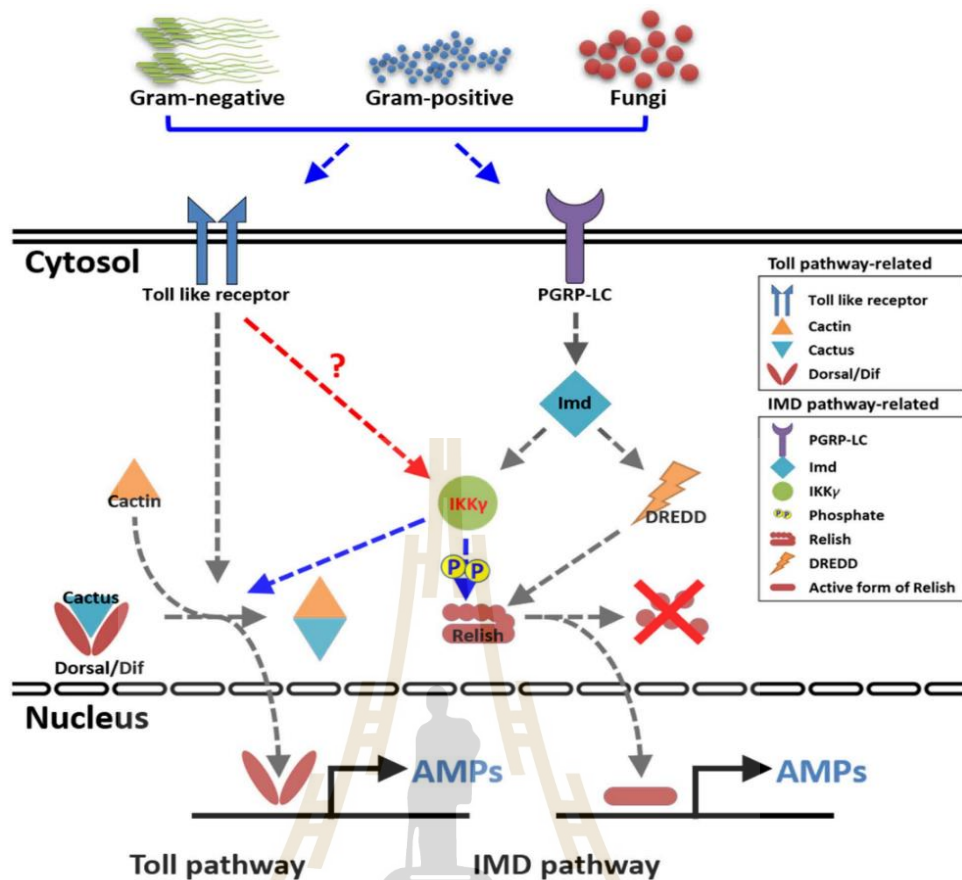
Figure 14. Toll and IMD signaling pathway (Ko et al., 2020).

2.4.2.2 The prophenoloxidase system

The prophenoloxidase system (proPO) is the origin of melanin production (melanization) and serves as an innate defense mechanism in penaeid shrimp. Commonly, proPO is an inactive form. These molecules induce the granulocyte secretion of inactive proPO granules and their transformation (cascade reaction) to proPO enzyme (Hellio et al., 2007; Lee et al., 2004). For example, the PAMPs (GLU, PGN, and LPS) were recognized by the PRPs (GLU-binding protein (βGBD), PGN-binding protein (PGBP), and LPS and GLU-binging protein (LGBD)). Then, the serine proteinase cadcase was activated, resulting in the cleavage of a final clip-domain serine proteinase (clip-SP) designated as a proPO-activating enzyme (PPAE). Subsequently, PPAE switches the inactive proPO into active phenoloxidase (PO). This oxidizes phenols into quinones, which may help to kill pathogens and are used for melanin production (Figure 15).
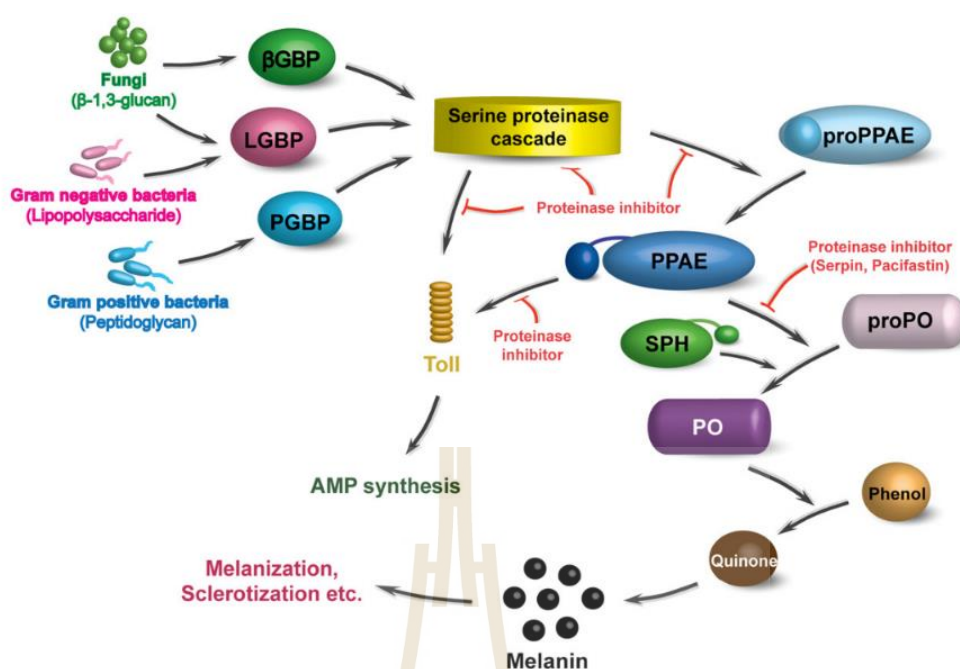
Figure 15. The prophenoloxidase (proPO)-activating system in arthropods (Amparyup et al., 2013).

2.4.2.3 Antimicrobial peptides

The antimicrobial peptides (AMPs) are an important element against the microbial infection. Therefore, the AMPs are considered as significant humoral immune effectors. AMPs are peptides encoded by genes, produced as precursor proteins, stored in granule-containing hemocytes, and released upon induction. These peptides exhibit a wide spectrum of activity, low specificity, and weak cytotoxicity to animal cells. They function by creating pores in the cell membranes of bacteria, fungi, parasites, and the envelopes of viruses.

- Penaeidin (PEN), a family of AMPs, was initially characterized from *L. vannamei*. It is synthesized and stored in the granulocytes and exhibits antibacterial and antifungal activities against Gram-positive bacteria (Destoumieux et al., 1997). In *P. monodon*, penaeidin 3 exhibits anti-fungal and antibacterial activities, while penaeidin 5 reduces bacterial growth (Hu et al., 2006) and demonstrates antiviral activity against WSSV infection (Destoumieux-Garzón et al., 2016).

- Lysozyme is a bacteriolytic enzyme. It can hydrolyze the β-1,4-glycosidic linkages between N-acetylmuramic acid and N-acetylglucosamine in

peptidoglycan lead to bacterial lysis. In shrimp, lysozyme was found to display antimicrobial activity against both gram-negative (-) and gram-positive (+) bacteria (Jollès and Jollès, 1984).

- Anti-lipopolysaccharide factors (ALFs) are a small polypeptide that belongs to an AMPs family. ALFs contain a hydrophobic N-terminal region with two conserved cysteine residues. The disulfide bond delimits a β-hairpin structure known as the LPS-binding domain. While most ALFs bind to Lipid A from Gram-negative bacteria, they can also interact with lipoteichoic acid (LTA) from Gram-positive bacteria and glucans from fungi. Therefore, the ALFs of penaeid shrimp exhibit a wide range of functions in shrimp immunity, including anti-bacterial, anti-fungal, and anti-viral activities (Tinwongger et al., 2019). Several ALFs have been identified in *P. monodon*, including ALF*Pm*2, ALF*Pm*3, and ALF*Pm*6. The expression patterns of ALFs genes respond to bacterial and viral infections. In terms of inhibition activities, ALF*Pm*3 inhibits fungi, Gram-positive and Gram-negative bacteria, *V. harveyi*, VP_{AHPND}, and WSSV infection (Methatham et al., 2017). ALF*Pm*6 also inhibits *V. harveyi*, YHV and WSSV infection (Kamsaeng et al., 2017).

2.5 non-coding RNAs

Non-coding RNAs (ncRNAs) are RNA molecules transcribed from the genome that do not encode proteins; instead, they function to regulate gene expression at both the transcriptional and post-transcriptional levels. The ncRNAs can be categorized into 2 types of housekeeping ncRNAs and regulatory ncRNAs to regulate gene expression (Zhang et al., 2019).

2.5.1 Housekeeping non-coding RNAs

Housekeeping ncRNAs, typically small in size (ranging from 50 to 500 nt), are expressed constitutively in all cells. These ncRNAs comprise of ribosomal RNAs (rRNAs), transfer RNAs (tRNAs), small nuclear RNAs (snRNAs), small nucleolar RNAs (snoRNAs), and telomer RNAs. They play essential roles in various cellular processes, such as protein synthesis (rRNAs and tRNAs), RNA splicing (snRNAs), and RNA modifications (snoRNAs) (Zhang et al., 2019).

2.5.2 Regulartory non-coding RNAs

Regulatory ncRNAs could be further categorized into small non-coding RNAs (sncRNAs), which are shorter than 200 nt, and long non-coding RNAs (lncRNAs), which exceed 200 nt in length. The main classes of sncRNAs are microRNAs (miRNAs), small interfering RNAs (siRNAs), and piwi-interaction RNAs (piRNAs). However, some ncRNAs with variable length might belong to two classifications at the same time (Zhang et al., 2019).

2.5.2.1 MicroRNAs

MicroRNAs (miRNAs) are the most abundant class of sncRNAs (approximately 18-24 oligonucleotides) that play important roles in the regulation of the gene expression process through RNA silencing and post-transcriptional regulation (Boonchuen et al., 2020). The miRNAs were transcribed into hairpin structures (100-1000 nt) within nucleas, called primary miRNAs (pi-miRNAs). The pi-miRNAs were then cleaved by drosha/DGCR8, producing precursor miRNAs (pre-miRNAs) hairpins. These pre-miRNAs were exported to the cytoplasm by Exportin-5 and subsequently processed by RNase III enzyme dicer, which removes the loop region of the hairpins, resulting in the production of mature miRNA duplexes approximately 22 oligonucleotides in length. The action of miRNAs begins when a mature miRNA is incorporated into the RNA-induced silencing complex (RISC), resulting in specific interactions with target mRNAs (seed region; typically, nt 2-8). The complementary target mRNA is degraded. Therefore, transcriptionally was repressed (Figure 16) (Azzam et al., 2012).
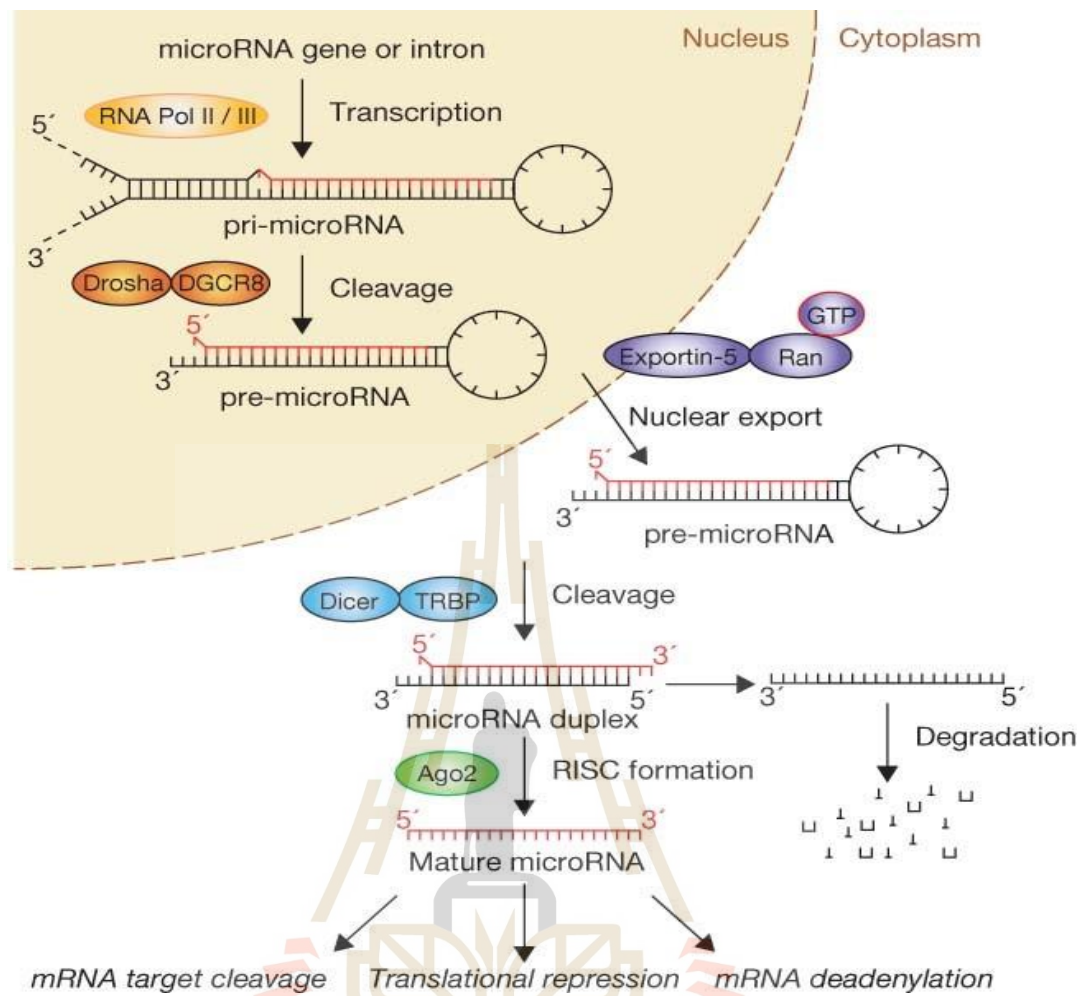
Figure 16. The miRNA processing pathway (Winter et al., 2009).

MiRNAs are involved in various biological processes including cellular proliferation, differentiation, apoptosis, development, and immune system. Previous studies reported that miRNAs are also implicated in viral infection response. For instance, shrimp miR-7 has the ability to suppress the wsv477 gene of WSSV, which is implicated in early DNA replication, resulting in a significant decrease in the number of WSSV copies (Figure 17) (Huang and Zhang, 2012). Furthermore, miRNA-965 was up-regulated in WSSV-infected shrimp (*M. japonicus*), which can decrease the number of WSSV copies and mortality in WSSV-infected shrimp by targeting the wsv240 gene (Shu et al., 2016). Therefore, these findings illustrate that miRNAs act as antiviral agents by targeting WSSV genes involved in replication.
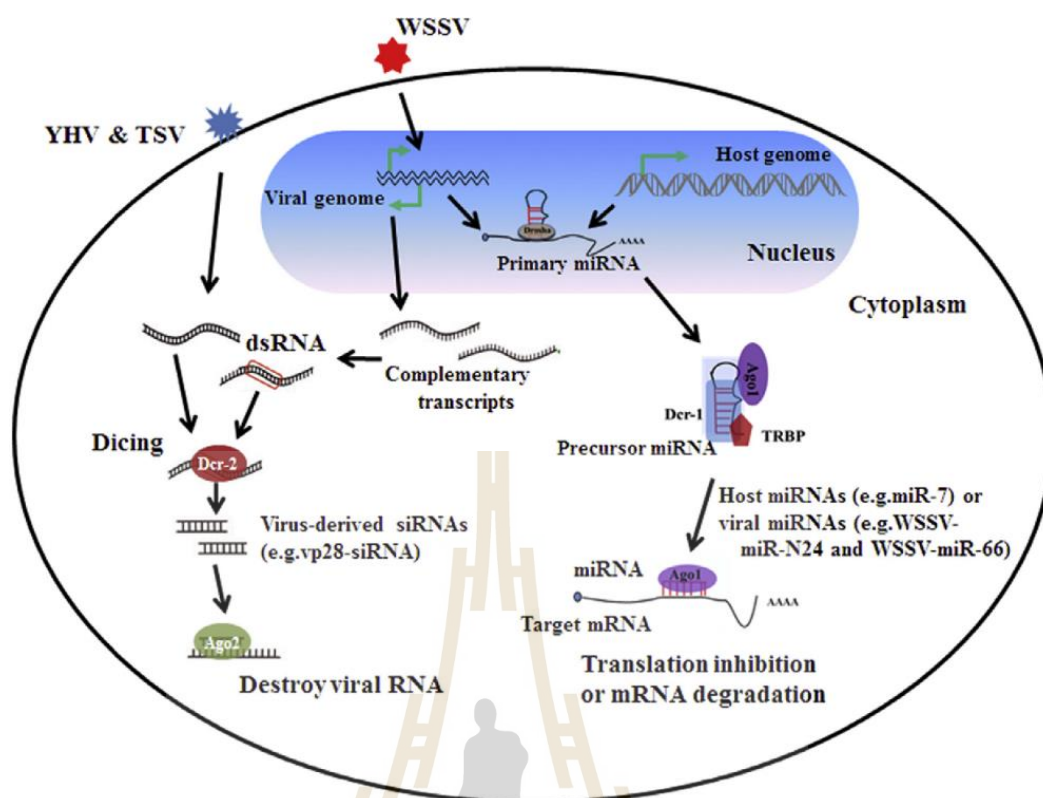
Figure 17. Schematic representation of miRNAs mediated antiviral immunity in shrimp (Xu et al., 2014).

2.5.2.2 Small interfering RNAs

Small interfering RNAs (siRNAs) are a class of double-stranded RNA (dsRNA) molecules and play important roles in RNA interference (RNAi) pathway (Zhang et al., 2019). This is a biological process in which small RNA molecules inhibit the gene expression process. The RNAi pathway is initiated through the cleavage of long dsRNAs into siRNAs (approximately 18–25 bp in length) by the RNase III–like enzyme Dicer. After that, single strand assembled into RISC. A perfect binding target of mRNA is cleaved by RISC in the middle of the siRNA:mRNA duplex. Therefore, transcriptionally was repressed (He et al., 2015). In shrimp, RNAi has been employed to suppress virus genes. The WSSV envelope protein VP28 plays a crucial role in the systemic infection of shrimp. This gene was used as a target for gene silencing through the siRNA strategy. The silencing of the *vp28* gene by vp28-siRNA leads to a significant reduction in virus replication and a reduced mortality rate of WSSV infection in shrimp (Xu et al., 2007). Additionally, the survival rate of WSSV-

infected shrimp was found to be enhanced by suppressing other genes, including DNA polymerase (*dnapol*), ribonucleotide reductase small subunit (*rr2*), thymidine kinase and thymidylate kinase (*tk-tmk*), *vp24*, and *vp15* (Westenberg et al., 2005; Wu et al., 2007).

2.5.2.3 piwi-interaction RNAs

piwi-interaction RNAs (piRNAs) constitute a class of sncRNAs, typically 24-32 nucleotides in length, that play crucial roles in regulating gene expression and maintaining genome stability, particularly in germ cells. Primary piRNAs originate from specific genomic loci known as piRNA clusters (Czech et al., 2018). In general, piRNAs have been categorized into five groups according to their origin: mRNAs-derived, tRNAs-derived, transposon-derived, long non-coding RNAs (lncRNAs)-derived, and snoRNAs-derived piRNAs. miRNAs-derived piRNAs are produced from mRNA 3′ untranslated regions (3′ UTRs) of mRNAs (Jensen et al., 2020). piRNAs derived from tRNAs originate from 5′-tRNAs halves rather than mature tRNAs (Honda et al., 2017; Keam et al., 2014). piRNAs derived from transposon are generated through single-strand clusters transcribed, generating both sense and antisense piRNAs (Czech and Hannon, 2016). piRNAs originating from lncRNAs are processed from exon regions of the lncRNA (Ha et al., 2014). piRNAs derived from snoRNAs originate from snoRNAs cleaved at the middle of their sequences (Zhong et al., 2015). The precursor piRNAs are initially translocated from the nucleus to the cytoplasm. Following cleavage and modification, the intermediate piRNAs subsequently associate with PIWI proteins, forming mature piRNA complexes (Y. Liu et al., 2019). piRNAs can regulate gene expression in somatic cells through transposon silencing, epigenetic programming, DNA rearrangements, mRNA turnover, and translational control (Wu et al., 2020). In the nematode *Caenorhabditis elegans*, piRNAs suppress several genes involved in germline development (Cornes et al., 2022; Montgomery et al., 2021). In *Drosophila melanogaster*, piRNAs have the function in transposon silencing (Chen et al., 2021). These piRNAs guide PIWI proteins to recognize and bind to complementary sequences within transposon element transcripts. Once bound, the piRNA/PIWI complex can induce silencing of transposon elements through mechanisms such as RNA degradation or transcriptional repression.

2.5.2.4 Long non-coding RNAs

Long non-coding RNAs (lncRNAs) are RNA molecules characterized by their size, typically more than 200 nt. Most lncRNAs are generated by RNA polymerase I, II, or III (Pol I, II, or III) (Mattick et al., 2023). Based on the locations in the genome, lncRNAs are classified into several categories: antisense lncRNAs, intronic lncRNAs, divergent lncRNAs, intergenic lncRNAs, promoter-associated lncRNAs, transcription start site-associated lncRNAs, and enhancer RNAs (eRNAs) (Gao et al., 2020). In recent years, long non-coding RNAs (lncRNAs) have emerged as crucial regulators in numerous biological processes such as gene expression, chromatin modification, cell apoptosis, and cell differentiation. Moreover, lncRNAs have been implicated in viral infection processes and the host's antiviral response (Li et al., 2022). In human cells, host lncRNAs exhibited differential expression in influenza A virus (IAV)-infected cells. Notably, one up-regulated lncRNA, ENST00000412690 (named VIN), is involved in IAV replication and viral protein synthesis (Winterling et al., 2014). Another example is the polyadenylated nuclear RNA (PAN RNA) produced by Kaposi's sarcoma-associated herpesvirus (KSHV), which plays a crucial role in the virus's evasion of host immune responses by suppressing the expression of various immune regulators and modulating KSHV's life cycle (Borah et al., 2011; Rossetto et al., 2013; Rossetto and Pari, 2012). Therefore, this evidence indicates that lncRNAs also play a critical role in the antivirus immune response.

2.5.2.5 Circular RNAs

Circular RNAs (circRNAs) represent a category of ncRNAs first detected in plant viral RNA pathogens, termed viroid (Sanger et al., 1976). Subsequently, it has shown that eukaryotic cells express circRNAs as well (Chen et al., 2015). circRNAs are generated from back-splicing events during mRNA maturation, where the 3′,5′-phosphodiester bond is formed between the upstream splice acceptor and the downstream splice donor region of a linear pre-mRNA, resulting in a closed-loop structure, lacking both the 5′ and 3′ terminal (Figure 18). The joining area is called a back-splice junction, which is a unique characteristic of circRNAs. Based on their formation location, three distinct types of circRNAs exist: exonic circRNAs, exonic-intronic circRNAs, and intronic circRNAs (Chen et al., 2015; Kristensen et al., 2019; Qu et al., 2015; Wang et al., 2017).

CircRNAs, though still largely mysterious in their individual biological functions, have increasingly emerged as key players in numerous biological processes, including cell proliferation, apoptosis, and the development of various diseases (Shang et al., 2019). Typically, circRNAs are anticipated to have different functions than their host genes. Despite the challenges posed by their low abundance, the study of circRNAs remains difficult (Kristensen et al., 2018). While further investigation is required for the majority of circRNAs, they have already illuminated multiple mechanisms of action including miRNA sponging, protein sponging, modulator of transcription, protein scaffolding, protein translocating, and translation (Figure 18). These findings underscore the importance of continued research to unravel the functional intricacies of circRNAs.

In the context of viral infections, circRNAs have been studied extensively. In human cells, distinct classes of circRNAs displayed up-regulation or down-regulation in hepatitis C virus (HCV)-infected cells. Notably, one up-regulated circRNA, circPSD3, exhibited a substantial impact on viral RNA levels in both hepatitis C virus- and Dengue virus- infected cells (Chen et al., 2020). In *D. melanogaster*, circRNA profiling revealed an age-related accumulation pattern from 10 to 40 days, extending the observations of Westholm et al. This provides evidence that global circRNA levels continue to rise from 20 to 40 days of age (Westholm et al., 2014). The white-spotted bamboo shark (*Chiloscyllium plagiosum*) employs at least two circRNAs, circ-38-1717 and circ-6-1096, which act as miRNA sponges (Zhang et al., 2020). Furthermore, circRNAs have been implicated in immune regulation in fish species, including grass carp (*Ctenopharyngodon idella*) (He et al., 2017), tilapia (*Oreochromis niloticus*) (Fan et al., 2019), Miiuy croaker (*Miichthys miiuy*) (Zheng et al., 2021), crucian carp (*Carassis auratus gibelio*) (Hu et al., 2019), and blunt snout bream (*Megalobrama amblycephala*) (Wang et al., 2021). When fish encounter bacterial or viral infections, differentially expressed circRNAs (DECs) containing miRNA binding sites may interact with miRNAs, influencing the expression of immunomodulatory proteins and thereby enhancing the immune response.

A previous study revealed the presence of circRNAs in shrimp infected with WSSV. Among the 290 circRNAs identified, 160 were up-regulated, while

130 were down-regulated upon WSSV infection. 8 DECs originating from specific parental genes involved in shrimp immune response were selected to confirm the characteristics of circRNAs and were predicted to act as miRNA sponges. This property is one of the functional attributes of circRNAs. This discovery offers insights into the landscape of WSSV-responsive circRNAs and their potential functions (Limkul et al., 2023). However, research on the identification of YHV-responsive circRNAs in shrimp has not been reported.
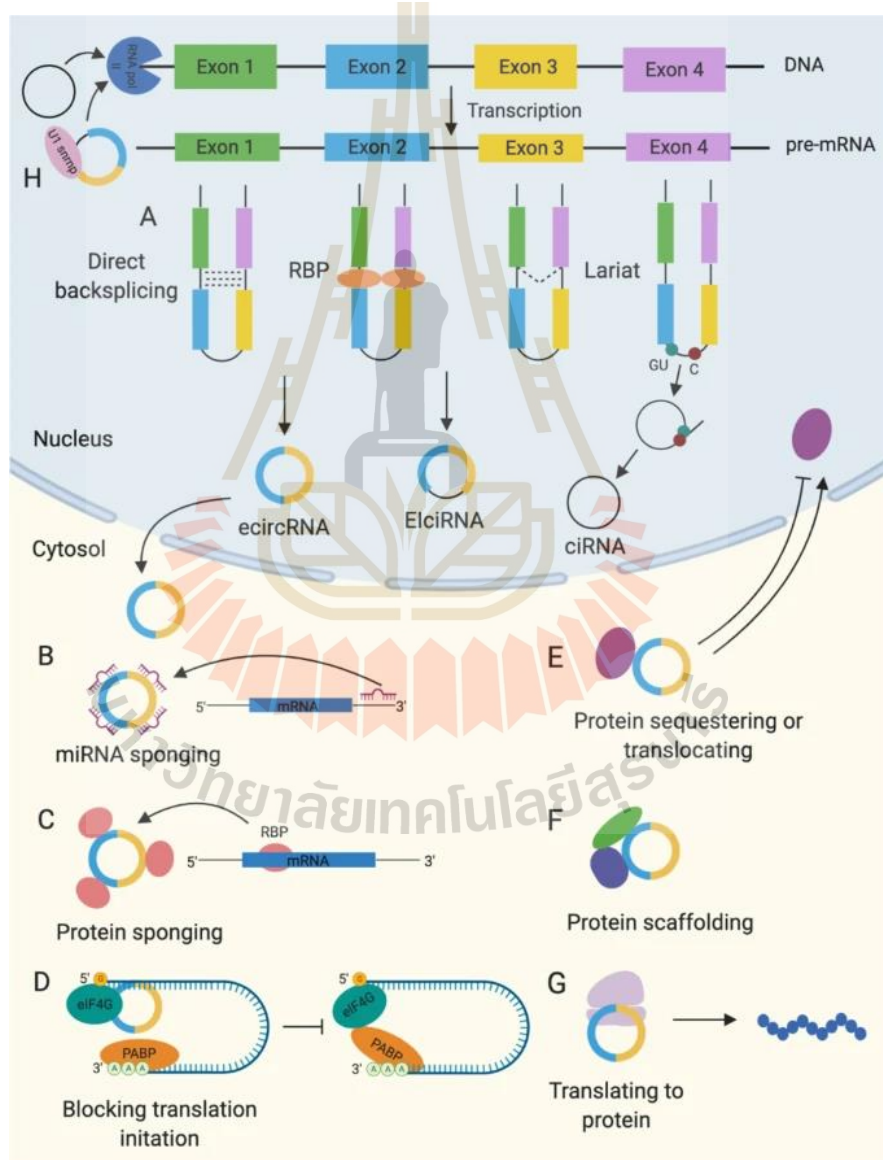
Figure 18. Biogenesis and functional mechanisms of circular RNAs (circRNAs) (He et al., 2021). (A) Back-splicing is initiated by the pairing of intronic complementary

sequences, RNA-binding proteins (RBPs), or lariat structures containing skipped exons or introns. (B) Sponging miRNA. (C) Sponging RNA-binding protein (RBP). (D) Interacting with eukaryotic translation initiation factor 4 G (eIF4G), poly(A)-binding protein (PABP), and associated mRNA. (E) Translocating proteins. (F) scaffolding protein complexes. (G) Translating to protein in a cap-independent manner. (H) Exon-intron circRNAs (EIcircRNAs) interact with U1 snRNP and RNA pol II to enhance transcription of parental genes. Intronic circRNAs (ciRNAs) similarly enhance transcription by interacting with the elongating RNA pol II complex.

CHAPTER III

MATERIALS AND METHODS

3.1 Ethics statement

According to the Ethical Principles and Guidelines for the Use of Animals in Scientific Research, as established by the National Research Council of Thailand, the experiments involving animals were conducted in compliance with Animal Use Protocol Number IACUC-66-17, which was approved by the Animal Care and Use Committee at Suranaree University of Technology. Additionally, the biosecurity concerns associated with this study underwent a thorough review and received approval from the Suranaree University of Technology under Approval Number IBC-66-09. These measures align with the risk levels associated with pathogens and animal toxins as outlined in "the Risk Group of Pathogen and Animal Toxin (2017)," as issued by the Department of Medical Sciences, Ministry of Public Health, and are consistent with the Pathogen and Animal Toxin Act (2015) and the Biosafety Guidelines for Modern Biotechnology, BIOTEC (2016).

3.2 Shrimp cultivation

Healthy Pacific white shrimp, *L. vannamei*, with an approximate body weight of 3–5 g, were raised in water with a salinity of 20 parts per thousand (ppt) and maintained at an ambient temperature of 30 ± 2°C with continuous aeration for 2 weeks before their use in experiments. During this period, the shrimp were provided with a commercial feed amounting to 5% of their body weight daily, and the commercial feed was used to feed the shrimp twice per day. Any uneaten food and feces were cleared from the rearing thanks before the next feeding.

3.3 Yellow head virus challenge

Pacific white shrimp (an approximate body weight of 3-5 g) were used in this experiment. A YHV stock solution was prepared following the method outlined by Jatuyosporn et al (Jatuyosporn et al., 2014). Subsequently, the YHV stock solution was diluted to a 10^6-fold concentration in normal saline (0.85% NaCl). Then, 50 µl from this diluted stock solution was injected intramuscularly into each shrimp at the second abdominal segment using a 1-mL insulin syringe with a 29G × ½" needle. It is worth noting that this injection resulted in 100% mortality of the shrimp within 5 days.

3.4 Total RNA extraction

Hemolymph samples were harvested from YHV-infected shrimp at 0-, 6-, 24-, and 48-hour post-infection (hpi) and mixed with an anticoagulant solution, specifically anticoagulant-modified Alsever's solution or MAS solution (containing 27 mM sodium citrate, 336 mM NaCl, 115 mM glucose, 9 mM EDTA, pH 7.4) (Perdomo-Morales et al., 2020). Then, hemocytes were isolated from the plasma by centrifugation at 800×g for 10 min at 4 °C. Subsequently, the hemocytes were used for total RNA extraction and purification using the Tissue Total RNA Purification Mini Kit from Favorgen following the manufacturer's instructions. In brief, hemocytes were homogenized in 350 µl of FARB buffer and 3.5 µl of β-mercaptoethanol and then vortexed vigorously for 1 min. Next, 40 µl of 3M Sodium acetate was added to precipitate nucleic acids (DNA and RNA). Subsequently, 500 µl of acid phenol and 100 µl of chloroform were mixed and vortexed for 30 sec. After that, the mixtures were centrifuged at 12,500×g for 15 min at 4 °C, and then the RNA-containing aqueous (upper) phase was transferred into the FARB mini-column. The supernatant was removed by centrifugation at 12,500×g for 1 min at 4 °C. Next, 75% ethanol 0.1% (v/v) diethylpyrocarbonate (DEPC)-treated water was added into the column and centrifuged at 12,500×g for 1 min at 4 °C, then discard the flow-through. Centrifugation at 12,500×g for 3-5 mins at 4 °C was applied to dry the column. Finally, 30 µl of DEPC-treated water was used for elution. The concentration of RNA

was determined using a Nanodrop 2000 Spectrophotometer (Thermo Scientific), and RNA integrity was assessed by visualizing it on agarose gel electrophoresis, which was stained with RedSafe Nucleic Acid Staining Solution (iNtRON). The eluted RNA was stored at -80°C until use.

3.5 CircRNA sequencing by Illumina

Library preparation was initiated using 2 μg of total RNA extracted from YHV-infected shrimp at 0 and 48 hpi, and the sequencing was performed by GENEWIZ in Suzhou, China. In summary, rRNA was eliminated from the total RNA using a single-stranded DNA probe. After adapter ligation, the adaptor-ligated DNA underwent size selection. Subsequently, libraries with distinct indexes were multiplexed and loaded onto an Illumina HiSeq instrument for sequencing in a 2×150 paired-end (PE) configuration, following the manufacturer's instructions.

The processed data underwent filtering using Cutadapt version 1.9.1 (Martin, 2011) to eliminate adapter sequences, N-containing bases at the 5′ or 3′ end, and reads shorter than 75 base pairs after trimming. The resulting sequences were then mapped to the reference genome using BWA version 0.7.5a-r405 (Li and Durbin, 2009). CircRNA prediction was executed using CIRI (Gao et al., 2015), and the expression of circRNAs was calculated based on back-splice junction reads, reported as spliced reads per billion mapping (Li et al., 2015).

Differentially expressed circRNAs (DECs) were selected for further analysis based on *P*-values < 0.05 and an absolute Log_2 (Fold change) ≥ 1. Gene Ontology (GO) and Kyoto Encyclopedia of Genes and Genomes (KEGG) enrichment analyses of the DECs were conducted, with GO terms or KEGG pathways having corrected *P*-values less than 0.05 considered significantly enriched in the set of DECs.

3.6 Quantitative real-time PCR (qRT-PCR) analysis

After the previously described procedure, total RNA was extracted from YHV-infected shrimp at 0, 6, 24, and 48 h post-infection (hpi). Subsequently, cDNA was synthesized using random hexamers and the RevertAid First Strand cDNA Synthesis

Kit from ThermoScientific, following the manufacturer's instructions. A total of 1 μg of total RNA was added to each 20 μl reaction system, and the resulting cDNA was employed as templates for PCR amplification.

For qRT-PCR, both convergent and divergent primers, as shown in the Figure 19 (Limkul et al., 2023), were designed, and their respective sequences are provided in Table 2. Quantitative real-time PCR (qRT-PCR) was conducted using these convergent and divergent primers with Luna Universal qPCR Master Mix from New England Biolabs on a CFX opus real-time PCR system manufactured by Bio-rad. Relative expression levels were calculated using the $2^{-\Delta\Delta ct}$ method (Livak and Schmittgen, 2001), with elongation factor-1 alpha (EF-1α) serving as the internal control. Each experiment was replicated three times.
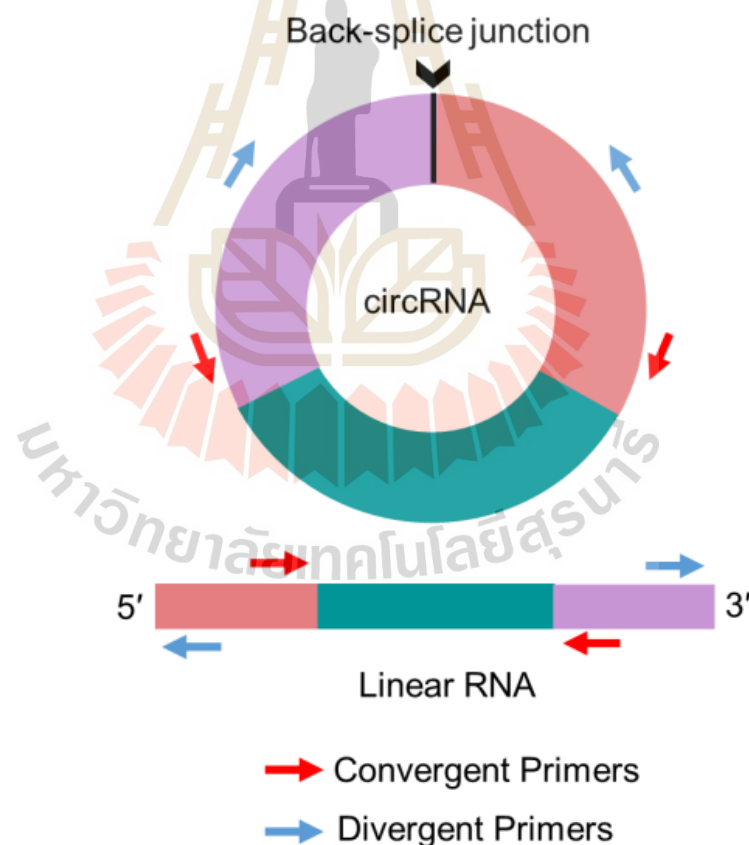
Figure 19. Diagram illustrating the designs of convergent and divergent primers (Limkul et al., 2023).

Table 2 List of synthetic oligonucleotide primers in qRT-PCR experiments.

Primer name	Sequences (5′-3′)	Annealing temperature (ºC)
Lv-Hemicentin2-li-F	GACACAACTGGTGGAGATG	58
Lv-Hemicentin2-li-R	CTGTCTGGCACTTGTACTC	58
Lv-Hemicentin2-circ-F	GCGCCATCATCTCCAAGAC	58
Lv-Hemicentin2-circ-R	ACTGAAGTGCTGTGCTCTC	58
Lv-Integrin-V-li-F	GCTGACCTTGCTGACCTATG	58
Lv-Integrin-V-li-R	CATCTTCGCAGCGAGAAGAG	58
Lv-Integrin-V-circ-F	CTCTTCTCGCTGCGAAGATG	58
Lv-Integrin-V-circ-R	GTCGACACGAGACACAACAG	58
Lv-Rab8b-li-F	GCATTCTGCAGGTATGTG	56
Lv-Rab8b-li-R	ATGGCAGTTGTTGCCAAG	56
Lv-Rab8b-circ-F	GAGCGGAATTCTGGTTGTG	58
Lv-Rab8b-circ-R	TGCTGTGTCCCACATCTG	58
Lv-Alpha-1-li-F	TACGACTTCCGGCTTCCTG	58
Lv-Alpha-1-li-R	CGACGTCACCCATACTTCG	58
Lv-Alpha-1-circ-F	GCATTCGTGTCCAGGGAAGAG	60
Lv-Alpha-1-circ-R	CTGCGGTGTGATCATGCTGAG	60
Lv-CDC42-li-F	ATCACGCAACAGCCACAG	58
Lv-CDC42-li-R	ACTGGCACAACCGTCAAC	58
Lv-CDC42-circ-F	AGCTGGTGCAACTGCAGAC	63
Lv-CDC42-circ-R	ACATCGCCGGCCATTGTAG	63
Lv-Kazal-li-F	CACTGACGGCAAGACCTAC	58
Lv-Kazal-li-R	CGTAGGTCTTGCCGTCAGTG	58
Lv-Kazal-circ-F	ACGACAAGACCTGCAATGG	58
Lv-Kazal-circ-R	CGTAGGTCTTGCCGTCAGTG	58
EF-1α-F	CGCAAGAGCGACAACTATGA	60
EF-1α-R	TGGCTTCAGGATACCAGTCT	60

3.7 Validation of circRNA by RNase R treatment, PCR, and Sanger sequencing

The total RNA from YHV-infected shrimp at 0 h post-infection (hpi) (20 μg) underwent treatment with RNase R (20U, Applied Biological Materials) and was incubated at 37 °C for 30 min. Subsequently, the RNase R-treated RNA was purified using the FavorPrep miRNA Isolation Kit from Favorgen to isolate large RNA fragments (>200 nt).

For cDNA synthesis, 100 ng of the RNase R-treated samples were used with random hexamers and the RevertAid First Strand cDNA Synthesis Kit from ThermoScientific. The resistance of circRNAs to RNase R digestion was quantitatively assessed by qRT-PCR using both convergent and divergent primers, and the results were calculated using a modified $2^{-\Delta\Delta ct}$ method (Panda and Gorospe, 2018).

Furthermore, these primers were applied to amplify amplicons from both genomic DNA (gDNA) and complementary DNA (cDNA). The resulting PCR products were visualized through agarose gel electrophoresis, with visualization aided by RedSafe Nucleic Acid Staining Solution from iNtRON. The circRNA-amplified PCR products were subsequently purified using the FavorPrep GEL/PCR Purification Kit from Favorgen and sent for Sanger sequencing at Celemics Inc. in South Korea.

3.8 Statistical analysis

The data were presented as the mean ± SD, derived from a minimum of three biological replications. Statistical differences in gene expression levels and circRNA validation were assessed using a paired-samples t-test. A significance threshold of P-value < 0.05 was employed to determine statistical significance.

CHAPTER IV

RESULTS

4.1 Shrimp RNA sample collection

From the experiment of total RNA extraction. The results shown that the extraction of total RNA at 0, 6, 24, and 48 hpi is of high quality, as evidenced by the integrity of the rRNA bands (Figure 20). Subsequently, the quality of the total RNA was validated, with the A_{260}/A_{280} ratio of the samples ranging from 1.8 to 2.0, as expected for acceptable RNA quality.
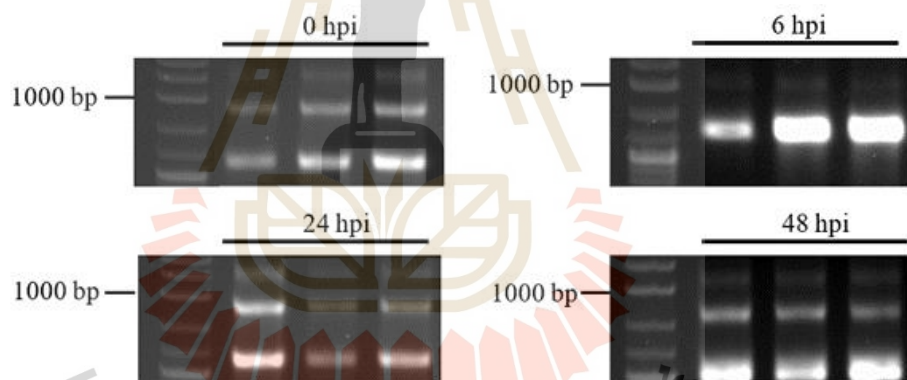
Figure 20. Visualization of total RNA in YHV-infected shrimp on 1.2% agarose gel electrophoresis, which was stained with RedSafe Nucleic Acid Staining Solution (iNtRON).

4.2 circRNA sequencing analysis, Gene Ontology (GO) and the Kyoto Encyclopedia of Genes and Genomes (KEGG) analysis

CircRNA sequencing (circRNA-Seq) was conducted on *L. vannamei* hemocytes at two distinct time points following YHV infection (0 hpi and 48 hpi), with each time point replicated three times. In total, six libraries were generated, comprising

approximately 181 million raw reads, with a Q20 quality score of ≥ 98% (Table 3). The clean reads underwent processing using Cutadapt version 1.9.1 and were subsequently aligned to the reference *L. vannamei* genome (GCA_003730335.1). This process identified a number of circRNAs, each with an abundance ranging from 20 to 500 reads (Table 4). Notably, over 75% of these circRNAs were exon circRNAs, around 20% were intergenic circRNAs, and close to 5% were intron circRNAs (as depicted in Figure 21).

A total of 358 differentially expressed circRNAs (DECs) were identified between the two groups of *L. vannamei* hemolymph post-YHV infection, comprising 177 up-regulated and 181 down-regulated DECs (Table 5; Figure 22). Further analysis involved categorizing and annotating these DECs using GO terms and KEGG pathways. GO term analysis provided insights into the functions associated with the genes, while KEGG pathways allowed for grouping these genes into specific biological pathways. GO categories were examined in relation to molecular functions, cellular components, and biological processes associated with the DECs (Figure   23A). Among these categories, the top 30 included 3 molecular functions, four cellular components, and 23 biological processes. Notably, the Wnt signaling pathway exhibited the highest level of enrichment among the GO terms. Pathway enrichment analysis of genes in the KEGG pathways revealed enrichment in taste transduction and endocytosis, with a Q-value of < 0.01 (Figure 23B).

Table 3 The circRNA-Seq data of the uninfected- (YHV-0h) and infected (YHV-48h) samples.

Sample	Raw reads	Clean reads	Bases	Q20 (%)	GC (%)
YHV-0h-1	173,612,428	173,385,578	25,673,517,691	98.34	59.98
YHV-0h-2	191,254,490	190,996,516	28,272,678,613	98.48	59.30
YHV-0h-3	176,700,102	176,422,030	26,119,617,488	98.32	60.74
YHV-48h-1	197,128,116	196,880,750	29,167,588,725	98.46	58.56
YHV-48h-2	177,311,678	177,062,858	26,250,428,110	98.32	59.67
YHV-48h-3	176,934,230	176,691,660	26,156,371,588	98.47	59.57

Table 4 Numbers of circRNAs in each library.

Sample	Numbers of circRNAs				
	10-20	20-50	50-100	100-500	>500
YHV-0h-1	400 (22.70%)	602 (34.17%)	285 (16.17%)	271 (15.38%)	59 (3.35%)
YHV-0h-2	301 (19.84%)	612 (40.34%)	241 (15.89%)	221 (14.57%)	46 (3.03%)
YHV-0h-3	410 (22.39%)	626 (34.19%)	316 (17.26%)	236 (12.89%)	47 (2.57%)
YHV-48h-1	413 (22.37%)	721 (39.06%)	275 (14.90%)	198 (10.73%)	46 (2.49%)
YHV-48h-2	424 (24.23%)	619 (35.37%)	226 (12.91%)	203 (11.60%)	43 (2.46%)
YHV-48h-3	376 (23.84%)	581 (36.84%)	244 (15.47%)	198 (12.56%)	40 (2.54%)

Table 5 Differentially expressed circRNAs.

circRNA_location	Gene ID	Log_2 (FoldChange)	P-value
NW_020871348.1:147107-178848	n/a	-10.04	4.23E-07
NW_020868607.1:154914-157224	n/a	-8.61	2.87E-05
NW_020869980.1:251041-252250	n/a	-8.53	3.46E-05
NW_020871094.1:388140-391147	n/a	-8.49	0.000037
NW_020870500.1:495713-497706	n/a	-8.44	4.41E-05
NW_020870911.1:1706753-1748423	n/a	-8.20	0.000103
NW_020870711.1:742350-765799	LOC113821134	-8.13	0.000123
NW_020870669.1:517200-615300	n/a	-8.02	0.000165
NW_020868415.1:1357071-1358196	LOC113808424	-8.00	0.000179
NW_020870945.1:265846-269286	LOC113823014	-7.33	0.001113
NW_020869083.1:141810-144850	LOC113806314	-7.08	0.001983
NW_020868581.1:726963-729120	LOC113824646	-7.02	0.002207
NW_020871204.1:256937-258476	n/a	-6.98	0.00246
NW_020871911.1:69767-71421	n/a	-6.84	0.003247
NW_020872637.1:1148083-1148775	LOC113830445	-6.83	0.003336
NW_020869777.1:175524-177089	LOC113812554	-6.81	0.00351
NW_020870059.1:359964-404080	n/a	-6.81	0.003527
NW_020871624.1:167169-192691	n/a	-6.74	0.006367

Table 5 Differentially expressed circRNAs (Continued).

circRNA_location	Gene ID	Log$_2$ (FoldChange)	*P*-value
NW_020872964.1:10581-11024	LOC113802844	-6.70	0.004847
NW_020870914.1:326740-330368	LOC113822783	-6.62	0.005651
NW_020871911.1:75358-81615	LOC113826981	-6.60	0.005807
NW_020868497.1:341265-341585	LOC113817908	-6.59	0.005951
NW_020869103.1:914233-1102795	n/a	-6.59	0.005299
NW_020871073.1:198922-200458	LOC113824171	-6.57	0.006197
NW_020872717.1:122201-152075	n/a	-6.54	0.006503
NW_020868810.1:1012234-1023575	n/a	-6.53	7.18E-06
NW_020868666.1:244132-246634	LOC113801149	-6.52	0.00674
NW_020869858.1:1060992-1063142	LOC113813276	-6.51	0.006871
NW_020870805.1:122392-124061	LOC113821981	-6.50	0.007045
NW_020868433.1:179592-183075	LOC113810466	-6.49	0.006422
NW_020869135.1:184437-186257	LOC113806936	-6.49	0.007182
NW_020871395.1:31177-33859	n/a	-6.48	0.008351
NW_020869195.1:527185-527725	LOC113807522	-6.48	0.008075
NW_020871514.1:449083-450974	LOC113825876	-6.48	0.008315
NW_020870771.1:319686-390648	LOC113821545	-6.48	0.007296
NW_020869023.1:192699-193527	LOC113805639	-6.47	0.006534
NW_020870440.1:150491-155612	n/a	-6.46	0.007572
NW_020869527.1:874891-890676	LOC113810417	-6.43	0.007874
NW_020870958.1:247595-254271	LOC113823118	-6.42	0.009891
NW_020868938.1:572704-628854	n/a	-6.40	0.009207
NW_020872868.1:39149-43063	LOC113802088	-6.40	0.009207
NW_020872854.1:14998-22612	LOC113801921	-6.39	0.008384
NW_020871628.1:158928-165558	LOC113826223	-6.38	0.008602
NW_020872839.1:113461-196026	LOC113801627	-6.32	0.010435
NW_020872860.1:402431-410302	LOC113801960	-6.30	0.010881
NW_020871094.1:385017-385785	n/a	-6.28	0.010122
NW_020871470.1:131024-137865	n/a	-6.28	0.010152
NW_020868954.1:245830-247329	LOC113805156	-6.27	0.010249
NW_020871911.1:69767-72041	n/a	-6.20	0.011498
NW_020872335.1:203787-205156	LOC113828265	-6.17	0.01198
NW_020868373.1:73259-79379	n/a	-6.17	0.012094
NW_020872479.1:639272-639853	n/a	-6.14	0.012546
NW_020871018.1:619574-623702	n/a	-6.14	0.01262
NW_020870179.1:147150-148359	n/a	-6.14	0.012658
NW_020870559.1:317438-317907	LOC113819749	-6.13	0.011547
NW_020870328.1:273437-275396	LOC113817832	-6.09	0.013719
NW_020870929.1:46850-108492	n/a	-6.06	0.014148

Table 5 Differentially expressed circRNAs (Continued).

circRNA_location	Gene ID	Log$_2$ (FoldChange)	P-value
NW_020870651.1:135605-159069	n/a	-6.01	0.015346
NW_020868539.1:298599-310285	LOC113820941	-6.00	0.014176
NW_020868615.1:428611-428768	n/a	-6.00	0.015537
NW_020870789.1:404680-404966	LOC113821714	-5.99	0.014298
NW_020870958.1:336550-336726	n/a	-5.99	0.015756
NW_020868364.1:170948-174203	LOC113804796	-5.99	0.015816
NW_020869317.1:199493-204509	LOC113808603	-5.98	0.016112
NW_020868551.1:58011-64224	LOC113821808	-5.95	0.016708
NW_020872468.1:37609-46520	LOC113829055	-5.95	0.016705
NW_020872203.1:167133-168407	LOC113827887	-5.93	0.017284
NW_020869429.1:1440707-1443113	n/a	-5.93	0.019259
NW_020870711.1:733897-765799	LOC113821134	-5.89	0.01663
NW_020871047.1:118851-122297	n/a	-5.86	0.019018
NW_020870273.1:169101-175335	LOC113817270	-5.85	0.019199
NW_020872715.1:20898-23143	LOC113800357	-5.85	0.019171
NW_020870025.1:123025-124876	LOC113814790	-5.84	0.019475
NW_020868760.1:1013711-1016491	LOC113803453	-5.84	0.019475
NW_020869252.1:140297-152503	LOC113808022	-5.82	0.019995
NW_020869093.1:349500-350685	LOC113806385	-5.81	0.020385
NW_020869102.1:322213-334283	LOC113806452	-5.77	0.021487
NW_020872953.1:247810-248067	n/a	-5.77	0.021663
NW_020870444.1:180544-187175	n/a	-5.77	0.021642
NW_020868337.1:916886-924408	n/a	-5.75	0.022163
NW_020870699.1:307894-309491	n/a	-5.74	0.022515
NW_020870529.1:318627-375389	n/a	-5.74	0.022515
NW_020871663.1:156166-156831	n/a	-5.72	0.023102
NW_020871010.1:571762-573028	LOC113823699	-5.71	0.023419
NW_020868810.1:1014405-1023575	n/a	-5.70	0.023707
NW_020869526.1:716473-720826	n/a	-5.70	0.023707
NW_020869188.1:102713-199605	LOC113807409	-5.69	0.023828
NW_020870955.1:308964-325866	n/a	-5.69	0.023844
NW_020872143.1:470172-472170	LOC113827612	-5.67	0.024566
NW_020870781.1:542645-543504	LOC113821621	-5.67	0.024566
NW_020872129.1:80741-82850	LOC113827561	-5.66	0.025016
NW_020870736.1:3268-155932	n/a	-5.64	0.025518
NW_020870479.1:391465-400073	n/a	-5.64	0.025518
NW_020869502.1:134491-135170	n/a	-5.64	0.025705
NW_020869284.1:251235-274157	n/a	-5.62	0.026061
NW_020872629.1:118020-129028	n/a	-5.62	0.026061

Table 5 Differentially expressed circRNAs (Continued).

circRNA_location	Gene ID	Log$_2$ (FoldChange)	*P*-value
NW_020869083.1:281805-283702	LOC113806319	-5.60	0.026826
NW_020872599.1:133675-155377	LOC113830023	-5.60	0.026826
NW_020869507.1:102766-105953	LOC113810245	-5.60	0.027007
NW_020872720.1:37587-193726	n/a	-5.59	0.027179
NW_020869429.1:1434432-1440911	n/a	-5.58	0.02766
NW_020870133.1:289927-291831	LOC113816016	-5.57	0.027729
NW_020868947.1:279906-282986	LOC113805082	-5.57	0.027729
NW_020872686.1:485985-487552	LOC113800045	-5.55	0.028556
NW_020870339.1:310820-337001	n/a	-5.50	0.030647
NW_020871030.1:154722-159658	n/a	-5.49	0.030821
NW_020870628.1:785565-787828	n/a	-5.49	0.030821
NW_020870958.1:247595-263272	LOC113823118	-5.47	0.031502
NW_020869299.1:204450-247143	n/a	-5.45	0.032168
NW_020869666.1:730247-746536	n/a	-5.45	0.029777
NW_020871712.1:158025-181618	LOC113826499	-5.45	0.032442
NW_020869060.1:826438-832887	LOC113806088	-5.44	0.032735
NW_020871231.1:45517-49234	LOC113824963	-5.42	0.033499
NW_020869294.1:79658-80286	LOC113808316	-5.39	0.03487
NW_020868793.1:125237-127079	n/a	-5.37	0.035451
NW_020869079.1:119909-120931	n/a	-5.37	0.035451
NW_020871072.1:35750-36806	n/a	-5.37	0.035451
NW_020871018.1:694564-695393	n/a	-5.36	0.036305
NW_020869299.1:160135-161955	n/a	-5.35	0.036358
NW_020870081.1:44686-45045	n/a	-5.35	0.036403
NW_020869206.1:646259-647569	LOC113807613	-5.34	0.036919
NW_020870376.1:254693-256239	LOC113818199	-5.33	0.037275
NW_020872866.1:219028-219513	LOC113802077	-5.32	0.037792
NW_020871382.1:192315-194659	LOC113825474	-5.31	0.038284
NW_020872229.1:220427-224523	LOC113827969	-5.31	0.038284
NW_020869844.1:608452-611044	LOC113813161	-5.31	0.038284
NW_020868637.1:371614-372660	LOC113829010	-5.30	0.038612
NW_020870425.1:285231-306076	LOC113818694	-5.30	0.038612
NW_020869010.1:128540-140721	n/a	-5.30	0.038612
NW_020869460.1:137801-155451	n/a	-5.30	0.038612
NW_020869103.1:24651-27036	n/a	-5.23	0.041722
NW_020869433.1:478139-479556	n/a	-5.22	0.04215
NW_020868733.1:120027-145317	n/a	-5.22	0.042403
NW_020870218.1:75083-79837	n/a	-5.22	0.042403
NW_020872191.1:139235-142674	n/a	-5.21	0.042852

Table 5 Differentially expressed circRNAs (Continued).

circRNA_location	Gene ID	Log$_2$ (FoldChange)	P-value
NW_020869818.1:24124-25642	n/a	-5.21	0.04311
NW_020869450.1:112945-147057	LOC113809725	-5.20	0.043112
NW_020872849.1:12377-18613	LOC113801846	-5.20	0.043112
NW_020871989.1:29666-36631	LOC113827240	-5.20	0.043299
NW_020872432.1:965178-990830	LOC113828758	-5.19	0.043652
NW_020869133.1:2544524-2546477	LOC113806872	-5.18	0.044183
NW_020869368.1:209284-226633	n/a	-5.18	0.044293
NW_020870097.1:1001914-1003937	LOC113815644	-5.18	0.044293
NW_020872855.1:77114-79752	n/a	-5.18	0.044293
NW_020869929.1:357181-367718	LOC113813926	-5.18	0.044293
NW_020869303.1:44112-45282	LOC113808477	-5.18	0.044293
NW_020870606.1:375798-388862	LOC113820163	-5.18	0.044476
NW_020870152.1:24806-27234	n/a	-5.15	0.045706
NW_020872468.1:101828-129822	n/a	-5.10	0.048463
NW_020870958.1:244321-246154	n/a	-5.10	0.048463
NW_020871989.1:35817-36631	n/a	-5.10	0.048463
NW_020870583.1:174193-181551	n/a	-5.09	0.049198
NW_020869731.1:16231-18514	n/a	-5.08	0.049331
NW_020872174.1:50650-50830	n/a	-5.08	0.049501
NW_020872590.1:817811-829514	n/a	-5.08	0.049527
NW_020871073.1:174217-185027	n/a	-4.09	0.003523
NW_020871911.1:64671-68980	LOC113826983	-4.00	0.011043
NW_020870001.1:421742-422491	LOC113814567	-3.56	0.018362
NW_020870878.1:169749-179877	LOC113822413	-2.88	0.026239
NW_020872788.1:913410-922899	LOC113800928	-2.63	0.000289
NW_020871975.1:85797-88133	LOC113827221	-2.37	0.049836
NW_020868412.1:178170-180078	n/a	-2.21	0.00002
NW_020869460.1:153451-155451	n/a	-2.11	7.42E-05
NW_020870421.1:50675-55560	LOC113818675	-2.03	0.00179
NW_020868337.1:922783-924408	LOC113802877	-1.71	0.02144
NW_020872556.1:137188-137771	LOC113829622	-1.71	0.005088
NW_020869929.1:357178-365104	LOC113813926	-1.56	0.002064
NW_020868973.1:908197-909215	n/a	-1.53	0.021643
NW_020872499.1:348327-351525	LOC113829200	-1.50	0.002196
NW_020870745.1:136124-138730	LOC113821353	-1.50	0.013355
NW_020868919.1:485865-488493	LOC113804840	-1.44	0.007083
NW_020869445.1:324929-329721	LOC113809688	-1.40	0.001325
NW_020872849.1:12377-13379	LOC113801846	-1.23	0.000834
NW_020868607.1:13249-50650	n/a	-1.22	0.020869

Table 5 Differentially expressed circRNAs (Continued).

circRNA_location	Gene ID	Log$_2$ (FoldChange)	*P*-value
NW_020870129.1:28048-41459	n/a	-1.17	0.015061
NW_020869939.1:164987-165557	LOC113814032	-1.17	0.030522
NW_020869844.1:1093-6788	LOC113813155	-1.15	0.046234
NW_020869839.1:127049-127718	LOC113813105	-1.11	0.003075
NW_020872556.1:42332-50158	LOC113829629	-1.07	0.04177
NW_020869450.1:126370-137191	LOC113809725	-1.06	0.022943
NW_020869704.1:677598-695917	LOC113811941	-1.02	0.008574
NW_020869419.1:1377285-1387049	LOC113809347	1.05	0.003938
NW_020872588.1:367082-367633	LOC113829916	1.08	0.045086
NW_020871435.1:177688-216066	n/a	1.11	0.047351
NW_020868353.1:274152-328283	n/a	1.17	8.96E-05
NW_020868700.1:496104-500476	n/a	1.22	0.001106
NW_020869193.1:95462-96225	LOC113807486	1.38	0.002402
NW_020869315.1:194930-195253	LOC113808587	1.48	0.043322
NW_020868495.1:925-36562	n/a	1.49	0.000315
NW_020872772.1:715077-719008	n/a	1.52	0.036887
NW_020871047.1:54242-55418	LOC113823946	1.60	0.004766
NW_020868810.1:1012234-1014554	LOC113803873	1.68	0.023304
NW_020871047.1:125721-129343	LOC113823934	1.84	0.002596
NW_020868547.1:429744-430605	LOC113821338	1.86	0.002728
NW_020870748.1:719976-723263	n/a	1.92	1.64E-07
NW_020870644.1:319835-329789	LOC113820463	2.26	0.000214
NW_020871991.1:144523-144974	n/a	2.68	8.34E-06
NW_020868353.1:274053-328283	n/a	2.81	1.54E-09
NW_020872184.1:101366-102694	LOC113827815	2.94	0.025897
NW_020869408.1:171079-171621	LOC113809241	3.28	0.039149
NW_020869295.1:654355-660002	LOC113808319	3.34	0.031951
NW_020871014.1:40857-42021	LOC113823758	5.08	0.049715
NW_020869419.1:1386947-1391706	LOC113809347	5.08	0.049784
NW_020868297.1:84517-87721	LOC113811649	5.13	0.047454
NW_020870418.1:310284-320568	n/a	5.13	0.047332
NW_020869419.1:1349997-1359997	LOC113809368	5.13	0.047332
NW_020868661.1:198286-199064	LOC113800566	5.14	0.046731
NW_020868721.1:462563-465614	LOC113803191	5.16	0.045697
NW_020871073.1:192111-193004	LOC113824171	5.16	0.045697
NW_020868792.1:1003450-1010618	LOC113803705	5.16	0.045697
NW_020872851.1:271029-282864	LOC113801904	5.17	0.045368
NW_020872659.1:312709-314016	LOC113830587	5.17	0.045368
NW_020870472.1:1193806-1200448	LOC113818995	5.17	0.045246

Table 5 Differentially expressed circRNAs (Continued).

circRNA_location	Gene ID	Log$_2$ (FoldChange)	P-value
NW_020870786.1:154101-156469	LOC113821664	5.18	0.04477
NW_020868952.1:589777-590159	LOC113805141	5.19	0.044047
NW_020868696.1:698904-742367	n/a	5.19	0.044047
NW_020872432.1:783673-786906	LOC113828743	5.19	0.044047
NW_020872452.1:197918-203445	LOC113828951	5.20	0.043987
NW_020870937.1:314375-315463	LOC113822944	5.20	0.043987
NW_020869335.1:823759-824973	LOC113808727	5.20	0.043987
NW_020871288.1:49982-54612	LOC113825142	5.25	0.041523
NW_020872420.1:197560-198039	LOC113828615	5.26	0.04085
NW_020872437.1:537679-555018	n/a	5.26	0.04085
NW_020872812.1:193595-194414	LOC113801201	5.26	0.04085
NW_020872437.1:469617-549122	n/a	5.26	0.04085
NW_020871072.1:16902-38068	LOC113824151	5.26	0.0407
NW_020870042.1:26653-84165	n/a	5.26	0.0407
NW_020870616.1:236897-239349	LOC113820235	5.30	0.039255
NW_020872715.1:137843-139411	n/a	5.30	0.038979
NW_020871204.1:278767-279376	LOC113824904	5.30	0.038979
NW_020869397.1:172506-173292	LOC113809176	5.30	0.03902
NW_020870614.1:382196-398359	LOC113820215	5.30	0.03902
NW_020870183.1:606974-651881	LOC113816457	5.32	0.038014
NW_020870673.1:71762-74965	LOC113820732	5.32	0.038014
NW_020872407.1:104858-105872	LOC113828531	5.34	0.037469
NW_020872537.1:314045-315679	LOC113829511	5.36	0.036468
NW_020869558.1:488191-488855	LOC113810815	5.36	0.036468
NW_020868721.1:24487-25090	LOC113803190	5.36	0.036468
NW_020870941.1:218823-219517	LOC113822989	5.38	0.035782
NW_020871581.1:355392-356437	n/a	5.39	0.035133
NW_020872961.1:122534-123011	LOC113802810	5.39	0.035133
NW_020868868.1:193710-202155	LOC113804377	5.42	0.03408
NW_020872437.1:469617-533213	n/a	5.46	0.032633
NW_020872717.1:226557-232031	LOC113800377	5.46	0.032633
NW_020871588.1:1113598-1181810	n/a	5.46	0.032579
NW_020868780.1:216659-227273	LOC113803580	5.46	0.032525
NW_020870042.1:26653-29596	LOC113814996	5.47	0.032186
NW_020872468.1:123333-129822	n/a	5.47	0.032186
NW_020869288.1:410790-411735	LOC113808290	5.47	0.032186
NW_020871158.1:239771-243696	LOC113824784	5.47	0.032007
NW_020869308.1:3264-5758	LOC113808526	5.49	0.031113
NW_020869344.1:41093-43882	LOC113808760	5.50	0.030804

Table 5 Differentially expressed circRNAs (Continued).

circRNA_location	Gene ID	Log$_2$ (FoldChange)	*P*-value
NW_020869967.1:792204-805729	n/a	5.50	0.030804
NW_020868549.1:376896-381292	n/a	5.54	0.029236
NW_020870249.1:71615-75889	LOC113817120	5.54	0.029217
NW_020870914.1:326740-330912	LOC113822783	5.55	0.029048
NW_020869205.1:96879-97471	LOC113807588	5.57	0.028388
NW_020870683.1:572814-575260	LOC113820821	5.57	0.028388
NW_020872342.1:203913-209253	LOC113828298	5.59	0.027552
NW_020868951.1:97810-128221	LOC113805128	5.62	0.026552
NW_020870042.1:34711-39123	LOC113814996	5.62	0.026552
NW_020871014.1:522788-561867	n/a	5.64	0.025774
NW_020868731.1:499-29460	n/a	5.64	0.0258
NW_020869227.1:562996-563516	LOC113807858	5.64	0.0258
NW_020870651.1:136860-137063	LOC113820520	5.65	0.025424
NW_020869873.1:130438-131894	LOC113813435	5.66	0.025247
NW_020868318.1:178124-241288	n/a	5.67	0.025051
NW_020870641.1:80723-80976	n/a	5.67	0.025051
NW_020869196.1:168669-170123	LOC113807532	5.67	0.025035
NW_020868353.1:274146-328283	n/a	5.69	0.024402
NW_020870120.1:210832-220109	LOC113815849	5.71	0.023565
NW_020870994.1:303392-305023	LOC113823448	5.75	0.022534
NW_020868474.1:310162-311984	LOC113814953	5.75	0.022534
NW_020870683.1:545984-546504	LOC113820821	5.77	0.021765
NW_020869852.1:639517-641410	LOC113813233	5.79	0.021245
NW_020869809.1:41849-42692	LOC113812833	5.81	0.020668
NW_020871047.1:46978-61741	LOC113823946	5.81	0.020609
NW_020870070.1:166244-167617	LOC113815263	5.81	0.020571
NW_020871204.1:517098-518233	LOC113824903	5.82	0.02039
NW_020872812.1:135962-169910	n/a	5.85	0.019824
NW_020868439.1:71348-85930	LOC113810935	5.85	0.017956
NW_020870416.1:211044-211926	LOC113818571	5.86	0.019311
NW_020869644.1:120060-123215	LOC113811476	5.87	0.019136
NW_020872734.1:1178976-1183818	n/a	5.87	0.019136
NW_020871744.1:310322-328382	LOC113826593	5.89	0.01858
NW_020869537.1:769894-788294	LOC113810587	5.90	0.018292
NW_020871411.1:39753-41097	LOC113825550	5.92	0.017861
NW_020869103.1:55857-66188	LOC113806460	5.92	0.017755
NW_020870600.1:187987-188274	LOC113820059	5.93	0.017599
NW_020868830.1:1042925-1054152	LOC113803987	5.93	0.017599
NW_020872849.1:358038-358186	LOC113801848	5.95	0.017048

Table 5 Differentially expressed circRNAs (Continued).

circRNA_location	Gene ID	Log$_2$ (FoldChange)	P-value
NW_020869021.1:667230-705961	n/a	5.96	0.017013
NW_020872950.1:49122-50150	LOC113802704	5.97	0.01667
NW_020868857.1:713933-715348	LOC113804207	5.97	0.016697
NW_020869914.1:191248-240308	n/a	5.97	0.016697
NW_020870396.1:306069-308828	LOC113818429	5.97	0.014998
NW_020869981.1:475301-476653	LOC113814385	5.97	0.014998
NW_020868548.1:131983-151462	LOC113821521	6.04	0.014935
NW_020868966.1:1241865-1242951	LOC113805254	6.08	0.014215
NW_020872734.1:1189792-1196100	n/a	6.07	0.014169
NW_020868353.1:273848-328283	n/a	6.07	0.012883
NW_020872588.1:352580-367633	LOC113829916	6.08	0.014179
NW_020869575.1:512765-515518	LOC113810932	6.09	0.012553
NW_020870146.1:2812-10559	LOC113816158	6.11	0.013439
NW_020869527.1:1543858-1560481	LOC113810427	6.14	0.012822
NW_020869306.1:466025-469615	n/a	6.17	0.012351
NW_020872129.1:73173-74116	LOC113827561	6.18	0.012004
NW_020872555.1:36247-36796	LOC113829607	6.23	0.01121
NW_020872432.1:1008729-1014642	LOC113828758	6.23	0.010079
NW_020870340.1:207200-207678	LOC113817901	6.26	0.010719
NW_020868803.1:393004-393591	LOC113803807	6.28	0.009245
NW_020872437.1:469617-541214	n/a	6.31	0.009984
NW_020868792.1:52691-55548	LOC113803688	6.33	0.008626
NW_020868696.1:22126-22682	n/a	6.34	0.009439
NW_020872703.1:176598-179405	LOC113800265	6.34	0.008417
NW_020869378.1:125906-167458	n/a	6.37	0.013186
NW_020870448.1:54611-55466	LOC113818846	6.40	0.008515
NW_020872327.1:324937-325591	LOC113828234	6.43	0.008116
NW_020869495.1:540742-541499	LOC113810117	6.43	0.008976
NW_020870270.1:531011-532242	LOC113817231	6.43	0.007264
NW_020872950.1:34628-59514	n/a	6.46	0.006875
NW_020872521.1:30087-34254	LOC113829394	6.47	0.006783
NW_020870688.1:526520-527443	LOC113820858	6.48	0.006699
NW_020870347.1:159967-162832	LOC113817988	6.54	0.006771
NW_020871855.1:212294-221578	n/a	6.55	0.006598
NW_020868629.1:5460-44852	n/a	6.58	0.006275
NW_020872521.1:32816-34254	LOC113829394	6.59	0.005517
NW_020870644.1:319835-325894	LOC113820463	6.59	0.006129
NW_020870461.1:155673-158871	LOC113818908	6.63	0.005118
NW_020870140.1:81823-83295	LOC113816135	6.64	0.004981

Table 5 Differentially expressed circRNAs (Continued).

circRNA_location	Gene ID	Log$_2$ (FoldChange)	P-value
NW_020869248.1:52146-243662	n/a	6.64	0.005603
NW_020868353.1:274152-327867	n/a	6.66	0.006469
NW_020872804.1:480471-481546	LOC113801036	6.67	0.004697
NW_020869005.1:539721-551521	n/a	6.70	0.005018
NW_020869429.1:1389419-1390510	LOC113809511	6.71	0.004359
NW_020870686.1:24062-41135	LOC113820835	6.74	0.004669
NW_020869213.1:20455-22928	LOC113807657	6.82	0.003549
NW_020870884.1:295630-296723	LOC113822494	6.88	0.003569
NW_020870878.1:169749-170010	LOC113822413	6.91	0.003399
NW_020869894.1:550636-640763	n/a	6.95	0.005014
NW_020868976.1:53300-54654	n/a	6.96	0.003061
NW_020870688.1:147087-151310	LOC113820837	6.96	0.003038
NW_020868495.1:205286-209598	LOC113817796	7.03	0.002266
NW_020870218.1:470141-471862	LOC113816891	7.10	0.00199
NW_020868629.1:5460-44891	n/a	7.11	0.001932
NW_020868756.1:133260-133988	LOC113803426	7.16	0.001736
NW_020869419.1:1377285-1387100	LOC113809347	7.24	0.001433
NW_020869419.1:1402739-1409356	LOC113809347	7.27	0.001362
NW_020868570.1:190248-190540	LOC113823309	7.34	0.001138
NW_020870690.1:300956-347453	n/a	7.48	0.000837
NW_020869318.1:286181-294242	LOC113808615	7.50	0.00077
NW_020869234.1:13955-15262	LOC113807911	7.66	0.000508
NW_020868493.1:745159-791483	n/a	7.80	0.000344
NW_020870600.1:163270-163936	LOC113820059	7.94	0.000249
NW_020869460.1:139323-141945	n/a	8.40	5.66E-05
NW_020868353.1:274152-328299	n/a	8.47	4.28E-05
NW_020870337.1:148797-152586	n/a	8.71	1.87E-05
NW_020871047.1:69451-75686	n/a	9.95	1.47E-07
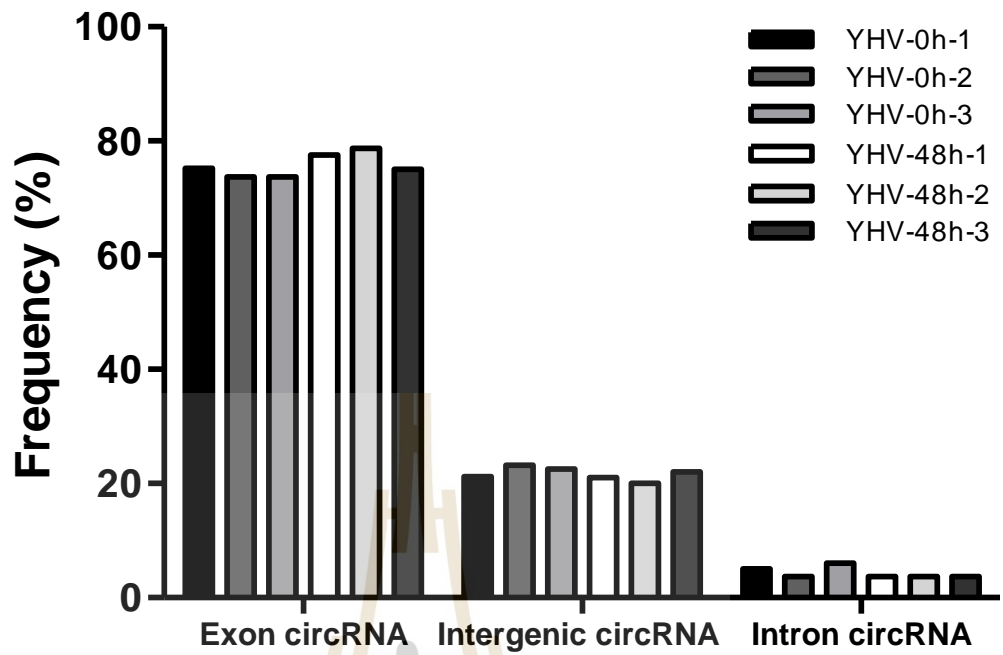
Figure 21. The frequency of circRNA types in the circRNA library of YHV-0h and YHV-48h. each library was conducted in three replications.
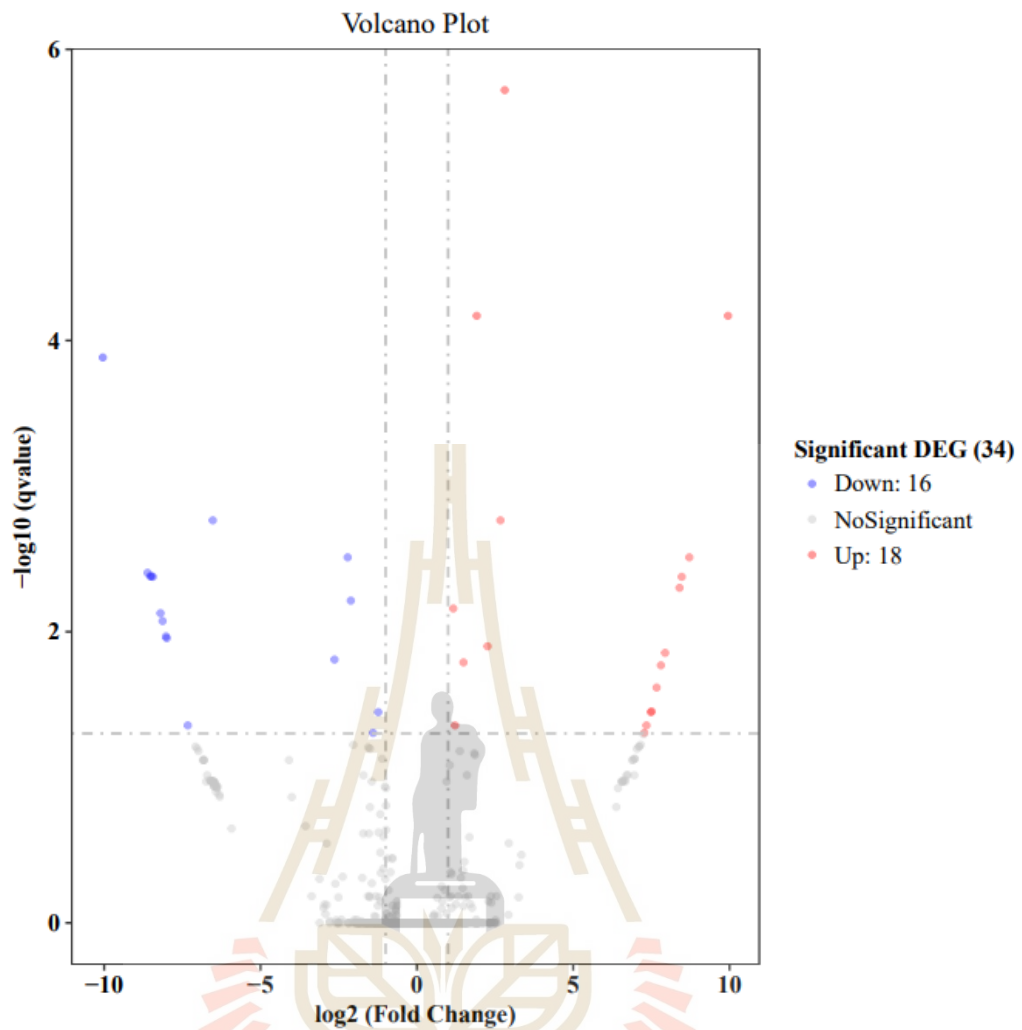
Figure 22. Volcano plots illustrating the $\log_2$(Fold Change) for YHV 48 hpi condition versus 0 hpi. The circRNAs that passed the significance threshold adjusted *P*-value < 0.05 and the expression cut-off $\log_2$(Fold Change) ≥ 1 are displayed in colored red, $\log_2$(Fold Change) ≤ – 1 are colored blue, and outside this range are colored black.
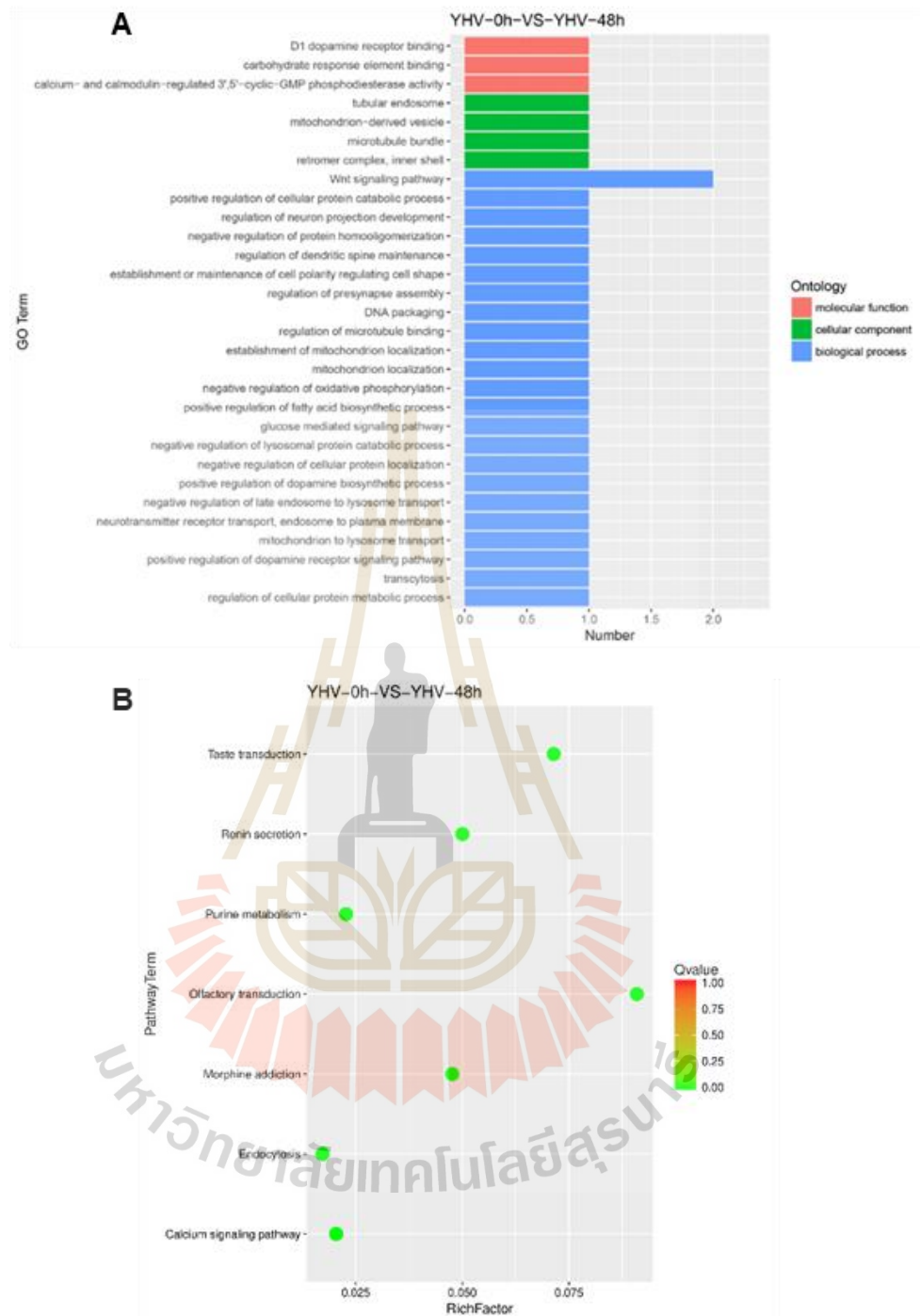
Figure 23. Gene Ontology (GO) and the Kyoto Encyclopedia of Genes and Genomes
(KEGG) analysis. (A) The GO terms for the top 30 enriched genes. In this
analysis, the differentially expressed circRNA were analyzed into
functional groups. The column corresponds to molecular function
(orange), cellular components (green) and biological process (blue),

respectively. Gene Ontology was used for this classification. (B) The genes with different expression levels were grouped into specific pathways using pathway enrichment analysis. In this presentation, circles with low q-values are depicted in green, while those with high q-values are shown in red. KEGG, which stands for Kyoto Encyclopedia of Genes and Genomes, was utilized for this purpose.

4.3 The expression level of immune-responsive circRNA in YHV-infected shrimp

To investigate the expression of selected *L. vannamei* circRNAs and their parental genes in response to YHV infection, the expression levels of 8 DECs were assessed. These DECs included circ_alpha-1-inhibitor 3, circ_cdc42 small effector protein 2, circ_hemicentin-2, circ_integrin alpha V, circ_kazal-type proteinase inhibitor, circ_phenoloxidase 3, circ_related protein rab-8B, and circ_protein toll-like, were conducted using quantitative reverse transcription polymerase chain reaction (qRT-PCR).

The expression levels of circ_phenoloxidase 3 and circ_hemicentin-2 exhibited up-regulation at 6, 24, and 48 hpi, with fold changes ranging from 1.53 to 4.26, 1.08 to 4.90, and 3.12 to 5.15, respectively. For circ_cdc42 small effector protein 2 and circ_kazal-type proteinase inhibitor 3, up-regulation was observed at 24 and 48 hpi, with fold changes ranging from 3.45 to 8.39 and 1.67 to 1.88, respectively. The expression levels of circ_alpha-1-inhibitor 3 and circ_ras-related protein Rab8B showed up-regulation at 48 hpi, with fold changes of 2.10 and 1.55, respectively. Notably, significant down-regulation was observed in the expression levels of circ_integrin alpha-V and circ_protein toll-like at 48 hpi, with fold changes of 0.34 and 0.41, respectively (Figure 24A).

The parental genes displayed a similar expression pattern. Notably, significant up-regulation of linear RNAs (li-RNAs) was observed at 6, 24, and 48 hpi. Specifically, li_kazal-type proteinase inhibitor and li_alpha-1-inhibitor 3 exhibited up-regulation by 1.35 to 1.51, 1.40 to 1.56, and 1.59 to 2.12-fold, respectively, during these time points. Conversely, li_cdc42 small effector protein 2 showed significant down-regulation at 6 and 24 hpi, with fold changes of 0.20 and 0.41, respectively. At 48 hpi,

the expression levels of li_hemicentin-2 and li_ras-related protein Rab8B were up-regulated by 2.50 and 2.91-fold, respectively, while li_protein toll-like displayed up-regulation at 6 and 24 hpi, with fold changes of 2.07 and 2.96, respectively. Furthermore, significant down-regulation of li-RNAs was observed at 24 and 48 hpi, particularly in li_integrin alpha-V, with fold changes of 0.52 and 0.45, respectively. Additionally, li_phenoloxidase 3 was down-regulated at 6 hpi, with a fold change of 0.74 (Figure 24B). The qRT-PCR results were consistent with the findings from circRNA-Seq analysis, confirming the correlation in expression patterns.
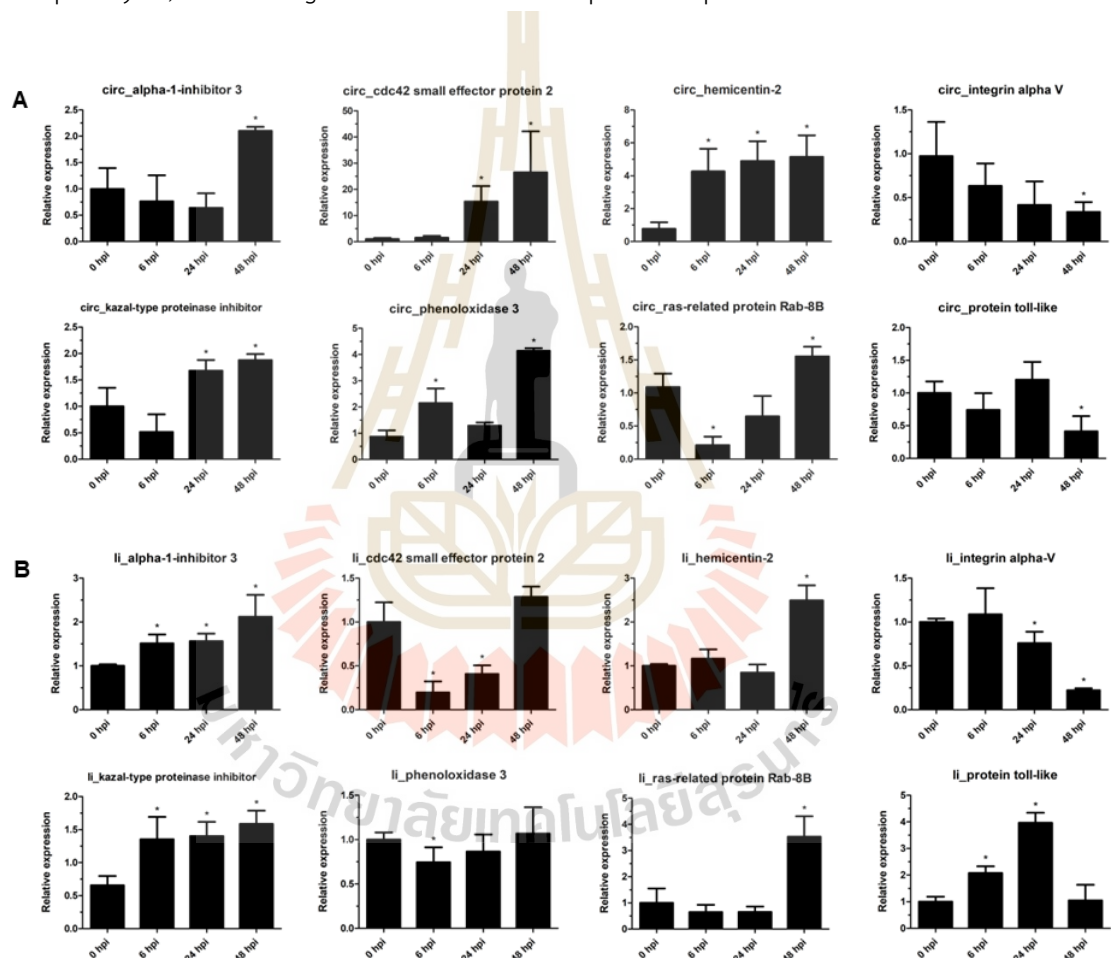
Figure 24. The expression of circRNAs and their parental li-RNA in shrimp upon YHV infection at 0, 6, 24, and 48 hpi. (A) The expression of circRNAs in shrimp upon YHV infection. (B) The expression of li-RNA in shrimp upon YHV infection. The expression levels were examined by qRT-PCR. Data were expressed as the relative expression value (means ± S.D., n = 9) and

normalized against EF-1α. Asterisks indicate significant differences between the data of 0 hpi and each time point postinfection (*P*-value < 0.05). The experiment was conducted in three replications.

4.4 Characterization of immune-responsive circRNA

To validate the characteristics of circRNAs, PCR, Sanger sequencing, and RNase R treatment experiments were employed. 8 differentially expressed genes (DEGs) were focused, which included circ_alpha-1-inhibitor 3, circ_cdc42 small effector protein 2, circ_hemicentin-2, circ_integrin alpha V, circ_kazal-type proteinase inhibitor, circ_phenoloxidase 3, circ_related protein rab-8B, and circ_protein toll-like.

4.4.1 Characterization of immune-responsive circRNA by PCR and Sanger sequencing

Both convergent and divergent primers were conducted to amplify PCR products from gDNA and cDNA. Interestingly, the amplicons generated by the divergent primers were only observed with the cDNA template, whereas the convergent primers successfully amplified PCR products from both gDNA and cDNA templates (Figure 25). Subsequently, the cDNA-derived amplicons generated by the divergent primers were subjected to Sanger sequencing. The sequencing results of these PCR products confirmed the characteristic features of circRNAs and displayed the back-splice junctions of the 8 DECs. These sequences corresponded to the positions and open-reading frames of the linear RNAs (li-RNAs) (Figure 26).
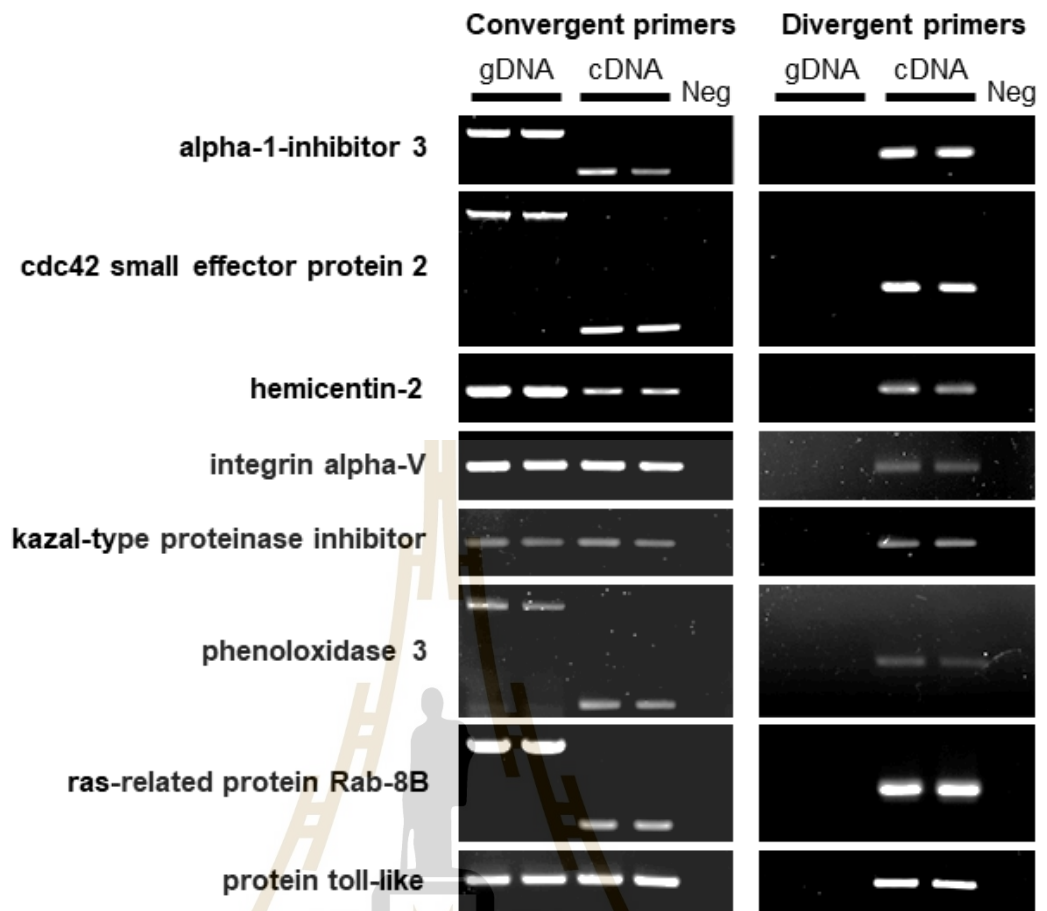
Figure 25. The PCR products of gDNA and cDNA amplification using convergent and divergent primers visualized on 1 % (w/v) agarose gel electrophoresis, which was stained with RedSafe Nucleic Acid Staining Solution (iNtRON).
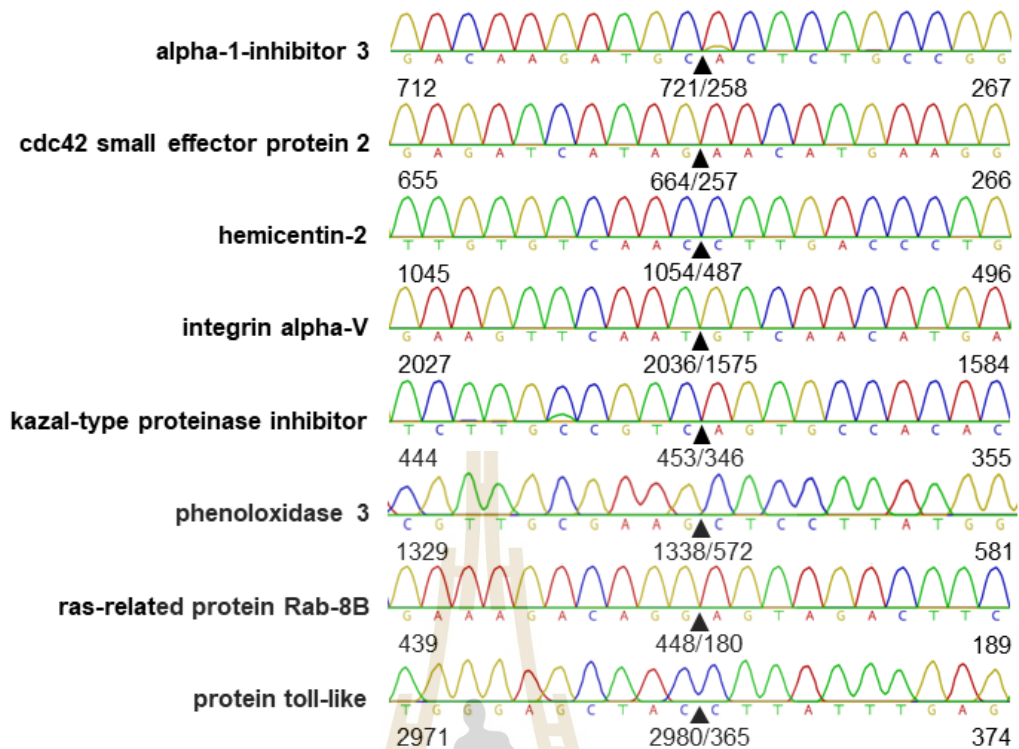
Figure 26. The Sanger sequencing of the amplicons amplified from divergent primers with cDNA as the template. The arrow and number represent the back-splice junction region and location on open-reading frames, respectively.

4.4.2 Characterization of immune-responsive circRNA by RNase R treatment

The impact of RNase R treatment on the enrichment of circRNAs was assessed. The relative expression of li-RNAs, amplified using convergent primers, including alpha-1-inhibitor 3, cdc42 small effector protein 2, hemicentin-2, integrin alpha V, kazal-type proteinase inhibitor, phenoloxidase 3, related protein rab-8B, and protein toll-like, as well as EF-1α (an internal control gene), decreased by nearly 10- to 1,000-fold following RNase R treatment. Conversely, the expression of circRNAs, amplified using divergent primers, increased by 10- to 10,000-fold after RNase R treatment, whereas no significant difference was observed for circ_protein toll-like (Figure 27). Therefore, it is evident that all 8 DECs possess the characteristic features of circRNAs.
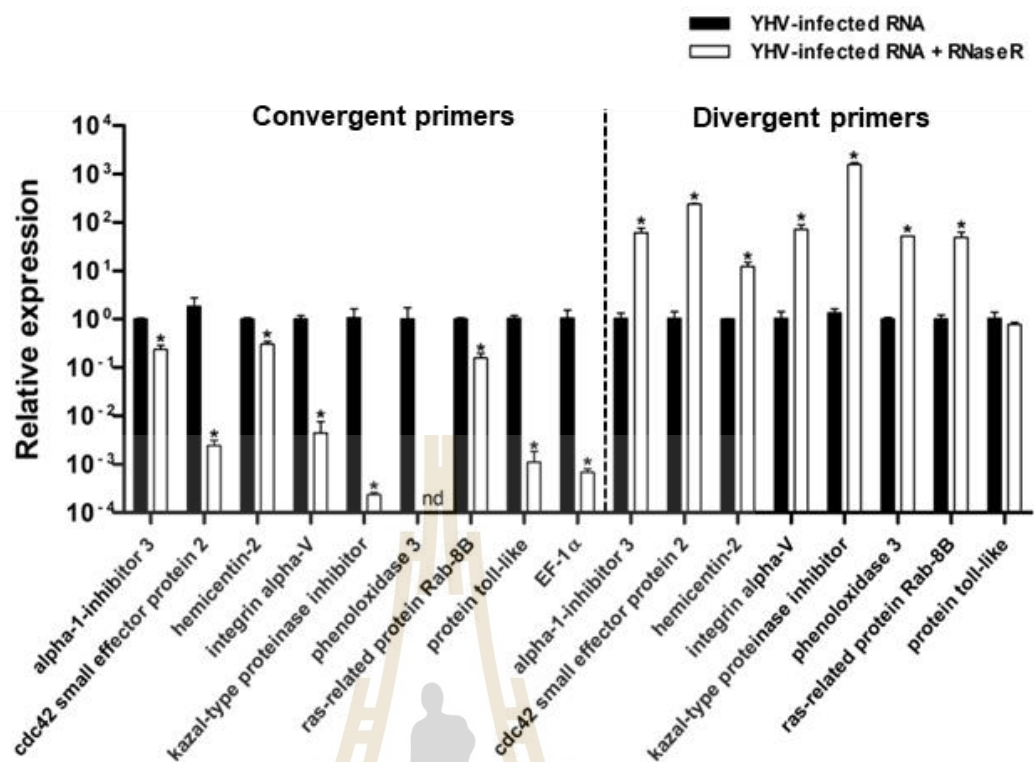
Figure 27. The resistance of circRNA to RNase R treatment. The circRNAs and their parental linear RNAs were quantitatively analyzed by qRT-PCR using cDNA synthesized from RNase R-untreated and -treated total RNA as templates and convergent and divergent primers. The relative expression was calculated by the modified $2^{-\Delta\Delta Ct}$ method and normalized against non-treatment groups. Bars depict mean ± S.D., and asterisks indicate significant difference (P-value < 0.05). The experiment was conducted in three replications (n = 9).

CHAPTER V

DISSCUSSION

In recent years, circRNAs have emerged as key players in various organisms across different species, contributing significantly to numerous biological processes, including cell proliferation, apoptosis, and the development of various diseases (Shang et al., 2019). Additionally, numerous studies have highlighted the role of circRNAs in viral infections and their ability to modulate the immune response. Notably, in humans, a distinct expression pattern was observed for 73 circRNAs during hepatitis C virus infection (Lu et al., 2020), while in fish, such as grass carp and miiuy croaker, 41 and 43 circRNAs were identified following infections with grass carp reovirus (GCRV) (He et al., 2017) and *Siniperca chuatsi* rhabdovirus (SCRV) (Chu et al., 2021), respectively. CircRNAs have also been detected in shrimp infected with WSSV, with a total of 290 differentially expressed circRNAs (DECs) identified in *L. vannamei* hemocytes after WSSV infection using high-throughput sequencing (Limkul et al., 2023). However, no reports on circRNAs in shrimp during YHV challenge have been documented.

In this study, circRNA profiling in Pacific white shrimp (*L. vannamei*) infected with YHV was conducted using high-throughput RNA sequencing, capable of processing a large number of input specimens in a single read (Meng et al., 2017; Zeng et al., 2017). From the results revealed 358 differentially expressed circRNAs in response to YHV infection compared to non-infected shrimp, comprising 177 up-regulated and 181 down-regulated circRNAs (Table 5; Figure 22). The number of circRNAs identified in *L. vannamei* was consistent with previous findings (Limkul et al., 2023). Furthermore, the expression profiles of circRNAs identified via circRNA-Seq were validated using other molecular biology techniques, including qRT-PCR technology (Panda and Gorospe, 2018). In previous studies, a random selection of the DECs identified in GCRV-infected Cytokine-induced killer cell (CIK) and porcine endemic diarrhea virus (PEDV) infection in the IPEC-J2 cell line underwent qRT-PCR

confirmation, and the results aligned with the sequencing data patterns (Chen et al., 2019; He et al., 2017; B. Liu et al., 2019). Therefore, in this study, qRT-PCR was employed to assess the accuracy of circRNA expression profiling, and the results from circRNA-Seq were consistent with those from qRT-PCR (Figure 24A).

Furthermore, the expression levels of the parent linear genes were examined using real-time PCR assay. Some parental genes exhibited a similar expression pattern to their corresponding circRNA transcripts, while others displayed an opposite expression pattern (Figure 24B). These findings suggest that both candidate circRNAs and their parent genes play an active role during YHV infection, underscoring their potential involvement in the host's response to viral infections (Chen et al., 2019). In this case, enhancing of shrimp immune system was accomplished by increasing the phenoloxidase (PO), prophenoloxidase (ProPO) (Jatuyosporn et al., 2023). The result found that the expression of phenoloxidase 3 circular forms were elevated but linear forms were steady. As previously reported, expression patterns and functions of circRNAs in human neuronal were studied and found highly increased circRNAs had higher fold-changes than their linear counterparts (Watts et al., 2023). From RT-PCR assay results supported initial evidence of circRNAs regulation in host response mechanisms during YHV infection.

Due to their lack of terminal structures, such as a 5′-terminal cap and a 3′-terminal poly (A) tail, which are covalently linked in canonical RNA molecules, circRNAs adopt a circular structure. Consequently, circRNAs demonstrate remarkable stability and resistance to nucleases, including RNase R (Xiao and Wilusz, 2019). These distinctive features have led to the development of various methods for circRNA validation, including qRT-PCR, sequencing, and RNase R treatment (Kristensen et al., 2019; Meng et al., 2017; Panda and Gorospe, 2018; Xiao and Wilusz, 2019). The cDNA derived from circRNAs contains exon-exon junction sequences, which are absent in conventionally spliced mRNAs. To analyze these junctions, divergent primers can be applied in qRT-PCR techniques to amplify across these specific junctions (Barrett and Salzman, 2016). However, it is essential to validate the presence of these junctions through Sanger sequencing to confirm their formation as perceived from the two reading frames of linear RNAs (Hu et al., 2019; Limkul et al., 2023; B. Liu et al., 2019; Wang et al., 2021). In this study, most of candidate DECs

exhibited circRNA-specific characteristics except for circ_protein toll-like, in which an increase of relative expression after RNase R treatment was not perceivable (Figure 27). Despite being resistant towards the cleavage by RNase R, some circRNAs have been found to be unsuccessfully enriched upon the RNase R validation. In mouse, no significant differences were discerned in five circRNAs including AUTs2, App, Samd4, Stk35, and Zfp609 after RNase R treatment; nevertheless, the confirmation by Northern blot showed the characteristics of circRNA (Gruner et al., 2016). Furthermore, the qPCR assay of recombinantly overexpressed circRNAs such as circRara and circPlce1 manifested the resistant cleavages in the presence of RNase R, thereby no up-regulated expression was observed following RNase R treatment (Lv et al., 2023; Xin et al., 2022). Therefore, the ineffectual enrichment of circ_protein toll-like by RNase R was comparatively correlated to the previous studies where the other circRNA validation techniques, for instance Sanger sequencing and PCR amplicons amplified by divergent primers, were implemented and unveiled the structural signatures of circRNAs. However, the behind reasons why some circRNAs are prone to RNase R digestion remain ambiguous and need investigating further.

CircRNAs exhibit various functions in response to pathogen infections, including their involvement in human cancers, where they influence tumorigenesis by orchestrating the tumor microenvironment's intricate communication between transformed cells and infiltrating immune cells, such as leukocytes (Patel et al., 2019). Recent insights into the role of the Wnt/β-catenin pathway in regulating immune cell infiltration within the tumor microenvironment have rekindled interest, given its potential impact on responses to immunotherapy treatments (Pai et al., 2017). From this study, analysis of GO categories revealed a connection between Wnt signaling and the immune system. Previous reports identified KEGG pathways associated with circRNA-derived genes, including central carbon metabolism in cancer, transcriptional misregulation in cancer, and the HIF-1 signaling pathway among the up-regulated circRNAs. Down-regulated circRNAs exhibited enrichment in processes linked to cancer, such as cell adhesion molecules (CAMs), ECM-receptor interaction, and the Rap 1 signaling pathway (Yan et al., 2019). Additionally, taste receptors in the airways potentially participate in three different immune pathways (Martens et al., 2021). Extracellular taste receptors play a significant role in

modulating the innate immune response by detecting pathogens (Patel et al., 2018). Furthermore, endocytosis plays a critical role in innate immunity, regulating microbial or pathogen infections in autoimmune and inflammatory diseases (Ding and Xiang, 2018). From this finding indicated that the KEGG pathways associated with circRNAs in this experiment were similar to those related to cancer metabolism, and distinct circRNAs could promote tumorigenesis, all of which are interconnected with the immune system. Finally, both GO term analysis and KEGG pathways were examined in shrimp, elucidating the circRNA metabolism-related biological processes following infection, which have been established as significant components of immune pathways and may be linked to the shrimp cells' immune response.

Being invertebrates, shrimp predominantly rely on their innate immune system to combat non-specific pathogenic microorganisms. Within this system, humoral responses serve as the first line of defense against pathogen infections. These responses encompass processes like blood clotting, activation of signaling pathways, and melanization, all of which are initiated by serine proteinase cascades (Jiravanichpaisal et al., 2006). Serine proteinase cascades are integral to various immunological pathways, including blood clotting in *L. vannamei* (Chaikeeratisak et al., 2012) and the activation of prophenoloxidase (proPO) in *Bombyx mori* (Tanaka and Yamakawa, 2011) and *L. vannamei* (Ponprateep et al., 2017). However, it is important to note that serine proteinases have the potential to cause significant tissue damage (Hiemstra, 2002). Consequently, the activity of serine proteinases must be carefully regulated. Various types of serine proteinase inhibitors play vital roles in modulating proteinase activities to mitigate the harmful effects of their active constituents. Furthermore, the suppression of specific serine proteinase inhibitors in crayfish hemolymph can inhibit the activation of the proPO cascade, resulting in reduced phenoloxidase levels (Hergenhahn et al., 1987). Finally, the phenoloxidase (PO) system is a crucial component of shrimp immunity, a major defense against viral pathogens. The enhancement of the shrimp immune system was accomplished by increasing the phenoloxidase (PO), prophenoloxidase (ProPO) (Jatuyosporn et al., 2023). From this study, the expression of phenoloxidase 3 circular forms were elevated but linear forms were steady. Additionally, an increase in the levels of linear and circular RNA in alpha-1-inhibitor-3 and a kazal-type proteinase inhibitor

following YHV infection in shrimp were observed. Both of these are serine proteinase inhibitors. These findings suggest that serine proteinase inhibitors may play a role in regulating the circular RNA proPO activation system, which is crucial in the innate immune response of *L. vannamei* to pathogens.

Pathogen recognition stands as a pivotal step in the host's immune response, initiated through PRRs identifying PAMPs. In shrimp, the principal signal transduction pathways implicated in the antiviral immune response encompass the Toll pathway, the immune deficiency (IMD) pathway, and the JAK-STAT pathway (Wang et al., 2014). These pathways collectively regulate the expression of antimicrobial peptides (AMPs) to combat pathogen infections. Toll-like proteins, which are germline-coded receptors for the innate immune system, are a class of proteins known to play a role in shrimp's immune response to both bacteria and viruses, as indicated by existing evidence (Li and Xiang, 2013b; Liu et al., 2021). Notably, the Toll pathway exerts a negative regulatory influence on AMP genes (Wang et al., 2013). In this study, a decrease in the expression of linear and circular RNA related to toll-like proteins following YHV infection in shrimp was observed. Consequently, the reduction in toll-like protein expression might facilitate the activation of AMP genes, bolstering the host's defense against pathogens. Furthermore, integrin alpha V as the cell membrane receptor responsible for Vago-dependent activation of the JAK/STAT pathway was identified, which in turn promotes the expression of antiviral immune factors (Gao et al., 2021). In the context of this finding, the down-regulation of both linear and circular integrin alpha V upon YHV infection in shrimp were noted. This decline in integrin alpha V levels may disrupt signaling transduction pathways, potentially rendering shrimp more vulnerable to YHV invasion.

Hemicentin is an extracellular matrix (ECM) protein and a member of the fibulin family. This protein plays a crucial role in tissue development and maintenance, particularly in the context of connective tissues (Feitosa et al., 2012). In *L. vannamei*, hemicentin-2 is up-regulated in response to Taura syndrome virus (TSV) infection (Zeng et al., 2013), demonstrating the involvement of these proteins during viral invasions. The results indicate that the expression of both linear and circular hemicentin-2 was increased after YHV infection. This increase in expression of both li-hemicentin-2 and circ-hemicentin could be attributed to the involvement in shrimp

during YHV infection. However, the pathways these molecules that could involve in during YHV invasion is ambiguous and need to be investigated further.

Small GTPase proteins serve a crucial function in membrane trafficking and phagocytosis pathways. This group of proteins comprises diverse families, including Rab, Rho, Ras, Sar1/Arf, and Ran. Ras-related protein Rab-8B, a member of the Rab family, plays a role in regulating intracellular membrane traffic (Wang et al., 2014). Rab8 proteins have been implicated in the trafficking of various viruses, such as the Dengue virus (Xu et al., 2008) and West Nile Virus (Kobayashi et al., 2016). From results indicate an up-regulation in the transcriptional levels of both linear and circular forms of Ras-related protein Rab-8B. Additionally, CDC42 small effector protein 2 (CDC42SE2), which is involved in cellular signaling and the regulation of the small GTPase protein CDC42, a member of the Rho GTPases (Swaine and Dittmar, 2015), exhibited increased expression following infection. These findings suggest that the increased expression of small GTPase proteins may facilitate YHV trafficking during shrimp infection, whereas the increased level of circRab8 and circ CDC42 small effector protein 2 might be employed by shrimp to modulate the expression of li-Rab8 and li-CDC42 small effector protein 2 involving in the viral pervasion through membrane trafficking pathways.

CHAPTER VI

CONCLUSION

In summary, a total of 358 differentially expressed circRNAs (DECs) were identified in YHV-infected shrimp through whole-transcriptome analysis. To validate these findings, qRT-PCR was applied to confirm the expression profiles of the identified DECs. The results obtained from circRNA-Seq and qRT-PCR were found to be consistent. The characteristics of circRNAs were further confirmed through RNase R treatment, PCR, and Sanger sequencing. The discovery of circRNAs in YHV-infected shrimp adds valuable insights to the shrimp genome, and these circRNAs hold promise as potential targets for preventing pathogen infections.

REFERENCES

Aguirre-Guzman, G., Sanchez-Martinez, J.G., Campa-Cordova, A.I., Luna-Gonzalez, A., Ascencio, F., 2009. Penaeid shrimp immune system. The Thai Journal of Veterinary Medicine 39, 205–215.

Amarakoon, A.G.U., Wijegoonawardane, P., 2017. A comparative analysis of Yellow Head Virus (YHD) diagnostic methods adopted in Sri Lanka to investigate the accuracy and specificity of the virus. World Scientific News 181–192.

Amparyup, P., Charoensapsri, W., Tassanakajon, A., 2013. Prophenoloxidase system and its role in shrimp immune responses against major pathogens. Fish & Shellfish Immunology 34, 990–1001.

Assavalapsakul, W., Tirasophon, W., Panyim, S., 2005. Antiserum to the gp116 glycoprotein of yellow head virus neutralizes infectivity in primary lymphoid organ cells of *Penaeus monodon*. Diseases of aquatic organisms 63, 85–88.

Azzam, G., Smibert, P., Lai, E.C., Liu, J.-L., 2012. *Drosophila* Argonaute 1 and its miRNA biogenesis partners are required for oocyte formation and germline cell division. Developmental biology 365, 384–394.

Bachère, E., Gueguen, Y., Gonzalez, M., De Lorgeril, J., Garnier, J., Romestand, B., 2004. Insights into the anti-microbial defense of marine invertebrates: the penaeid shrimps and the oyster *Crassostrea gigas*. Immunological reviews 198, 149–168.

Bailey-Brock, J.H., Moss, S.M., 1992. Penaeid taxonomy, biology ans zoogeography. Developments in aquaculture and fisheries science 23, 9–27.

Bao, S., Zheng, Z., Aweya, J.J., Yao, D., Li, S., Sun, C., Hong, Y., Zhang, Y., 2020. MicroRNA-589-5p modulates the expression of hemocyanin as part of the anti-WSSV immune response in *Litopenaeus vannamei*. Developmental & Comparative Immunology 107, 103642.

Barrett, S.P., Salzman, J., 2016. Circular RNAs: analysis, expression and potential functions. Development 143, 1838–1847.

Beutler, B., 2004. Innate immunity: an overview. Molecular immunology 40, 845–859.

Boonchuen, P., Maralit, B.A., Jaree, P., Tassanakajon, A., Somboonwiwat, K., 2020. MicroRNA and mRNA interactions coordinate the immune response in non-lethal heat stressed *Litopenaeus vannamei* against AHPND-causing *Vibrio parahaemolyticus*. Scientific reports 10, 787.

Boonyaratpalin, S., Supamattaya, K., Kasornchandra, J., Direkbusaracom, S., Aekpanithanpong, U., Chantanachooklin, C., 1993. Non-occluded baculo-like virus, the causative agent of yellow head disease in the black tiger shrimp (*Penaeus monodon*). Fish Pathology 28, 103–109.

Borah, S., Darricarrère, N., Darnell, A., Myoung, J., Steitz, J.A., 2011. A viral nuclear noncoding RNA binds re-localized poly (A) binding protein and is required for late KSHV gene expression. PLoS pathogens 7, e1002300.

Borsa, M., Seibert, C.H., Rosa, R.D., Stoco, P.H., Cargnin-Ferreira, E., Pereira, A.M., Grisard, E.C., Zanetti, C.R., Pinto, A.R., 2011. Detection of infectious myonecrosis virus in penaeid shrimps using immunoassays: usefulness of monoclonal antibodies directed to the viral major capsid protein. Archives of virology 156, 9–16.

Canton, J., 2014. Phagosome maturation in polarized macrophages. Journal of leukocyte biology 96, 729–738.

Cedano-Thomas, Y., De La Rosa-Vélez, J., Bonami, J.R., Vargas-Albores, F., 2010. Gene expression kinetics of the yellow head virus in experimentally infected *Litopenaeus vannamei*. Aquaculture research 41, 1432–1443.

Cerenius, L., Kawabata, S., Lee, B.L., Nonaka, M., Söderhäll, K., 2010. Proteolytic cascades and their involvement in invertebrate immunity. Trends in biochemical sciences 35, 575–583.

Chaikeeratisak, V., Somboonwiwat, K., Tassanakajon, A., 2012. Shrimp alpha-2-macroglobulin prevents the bacterial escape by inhibiting fibrinolysis of blood clots.

Chandrakala, N., Priya, S., 2017. Vibriosis in shrimp aquaculture a review. International Journal of Scientific Research in Science, Engineering and Technology 3, 27–33.

Chantanachookin, C., Boonyaratpalin, S., Kasornchandra, J., Direkbusarakom, S., Ekpanithanpong, U., Supamataya, K., Sriurairatana, S., Flegel, T., 1993.

Histology and ultrastructure reveal a new granulosis-like virus in Penaeus monodon affected by yellow-head disease. Diseases of Aquatic Organisms 17, 145–145.

Chayaburakul, K., Nash, G., Pratanpipat, P., Sriurairatana, S., Withyachumnarnkul, B., 2004. Multiple pathogens found in growth-retarded black tiger shrimp *Penaeus monodon* cultivated in Thailand. Diseases of aquatic organisms 60, 89–96.

Chen, D., 1992. An overview of the disease situation, diagnostic techniques, treatments and preventatives used on shrimp farms in China. Diseases of Cultured Penaeid Shrimp in Asia and the Unites States. The Oceanic Institute, Hawaii 47–55.

Chen, J., Wang, H., Jin, L., Wang, L., Huang, X., Chen, W., Yan, M., Liu, G., 2019. Profile analysis of circRNAs induced by porcine endemic diarrhea virus infection in porcine intestinal epithelial cells. Virology 527, 169–179.

Chen, L., Huang, C., Wang, X., Shan, G., 2015. Circular RNAs in eukaryotic cells. Current genomics 16, 312–318.

Chen, P., Kotov, A.A., Godneeva, B.K., Bazylev, S.S., Olenina, L.V., Aravin, A.A., 2021. piRNA-mediated gene regulation and adaptation to sex-specific transposon expression in *D. melanogaster* male germline. Genes & development 35, 914–935.

Chen, T.-C., Tallo-Parra, M., Cao, Q.M., Kadener, S., Böttcher, R., Pérez-Vilaró, G., Boonchuen, P., Somboonwiwat, K., Díez, J., Sarnow, P., 2020. Host-derived circular RNAs display proviral activities in Hepatitis C virus-infected cells. PLoS pathogens 16, e1008346.

Chou, H., Huang, C., Wang, C., Chiang, H., Lo, C., 1995. Pathogenicity of a baculovirus infection causing white spot syndrome in cultured penaeid shrimp in Taiwan. Diseases of aquatic organisms 23, 165–173.

Chu, Q., Zheng, W., Su, H., Zhang, L., Chang, R., Gao, W., Xu, T., 2021. A highly conserved circular RNA, circRasGEF1B, enhances antiviral immunity by regulating the miR-21-3p/MITA pathway in lower vertebrates. Journal of Virology 95, 10–1128.

Cornes, E., Bourdon, L., Singh, M., Mueller, F., Quarato, P., Wernersson, E., Bienko, M., Li, B., Cecere, G., 2022. piRNAs initiate transcriptional silencing of spermatogenic genes during *C. elegans* germline development. Developmental cell 57, 180–196.

Cowley, J.A., Cadogan, L.C., Spann, K.M., Sittidilokratna, N., Walker, P.J., 2004. The gene encoding the nucleocapsid protein of gill-associated nidovirus of *Penaeus monodon* prawns is located upstream of the glycoprotein gene. Journal of virology 78, 8935–8941.

Cruz-Flores, R., Mai, H.N., Dhar, A.K., 2021. Complete genome reconstruction and genetic analysis of Taura syndrome virus of shrimp from archival Davidson's-fixed paraffin embedded tissue. Virology 553, 117–121.

Czech, B., Hannon, G.J., 2016. One loop to rule them all: the ping-pong cycle and piRNA-guided silencing. Trends in biochemical sciences 41, 324–337.

Czech, B., Munafò, M., Ciabrelli, F., Eastwood, E.L., Fabry, M.H., Kneuss, E., Hannon, G.J., 2018. piRNA-guided genome defense: from biogenesis to silencing. Annual review of genetics 52, 131–157.

Destoumieux, D., Bulet, P., Loew, D., Van Dorsselaer, A., Rodriguez, J., Bachere, E., 1997. Penaeidins, a new family of antimicrobial peptides isolated from the shrimp *Penaeus vannamei* (Decapoda). Journal of Biological Chemistry 272, 28398–28406.

Destoumieux-Garzón, D., Rosa, R.D., Schmitt, P., Barreto, C., Vidal-Dupiol, J., Mitta, G., Gueguen, Y., Bachere, E., 2016. Antimicrobial peptides in marine invertebrate health and disease. Philosophical Transactions of the Royal Society B: Biological Sciences 371, 20150300.

Dhar, A.K., Cowley, J.A., Hasson, K.W., Walker, P.J., 2004. Genomic organization, biology, and diagnosis of Taura syndrome virus and yellowhead virus of penaeid shrimp. Advances in virus research 63, 353.

Ding, X., Xiang, S., 2018. Endocytosis and human innate immunity. Journal of Immunological Sciences 2.

Duangsuwan, P., Tinikul, Y., Withyachumnarnkul, B., Chotwiwatthanakun, C., Sobhon, P., 2011. Cellular targets and pathways of yellow head virus infection in

lymphoid organ of *Penaeus monodon* as studied by transmission electron microscopy. Songklanakarin Journal of Science & Technology 33.

Dugassa, H., Gaetan, D., 2018. Biology of White Leg Shrimp , *Penaeus vannamei* : Review.

El-Saadony, M.T., Swelum, A.A., Ghanima, M.M.A., Shukry, M., Omar, A.A., Taha, A.E., Salem, H.M., El-Tahan, A.M., El-Tarabily, K.A., Abd El-Hack, M.E., 2022. Shrimp production, the most important diseases that threaten it, and the role of probiotics in confronting these diseases: a review. Research in veterinary science 144, 126–140.

Fadilah, A., Fasya, A., 2021. Examination of Taura Syndrome Virus (TSV) in white shrimp (*Litopenaeus vannamei*) and tiger prawn (*Penaeus monodon*) with Polymerase Chain Reaction (PCR) method. Presented at the IOP Conference Series: Earth and Environmental Science, IOP Publishing, p. 012069.

Fan, B., Chen, F., Li, Y., Wang, Zhongliang, Wang, Zhiwen, Lu, Y., Wu, Z., Jian, J., Wang, B., 2019. A comprehensive profile of the tilapia (*Oreochromis niloticus*) circular RNA and circRNA–miRNA network in the pathogenesis of meningoencephalitis of teleosts. Molecular omics 15, 233–246.

Feitosa, N.M., Zhang, J., Carney, T.J., Metzger, M., Korzh, V., Bloch, W., Hammerschmidt, M., 2012. Hemicentin 2 and Fibulin 1 are required for epidermal–dermal junction formation and fin mesenchymal cell migration during zebrafish development. Developmental biology 369, 235–248.

Flegel, T., 2006. Detection of major penaeid shrimp viruses in Asia, a historical perspective with emphasis on Thailand. Aquaculture 258, 1–33.

Flegel, T.W., 2012. Historic emergence, impact and current status of shrimp pathogens in Asia. Journal of invertebrate pathology 110, 166–173.

Flegel, T.W., 1997. Major viral diseases of the black tiger prawn (*Penaeus monodon*) in Thailand. World Journal of Microbiology and Biotechnology 13, 433–442.

Gao, J., Zhao, B.-R., Zhang, H., You, Y.-L., Li, F., Wang, X.-W., 2021. Interferon functional analog activates antiviral Jak/Stat signaling through integrin in an arthropod. Cell reports 36.

Gao, N., Li, Yueheng, Li, J., Gao, Z., Yang, Z., Li, Yong, Liu, H., Fan, T., 2020. Long non-coding RNAs: the regulatory mechanisms, research strategies, and future directions in cancers. Frontiers in Oncology 10, 598817.

Gao, Y., Wang, J., Zhao, F., 2015. CIRI: an efficient and unbiased algorithm for de novo circular RNA identification. Genome biology 16, 1–16.

Gruner, H., Cortés-López, M., Cooper, D.A., Bauer, M., Miura, P., 2016. CircRNA accumulation in the aging mouse brain. Scientific reports 6, 38907.

Ha, H., Song, J., Wang, S., Kapusta, A., Feschotte, C., Chen, K.C., Xing, J., 2014. A comprehensive analysis of piRNAs from adult human testis and their relationship with genes and mobile elements. BMC genomics 15, 1–16.

Han, J.E., Tang, K.F., Tran, L.H., Lightner, D.V., 2015. Photorhabdus insect-related (Pir) toxin-like genes in a plasmid of *Vibrio parahaemolyticus*, the causative agent of acute hepatopancreatic necrosis disease (AHPND) of shrimp. Diseases of aquatic organisms 113, 33–40.

He, A.T., Liu, J., Li, F., Yang, B.B., 2021. Targeting circular RNAs as a therapeutic approach: current strategies and challenges. Signal transduction and targeted therapy 6, 185.

He, L., Zhang, A., Xiong, L., Li, Y., Huang, R., Liao, L., Zhu, Z., Wang, Y., 2017. Deep circular RNA sequencing provides insights into the mechanism underlying grass carp reovirus infection. International journal of molecular sciences 18, 1977.

He, Y., Ju, C., Zhang, X., 2015. Roles of small RNAs in the immune defense mechanisms of crustaceans. Molecular immunology 68, 399–403.

Hellio, C., Bado-Nilles, A., Gagnaire, B., Renault, T., Thomas-Guyon, H., 2007. Demonstration of a true phenoloxidase activity and activation of a ProPO cascade in Pacific oyster, *Crassostrea gigas* (Thunberg) in vitro. Fish & shellfish immunology 22, 433–440.

Hergenhahn, H.-G., Aspan, A., Söderhäll, K., 1987. Purification and characterization of a high-M r proteinase inhibitor of pro-phenol oxidase activation from crayfish plasma. Biochemical Journal 248, 223–228.

Hiemstra, P., 2002. Novel roles of protease inhibitors in infection and inflammation. Biochemical Society Transactions 30, 116–120.

Honda, S., Kawamura, T., Loher, P., Morichika, K., Rigoutsos, I., Kirino, Y., 2017. The biogenesis pathway of tRNA-derived piRNAs in *Bombyx* germ cells. Nucleic acids research 45, 9108–9120.

Hu, S.-Y., Huang, J.-H., Huang, W.-T., Yeh, Y.-H., Chen, M.H.-C., Gong, H.-Y., Chiou, T.-T., Yang, T.-H., Chen, T.T., Lu, J.-K., 2006. Structure and function of antimicrobial peptide penaeidin-5 from the black tiger shrimp *Penaeus monodon.* Aquaculture 260, 61–68.

Hu, X., Dai, Y., Zhang, X., Dai, K., Liu, B., Yuan, R., Feng, Y., Liang, Z., Zhu, M., Zhang, M., 2019. Identification and characterization of novel type of RNAs, circRNAs in crucian carp Carassius auratus gibelio. Fish & shellfish immunology 94, 50–57.

Huang, T., Zhang, X., 2012. Functional analysis of a crustacean microRNA in host-virus interactions. Journal of virology 86, 12997–13004.

Jaroenlak, P., Boakye, D.W., Vanichviriyakit, R., Williams, B.A., Sritunyalucksana, K., Itsathitphaisarn, O., 2018. Identification, characterization and heparin binding capacity of a spore-wall, virulence protein from the shrimp microsporidian, *Enterocytozoon hepatopenaei* (EHP). Parasites & vectors 11, 1–15.

Jatuyosporn, T., Laohawutthichai, P., Romo, J.P.O., Gallardo-Becerra, L., Lopez, F.S., Tassanakajon, A., Ochoa-Leyva, A., Krusong, K., 2023. White spot syndrome virus impact on the expression of immune genes and gut microbiome of black tiger shrimp *Penaeus monodon*. Scientific Reports 13, 996.

Jatuyosporn, T., Supungul, P., Tassanakajon, A., Krusong, K., 2014. The essential role of clathrin-mediated endocytosis in yellow head virus propagation in the black tiger shrimp *Penaeus monodon*. Developmental & Comparative Immunology 44, 100–110.

Jayasree, L., Janakiram, P., Madhavi, R., 2006. Characterization of *Vibrio* spp. associated with diseased shrimp from culture ponds of Andhra Pradesh (India). Journal of the world aquaculture society 37, 523–532.

Jensen, S., Brasset, E., Parey, E., Roest Crollius, H., Sharakhov, I.V., Vaury, C., 2020. Conserved small nucleotidic elements at the origin of concerted piRNA biogenesis from genes and lncRNAs. Cells 9, 1491.

Jiravanichpaisal, P., Lee, B.L., Söderhäll, K., 2006. Cell-mediated immunity in arthropods: hematopoiesis, coagulation, melanization and opsonization. Immunobiology 211, 213–236.

Jitrapakdee, S., Unajak, S., Sittidilokratna, N., Hodgson, R.A., Cowley, J.A., Walker, P.J., Panyim, S., Boonsaeng, V., 2003. Identification and analysis of gp116 and gp64 structural glycoproteins of yellow head nidovirus of *Penaeus monodon* shrimp. Journal of General Virology 84, 863–873.

Jollès, P., Jollès, J., 1984. What's new in lysozyme research? Always a model system, today as yesterday. Molecular and cellular biochemistry 63, 165–189.

Kamsaeng, P., Tassanakajon, A., Somboonwiwat, K., 2017. Regulation of antilipopolysaccharide factors, ALF *Pm* 3 and ALF *Pm* 6, in *Penaeus monodon*. Scientific Reports 7, 12694.

Karunasagar, Indrani, Otta, S., Karunasagar, Iddya, 1997. Histopathological and bacteriological study of white spot syndrome of *Penaeus monodon* along the west coast of India. Aquaculture 153, 9–13.

Keam, S.P., Young, P.E., McCorkindale, A.L., Dang, T.H., Clancy, J.L., Humphreys, D.T., Preiss, T., Hutvagner, G., Martin, D.I., Cropley, J.E., 2014. The human Piwi protein Hiwi2 associates with tRNA-derived piRNAs in somatic cells. Nucleic acids research 42, 8984–8995.

Ko, H.J., Jo, Y.H., Patnaik, B.B., Park, K.B., Kim, C.E., Keshavarz, M., Jang, H.A., Lee, Y.S., Han, Y.S., 2020. IKKγ/NEMO is required to confer antimicrobial innate immune responses in the yellow mealworm, Tenebrio Molitor. International Journal of Molecular Sciences 21, 6734.

Kobayashi, M., Johansson, M.W., Söderhäll, K., 1990. The 76 kD cell-adhesion factor from crayfish haemocytes promotes encapsulation in vitro. Cell and Tissue Research 260, 13–18.

Kobayashi, S., Suzuki, T., Kawaguchi, A., Phongphaew, W., Yoshii, K., Iwano, T., Harada, A., Kariwa, H., Orba, Y., Sawa, H., 2016. Rab8b regulates transport of West Nile virus particles from recycling endosomes. Journal of Biological Chemistry 291, 6559–6568.

Kristensen, L.S., Andersen, M.S., Stagsted, L.V., Ebbesen, K.K., Hansen, T.B., Kjems, J., 2019. The biogenesis, biology and characterization of circular RNAs. Nature Reviews Genetics 20, 675–691.

Kristensen, L.S., Hansen, T.B., Venø, M.T., Kjems, J., 2018. Circular RNAs in cancer: opportunities and challenges in the field. Oncogene 37, 555–565.

Kulkarni, A., Krishnan, S., Anand, D., Kokkattunivarthil Uthaman, S., Otta, S.K., Karunasagar, I., Kooloth Valappil, R., 2021. Immune responses and immunoprotection in crustaceans with special reference to shrimp. Reviews in Aquaculture 13, 431–459.

Kumar, B., Deepika, A., Arumugam, M., Mullainadhan, P., Makesh, M., Tripathi, G., Purushothaman, C., Rajendran, K., 2013. Microscopic and cytochemical characterisation of haemocytes of the mud crab *Scylla serrata* (Forskål, 1775)(Decapoda, Portunidae). Crustaceana 86, 1234–1249.

Kumar, R., Huang, J., Ng, Y., Chen, C., Wang, H., 2022. The regulation of shrimp metabolism by the white spot syndrome virus (WSSV). Reviews in Aquaculture 14, 1150–1169.

Kumar, R., Ng, T., Wang, H., 2020. Acute hepatopancreatic necrosis disease in penaeid shrimp. Rev Aquac 12: 1867–1880.

Kumar, T.S., Praveena, P.E., Sivaramakrishnan, T., Rajan, J.J.S., Makesh, M., Jithendran, K., 2022. Effect of *Enterocytozoon hepatopenaei* (EHP) infection on physiology, metabolism, immunity, and growth of *Penaeus vannamei*. Aquaculture 553, 738105.

Leaño, E.M., Mohan, C., 2012. Early mortality syndrome threatens Asia's shrimp farms. Global Aquaculture Advocate 2012, 38–9.

Lee, C.-T., Chen, I.-T., Yang, Y.-T., Ko, T.-P., Huang, Y.-T., Huang, J.-Y., Huang, M.-F., Lin, S.-J., Chen, C.-Y., Lin, S.-S., 2015. The opportunistic marine pathogen *Vibrio parahaemolyticus* becomes virulent by acquiring a plasmid that expresses a deadly toxin. Proceedings of the National Academy of Sciences 112, 10798–10803.

Lee, D., Yu, Y.-B., Choi, J.-H., Jo, A.-H., Hong, S.-M., Kang, J.-C., Kim, J.-H., 2022. Viral shrimp diseases listed by the OIE: a review. Viruses 14, 585.

Lee, M.H., Osaki, T., Lee, J.Y., Baek, M.J., Zhang, R., Park, J.W., Kawabata, S., Soderhall, K., Lee, B.L., 2004. Peptidoglycan recognition proteins involved in 1, 3-β-D-glucan-dependent prophenoloxidase activation system of insect. Journal of biological chemistry 279, 3218–3227.

Lee, S.Y., Söderhäll, K., 2002. Early events in crustacean innate immunity. Fish & shellfish immunology 12, 421–437.

Li, C., Ren, Y., Dong, X., Wang, C., Huang, J., 2019. Extraction of assembling complexes of viral capsomers from shrimp tissue infected with yellow head virus genotype 8 (YHV-8). Journal of fish diseases 42, 613–616.

Li, F., Xiang, J., 2013a. Recent advances in researches on the innate immunity of shrimp in China. Developmental & Comparative Immunology 39, 11–26.

Li, F., Xiang, J., 2013b. Signaling pathways regulating innate immune responses in shrimp. Fish & shellfish immunology 34, 973–980.

Li, H., Durbin, R., 2009. Fast and accurate short read alignment with Burrows–Wheeler transform. bioinformatics 25, 1754–1760.

Li, Y., Zheng, Q., Bao, C., Li, S., Guo, W., Zhao, J., Chen, D., Gu, J., He, X., Huang, S., 2015. Circular RNA is enriched and stable in exosomes: a promising biomarker for cancer diagnosis. Cell research 25, 981–984.

Li, Z., Gao, J., Xiang, X., Deng, J., Gao, D., Sheng, X., 2022. Viral long non-coding RNA regulates virus life-cycle and pathogenicity. Molecular Biology Reports 49, 6693–6700.

Lightner, D., 2011. Virus diseases of farmed shrimp in the Western Hemisphere (the Americas): a review. Journal of invertebrate pathology 106, 110–130.

Lightner, D., Redman, R., Bell, T., Brock, J., 1983. Detection of IHHN virus in *Penaeus stylirostris* and *P. vannamei* imported into Hawaii. Journal of the World Mariculture Society 14, 212–225.

Lightner, D.V., 1996. A handbook of shrimp pathology and diagnostic procedures for diseases of cultured penaeid shrimp.

Limkul, S., Phiwthong, T., Massu, A., Boonanuntanasarn, S., Teaumroong, N., Somboonwiwat, K., Boonchuen, P., 2023. Transcriptome-based insights into the regulatory role of immune-responsive circular RNAs in *Litopanaeus vannamei* upon WSSV infection. Fish & Shellfish Immunology 132, 108499.

Lin, X., Söderhäll, I., 2011. Crustacean hematopoiesis and the astakine cytokines. Blood, The Journal of the American Society of Hematology 117, 6417–6424.

Liu, B., Yuan, R., Liang, Z., Zhang, T., Zhu, M., Zhang, X., Geng, W., Fang, P., Jiang, M., Wang, Z., 2019. Comprehensive analysis of circRNA expression pattern and circRNA–mRNA–miRNA network in *Ctenopharyngodon idellus* kidney (CIK) cells after grass carp reovirus (GCRV) infection. Aquaculture 512, 734349.

Liu, H., Guo, S., He, Y., Shi, Q., Yang, M., You, X., 2021. Toll protein family structure, evolution and response of the whiteleg shrimp (*Litopenaeus vannamei*) to exogenous iridescent virus. Journal of Fish Diseases 44, 1131–1145.

Liu, Y., Dou, M., Song, X., Dong, Y., Liu, S., Liu, H., Tao, J., Li, W., Yin, X., Xu, W., 2019. The emerging role of the piRNA/piwi complex in cancer. Molecular cancer 18, 1–15.

Livak, K.J., Schmittgen, T.D., 2001. Analysis of relative gene expression data using real-time quantitative PCR and the 2− ΔΔCT method. methods 25, 402–408.

Lu, S., Zhu, N., Guo, W., Wang, X., Li, K., Yan, J., Jiang, C., Han, S., Xiang, H., Wu, X., 2020. RNA-Seq revealed a circular RNA-microRNA-mRNA regulatory network in Hantaan virus infection. Frontiers in cellular and infection microbiology 10, 97.

Lv, X., Luo, Q., Xin, S., Zheng, W., Xu, T., Sun, Y., 2023. Circular RNA circPlce1 regulates innate immune response in miiuy croaker, *Miichthys miiuy*. Fish & Shellfish Immunology 133, 108561.

Martens, K., Steelant, B., Bullens, D.M., 2021. Taste receptors: the gatekeepers of the airway epithelium. Cells 10, 2889.

Martin, M., 2011. Cutadapt removes adapter sequences from high-throughput sequencing reads. EMBnet. journal 17, 10–12.

Mattick, J.S., Amaral, P.P., Carninci, P., Carpenter, S., Chang, H.Y., Chen, L.-L., Chen, R., Dean, C., Dinger, M.E., Fitzgerald, K.A., 2023. Long non-coding RNAs: definitions, functions, challenges and recommendations. Nature Reviews Molecular Cell Biology 24, 430–447.

Meng, X., Li, X., Zhang, P., Wang, J., Zhou, Y., Chen, M., 2017. Circular RNA: an emerging key player in RNA world. Briefings in bioinformatics 18, 547–557.

Methatham, T., Boonchuen, P., Jaree, P., Tassanakajon, A., Somboonwiwat, K., 2017. Antiviral action of the antimicrobial peptide ALF*Pm*3 from *Penaeus monodon*

against white spot syndrome virus. Developmental & Comparative Immunology 69, 23–32.

Montgomery, B.E., Vijayasarathy, T., Marks, T.N., Cialek, C.A., Reed, K.J., Montgomery, T.A., 2021. Dual roles for piRNAs in promoting and preventing gene silencing in *C. elegans*. Cell reports 37.

Motte, E., Yugcha, E., Luzardo, J., Castro, F., Leclercq, G., Rodríguez, J., Miranda, P., Borja, O., Serrano, J., Terreros, M., 2003. Prevention of IHHNV vertical transmission in the white shrimp *Litopenaeus vannamei*. Aquaculture 219, 57–70.

Pai, S.G., Carneiro, B.A., Mota, J.M., Costa, R., Leite, C.A., Barroso-Sousa, R., Kaplan, J.B., Chae, Y.K., Giles, F.J., 2017. Wnt/beta-catenin pathway: modulating anticancer immune response. Journal of hematology & oncology 10, 1–12.

Panda, A.C., Gorospe, M., 2018. Detection and analysis of circular RNAs by RT-PCR. Bio-protocol 8, e2775–e2775.

Park, J., Lee, YS, Lee, S., Lee, Y, 1998. An infectious viral disease of penaeid shrimp newly found in Korea. Diseases of aquatic organisms 34, 71–75.

Patel, N.N., Workman, A.D., Cohen, N.A., 2018. Role of taste receptors as sentinels of innate immunity in the upper airway. Journal of pathogens 2018.

Patel, S., Alam, A., Pant, R., Chattopadhyay, S., 2019. Wnt signaling and its significance within the tumor microenvironment: novel therapeutic insights. Frontiers in immunology 10, 2872.

Perdomo-Morales, R., Montero-Alejo, V., Rodríguez-Viera, L., Perera, E., 2020. Evaluation of anticoagulants and hemocyte-maintaining solutions for the study of hemolymph components in the spiny lobster *Panulirus argus* (Latreille, 1804)(Decapoda: Achelata: Palinuridae). The Journal of Crustacean Biology 40, 213–217.

Ponprateep, S., Vatanavicharn, T., Lo, C.F., Tassanakajon, A., Rimphanitchayakit, V., 2017. Alpha-2-macroglobulin is a modulator of prophenoloxidase system in pacific white shrimp *Litopenaeus vannamai*. Fish & shellfish immunology 62, 68–74.

Poulos, B.T., Tang, K.F., Pantoja, C.R., Bonami, J.R., Lightner, D.V., 2006. Purification and characterization of infectious myonecrosis virus of penaeid shrimp. Journal of General Virology 87, 987–996.

Qiu, W., Geng, R., Zuo, H., Weng, S., He, J., Xu, X., 2021. Toll receptor 2 (Toll2) positively regulates antibacterial immunity but promotes white spot syndrome virus (WSSV) infection in shrimp. Developmental & Comparative Immunology 115, 103878.

Qu, S., Yang, X., Li, X., Wang, J., Gao, Y., Shang, R., Sun, W., Dou, K., Li, H., 2015. Circular RNA: a new star of noncoding RNAs. Cancer letters 365, 141–148.

Robalino, J., Browdy, C.L., Prior, S., Metz, A., Parnell, P., Gross, P., Warr, G., 2004. Induction of antiviral immunity by double-stranded RNA in a marine invertebrate. Journal of virology 78, 10442–10448.

Rossetto, C.C., Pari, G., 2012. KSHV PAN RNA associates with demethylases UTX and JMJD3 to activate lytic replication through a physical interaction with the virus genome. PLoS pathogens 8, e1002680.

Rossetto, C.C., Tarrant-Elorza, M., Verma, S., Purushothaman, P., Pari, G.S., 2013. Regulation of viral and cellular gene expression by Kaposi's sarcoma-associated herpesvirus polyadenylated nuclear RNA. Journal of virology 87, 5540–5553.

Ruppert, E.E., Barnes, R.D., 1994. Invertebrate zoology. Saunders College Publishing New York.

Sahul Hameed, A., Abdul Majeed, S., Vimal, S., Madan, N., Rajkumar, T., Santhoshkumar, S., Sivakumar, S., 2017. Studies on the occurrence of infectious myonecrosis virus in pond-reared *Litopenaeus vannamei* (Boone, 1931) in India. Journal of fish diseases 40, 1823–1830.

Samocha, T.M., 2019. Sustainable biofloc systems for marine shrimp. Academic Press.

Sánchez-Paz, A., 2010. White spot syndrome virus: an overview on an emergent concern. Veterinary research 41.

Sanger, H.L., Klotz, G., Riesner, D., Gross, H.J., Kleinschmidt, A.K., 1976. Viroids are single-stranded covalently closed circular RNA molecules existing as highly base-paired rod-like structures. Proceedings of the National Academy of Sciences 73, 3852–3856.

Shang, Q., Yang, Z., Jia, R., Ge, S., 2019. The novel roles of circRNAs in human cancer. Molecular cancer 18, 1–10.

Shen, H., Zhang, W., Shao, S., 2015. Phylogenetic and recombination analysis of genomic sequences of IHHNV. Journal of Basic Microbiology 55, 1048–1052.

Shu, L., Li, C., Zhang, X., 2016. The role of shrimp miR-965 in virus infection. Fish & Shellfish Immunology 54, 427–434.

Sittidilokratna, N., Dangtip, S., Cowley, J.A., Walker, P.J., 2008. RNA transcription analysis and completion of the genome sequence of yellow head nidovirus. Virus research 136, 157–165.

Srisuvan, T., Tang, K.F., Lightner, D.V., 2005. Experimental infection of *Penaeus monodon* with Taura syndrome virus (TSV). Diseases of aquatic organisms 67, 1–8.

Suresh, K., Srinu, R., Pillai, D., Rajesh, G., 2018. Hepatopancreatic microsporidiasis (HPM) in shrimp culture: a review. International journal of current microbiology and applied sciences 7, 3208–3215.

Swaine, T., Dittmar, M.T., 2015. CDC42 use in viral cell entry processes by RNA viruses. Viruses 7, 6526–6536.

Tanaka, H., Yamakawa, M., 2011. Regulation of the innate immune responses in the silkworm, *Bombyx mori*. Invertebrate Survival Journal 8, 59–69.

Tang, K.F., Pantoja, C.R., Poulos, B.T., Redman, R.M., Lightner, D.V., 2005. *In situ* hybridization demonstrates that *Litopenaeus vannamei*, *L. stylirostris* and *Penaeus monodon* are susceptible to experimental infection with infectious myonecrosis virus (IMNV). Diseases of aquatic organisms 63, 261–265.

Tassanakajon, A., Somboonwiwat, K., Supungul, P., Tang, S., 2013. Discovery of immune molecules and their crucial functions in shrimp immunity. Fish & shellfish immunology 34, 954–967.

Tinwongger, S., Thawonsuwan, J., Kondo, H., Hirono, I., 2019. Identification of an anti-lipopolysaccharide factor AV-R isoform (*Lv*ALF AV-R) related to Vp_PirAB-like toxin resistance in *Litopenaeus vannamei*. Fish & shellfish immunology 84, 178–188.

Tran, L., Nunan, L., Redman, R.M., Mohney, L.L., Pantoja, C.R., Fitzsimmons, K., Lightner, D.V., 2013. Determination of the infectious nature of the agent of

acute hepatopancreatic necrosis syndrome affecting penaeid shrimp. Diseases of aquatic organisms 105, 45–55.

Tsai, J.-M., Wang, H.-C., Leu, J.-H., Wang, A.H.-J., Zhuang, Y., Walker, P.J., Kou, G.-H., Lo, C.-F., 2006. Identification of the nucleocapsid, tegument, and envelope proteins of the shrimp white spot syndrome virus virion. Journal of virology 80, 3021–3029.

Walker, P., Bonami, J., Boonsaeng, V., Chang, P., Cowley, J., Enjuanes, L., Flegel, T., Lightner, D., Loh, P., Snijder, E., 2005. Family roniviridae.

Wang, G., Sun, Q., Wang, H., Liu, H., 2021. Identification and characterization of circRNAs in the liver of blunt snout bream (*Megalobrama amblycephala*) infected with *Aeromonas hydrophila*. Developmental & Comparative Immunology 124, 104185.

Wang, M., Yu, F., Wu, W., Zhang, Y., Chang, W., Ponnusamy, M., Wang, K., Li, P., 2017. Circular RNAs: a novel type of non-coding RNA and their potential implications in antiviral immunity. International journal of biological sciences 13, 1497.

Wang, P.-H., Gu, Z.-H., Wan, D.-H., Zhu, W.-B., Qiu, W., Chen, Y.-G., Weng, S.-P., Yu, X.-Q., He, J.-G., 2013. *Litopenaeus vannamei* Toll-interacting protein (*Lv*Tollip) is a potential negative regulator of the shrimp Toll pathway involved in the regulation of the shrimp antimicrobial peptide gene penaeidin-4 (PEN4). Developmental & Comparative Immunology 40, 266–277.

Wang, P.-H., Huang, T., Zhang, X., He, J.-G., 2014. Antiviral defense in shrimp: from innate immunity to viral infection. Antiviral research 108, 129–141.

Watts, M.E., Oksanen, M., Lejerkrans, S., Mastropasqua, F., Gorospe, M., Tammimies, K., 2023. Circular RNAs arising from synaptic host genes during human neuronal differentiation are modulated by SFPQ RNA-binding protein. BMC biology 21, 1–18.

Westenberg, M., Heinhuis, B., Zuidema, D., Vlak, J.M., 2005. siRNA injection induces sequence-independent protection in *Penaeus monodon* against white spot syndrome virus. Virus research 114, 133–139.

Westholm, J.O., Miura, P., Olson, S., Shenker, S., Joseph, B., Sanfilippo, P., Celniker, S.E., Graveley, B.R., Lai, E.C., 2014. Genome-wide analysis of *Drosophila*

circular RNAs reveals their structural and sequence properties and age-dependent neural accumulation. Cell reports 9, 1966–1980.

Wijegoonawardane, P.K., Cowley, J.A., Phan, T., Hodgson, R.A., Nielsen, L., Kiatpathomchai, W., Walker, P.J., 2008. Genetic diversity in the yellow head nidovirus complex. Virology 380, 213–225.

Winter, J., Jung, S., Keller, S., Gregory, R.I., Diederichs, S., 2009. Many roads to maturity: microRNA biogenesis pathways and their regulation. Nature cell biology 11, 228–234.

Winterling, C., Koch, M., Koeppel, M., Garcia-Alcalde, F., Karlas, A., Meyer, T.F., 2014. Evidence for a crucial role of a host non-coding RNA in influenza A virus replication. RNA biology 11, 66–75.

Wongteerasupaya, C., Sriurairatana, S., Vickers, J.E., Akrajamorn, A., Boonsaeng, V., Panyim, S., Tassanakajon, A., Withyachumnarnkul, B., Flegel, T., 1995. Yellow-head virus of *Penaeus monodon* is an RNA virus. Diseases of Aquatic Organisms 22, 45–50.

Wu, X., Pan, Y., Fang, Y., Zhang, J., Xie, M., Yang, F., Yu, T., Ma, P., Li, W., Shu, Y., 2020. The biogenesis and functions of piRNAs in human diseases. Molecular Therapy-Nucleic Acids 21, 108–120.

Wu, Y., Lü, L., Yang, L.-S., Weng, S.-P., Chan, S.-M., He, J.-G., 2007. Inhibition of white spot syndrome virus in *Litopenaeus vannamei* shrimp by sequence-specific siRNA. Aquaculture 271, 21–30.

Xiao, M.-S., Wilusz, J.E., 2019. An improved method for circular RNA purification using RNase R that efficiently removes linear RNAs containing G-quadruplexes or structured 3′ ends. Nucleic acids research 47, 8755–8769.

Xin, S., Lv, X., Zheng, W.W., Wang, L., Xu, T., Sun, Y., 2022. Circular RNA circRara promote the innate immune responses in miiuy croaker, *Miichthys miiuy*. Fish & Shellfish Immunology 128, 557–564.

Xu, D., Liu, W., Alvarez, A., Huang, T., 2014. Cellular immune responses against viral pathogens in shrimp. Developmental & comparative immunology 47, 287–297.

Xu, J., Han, F., Zhang, X., 2007. Silencing shrimp white spot syndrome virus (WSSV) genes by siRNA. Antiviral research 73, 126–131.

Xu, X.-F., Chen, Z.-T., Zhang, J.-L., Chen, W., Wang, J.-L., Tian, Y.-P., Gao, N., An, J., 2008. Rab8, a vesicular traffic regulator, is involved in dengue virus infection in HepG2 cells. Intervirology 51, 182–188.

Yan, Y., Zhang, R., Zhang, X., Zhang, A., Zhang, Y., Bu, X., 2019. RNA-Seq profiling of circular RNAs and potential function of hsa_circ_0002360 in human lung adenocarcinom. American Journal of Translational Research 11, 160.

Yang, Y.-T., Chen, I.-T., Lee, C.-T., Chen, C.-Y., Lin, S.-S., Hor, L.-I., Tseng, T.-C., Huang, Y.-T., Sritunyalucksana, K., Thitamadee, S., 2014. Draft genome sequences of four strains of *Vibrio parahaemolyticus*, three of which cause early mortality syndrome/acute hepatopancreatic necrosis disease in shrimp in China and Thailand. Genome Announcements 2, 10–1128.

Zeng, D., Chen, X., Xie, D., Zhao, Y., Yang, C., Li, Y., Ma, N., Peng, M., Yang, Q., Liao, Z., 2013. Transcriptome analysis of Pacific white shrimp (*Litopenaeus vannamei*) hepatopancreas in response to Taura syndrome Virus (TSV) experimental infection. PloS one 8, e57515.

Zeng, X., Lin, W., Guo, M., Zou, Q., 2017. A comprehensive overview and evaluation of circular RNA detection tools. PLoS computational biology 13, e1005420.

Zhan, W., Wang, Y., Fryer, J.L., Yu, K., Fukuda, H., Meng, Q., 1998. White spot syndrome virus infection of cultured shrimp in China. Journal of aquatic animal health 10, 405–410.

Zhang, P., Wu, W., Chen, Q., Chen, M., 2019. Non-coding RNAs and their integrated networks. Journal of integrative bioinformatics 16.

Zhang, W., Qin, P., Gong, X., Huang, L., Wang, C., Chen, G., Chen, J., Wang, L., Lv, Z., 2020. Identification of circRNAs in the liver of whitespotted bamboo shark (*Chiloscyllium plagiosum*). Frontiers in genetics 11, 596308.

Zhang, Z.F., Shao, M., Kang, K.H., 2006. Classification of haematopoietic cells and haemocytes in Chinese prawn *Fenneropenaeus chinensis*. Fish & Shellfish Immunology 21, 159–169.

Zheng, W., Sun, L., Yang, L., Xu, T., 2021. The circular RNA circBCL2L1 regulates innate immune responses via microRNA-mediated downregulation of TRAF6 in teleost fish. Journal of Biological Chemistry 297.

Zhong, F., Zhou, N., Wu, K., Guo, Y., Tan, W., Zhang, H., Zhang, X., Geng, G., Pan, T., Luo, H., 2015. A SnoRNA-derived piRNA interacts with human interleukin-4 pre-mRNA and induces its decay in nuclear exosomes. Nucleic acids research 43, 10474–10491.

BIOGRAPHY

Mr. Amarin Massu was born on November 1st, 1998 in Lopburi Province, Thailand. He received his Bachelor's Degree of Science (Biomedical Science) form Burapha University in 2021. After graduation, he has been employed under the position of research assistant at School of Biotechnology, Institute of Agricultural Technology, Suranaree University of Technology (SUT). In 2022, he continued with his graduate studies in School of Biotechnology, Institute of Agricultural Technology, SUT. He was supported by One Research One Graduate fellowships from SUT under supervision of Assist. Prof. Pakpoom Boonchuen, Ph.D.

Publication

Massu, A., Mahanil, K., Limkul, S., Phiwthong, T., Boonanuntanasarn, S., Teaumroong, N., Somboonwiwat, K., & Boonchuen, P. (2024). Identification of immune-responsive circular RNAs in shrimp (*Litopenaeus vannamei*) upon yellow head virus infection. *Fish & Shellfish Immunology*, 144, 109246.

Sriphuttha, C., Limkul, S., Pongsetkul, J., Phiwthong, T., **Massu, A.,** Sumniangyen, N., Boontawan, P., Ketudat-Cairns, M., Boontawan, A., & Boonchuen, P. (2023). Effect of fed dietary yeast (*Rhodotorula paludigena* CM33) on shrimp growth, gene expression, intestinal microbial, disease resistance, and meat composition of *Litopenaeus vannamei. Developmental & Comparative Immunology*, 147, 104896.

Limkul, S., Phiwthong, T., **Massu, A.,** Boonanuntanasarn, S., Teaumroong, N., Somboonwiwat, K., & Boonchuen, P. (2023). Transcriptome-based insights into the regulatory role of immune-responsive circular RNAs in *Litopanaeus vannamei* upon WSSV infection. *Fish & Shellfish Immunology*, 132, 108499.

Limkul, S., Phiwthong, T., **Massu, A.,** Jaree, P., Thawonsuwan, J., Teaumroong, N., Boonanuntanasarn, S., Somboonwiwat, K., & Boonchuen, P. (2022). The interferon-like proteins, Vagos, in *Fenneropenaeus merguiensis* elicit antimicrobial responses against WSSV and VPAHPND infection. *Fish & Shellfish Immunology*, 131, 718-728.